2012

Robot manipulator control using adaptive-gain sliding modes

Tetsuya Toyama

ROBOT MANIPULATOR CONTROL USING ADAPTIVE-GAIN SLIDING MODES

BY

TETSUYA TOYAMA

A THESIS

Submitted in partial fulfillment of the requirements
for the degree of Master of Science
in
The Department of Electrical and Computer Engineering
to
The School of Graduate Studies
of
The University of Alabama in Huntsville

HUNTSVILLE, ALABAMA

2012

In presenting this thesis in partial fulfillment of the requirements for a master's degree from The University of Alabama in Huntsville, I agree that the Library of this University shall make it freely available for inspection. I further agree that permission for extensive copying for scholarly purposes may be granted by my advisor or, in his/her absence, by the Chair of the Department or the Dean of the School of Graduate Studies. It is also understood that due recognition shall be given to me and to The University of Alabama in Huntsville in any scholarly use which may be made of any material in this thesis.

Tetsuya Toyama 3/12/2012

(student signature) (date)

THESIS APPROVAL FORM

Submitted by Tetsuya Toyama in partial fulfillment of the requirements for the degree of Master of Science in Engineering and accepted on behalf of the Faculty of the School of Graduate Studies by the thesis committee.

We, the undersigned members of the Graduate Faculty of The University of Alabama in Huntsville, certify that we have advised and/or supervised the candidate on the work described in this thesis. We further certify that we have reviewed the thesis manuscript and approve it in partial fulfillment of the requirements for the degree of Master of Science in Engineering.

03/12/2012 Committee Chair

(Date)

03/12/2012

3/14/2012

3/14/12 Department Chair

College Dean

3/28/12 Graduate Dean

ABSTRACT
The School of Graduate Studies
The University of Alabama in Huntsville

Degree Master of Science in Engineering College/Dept. Engineering/Electrical and Computer Engineering.

Name of Candidate Tetsuya Toyama

Title Robot Manipulator Control Using Adaptive-Gain Sliding Modes

In this thesis, adaptive sliding mode controls are presented as robust controls for robot manipulators. The objective of the study is to design controls for robot manipulators without the knowledge of the boundary of the uncertainties/disturbances by using an adaptive sliding mode control while elucidating the robustness of the adaptive sliding mode control. A sliding mode control provides for ultimate accuracy in the presence of the bounded disturbances/uncertainties, although the sliding mode control also causes chattering. Chattering is undesirable for use with actual components, since it might cause damage to them with a subsequent loss of accuracy. Such chatter is caused by overestimation of the controller gain. An adaptive sliding mode is proposed as a solution to the problems created by chattering; to illustrate, a 2-link robot manipulator is simulated with an adaptive sliding mode control. The performance of each adaptive sliding mode control is demonstrated through the simulation results. The results of the simulations show the effectiveness for chattering mitigation by means of avoiding overestimation, and the robustness of an adaptive sliding mode control.

Abstract Approval: Committee Chair Yuri Shtessel 03/12/2012

Department Chair Quiltaker for Dr. Lindquist 3/14/12

Graduate Dean Rhonda Kay Dade 3/28/12

ACKNOWLEDGMENTS

The work described in this thesis would not have been possible without the assistance of a number of people who deserve special mention. First, I would like to thank Dr. Yuri Shtessel for his suggestion of the research topic and his guidance throughout all the stages of the work. His advice and patient support were invaluable during the construction of this work.

I would also like to thank my family and my friends, who not only encouraged me to begin work on this degree and but also helped me to complete this work.

TABLE OF CONTENTS

Page

LIST OF FIGURES

CHAPTER 1

INTRODUCTION

1.1 Statement of the Problem

Designing an effective and robust control for a nonlinear system with unmodeled dynamics and system disturbances/uncertainties is one of the most significant issues facing control engineers [12]. In the real world, system dynamics are seldom fully known, and more unknown disturbances will arise during the operation. Because there are some uncertainties or unknown disturbances within the system, many engineers have developed a dedicated design control which is insensitive to changes in system dynamics; this dedicated control has become known as a robust control [9, 11]. The sliding mode control is an example of a dedicated design control that is used as a robust control [9]. The main feature of the sliding mode control is that it is insensitive to disturbances and uncertainties, if those are bounded.

However, the sliding mode control introduces chattering, which is one of the most significant problems in the field of sliding mode control [9, 10]. Overestimating the boundaries of uncertainties and disturbances leads to high sliding mode controller gains and thus increases chattering. Chattering in systems with a sliding mode control is usually caused by the unmodeled dynamics and can be observed as high frequency (but

less than infinity) control switching. The chattering effect in control results in oscillations in the sliding variable dynamics. These oscillations prevent sliding variables from being constrained to zero, which results in the degradation of the accuracy of sliding variable stabilization. As a solution to this issue, a sliding mode control with gain adaptation has been proposed, because of its ability to reduce the chattering; it retains the main properties of a sliding mode control but can also control a system with matched bounded disturbances, in which the bounds are unknown.

This paper examines and compares two strategies for creating robust controls in an atmosphere of dynamic disturbances and uncertainties. The first strategy utilizes a sliding mode control while the second utilizes a sliding mode control with a gain adaptation. Using the nonlinear system to compare these strategies, this paper shows that the sliding mode control with gain adaptation is a better strategy to design successful control models for use in the presence of the unknown bounded disturbances or uncertainties with unknown boundaries, since the adaptive gain sliding mode control mitigates chattering.

The robot manipulator is chosen as the nonlinear system. Robot manipulators are designed to move material, parts, tools, and specialized devices by having various programmed motions for different tasks. These manipulators consist of links connected by joints; those connected links then form a kinematic chain. The robot manipulators have several features that make them attractive in an industrial environment. Among the advantages often mentioned are decreased labor costs, increased precision, and more humane working conditions, as dull, repetitive, or hazardous jobs are performed by the

robot manipulators rather than by humans. The following picture shows the robot manipulators in operation.

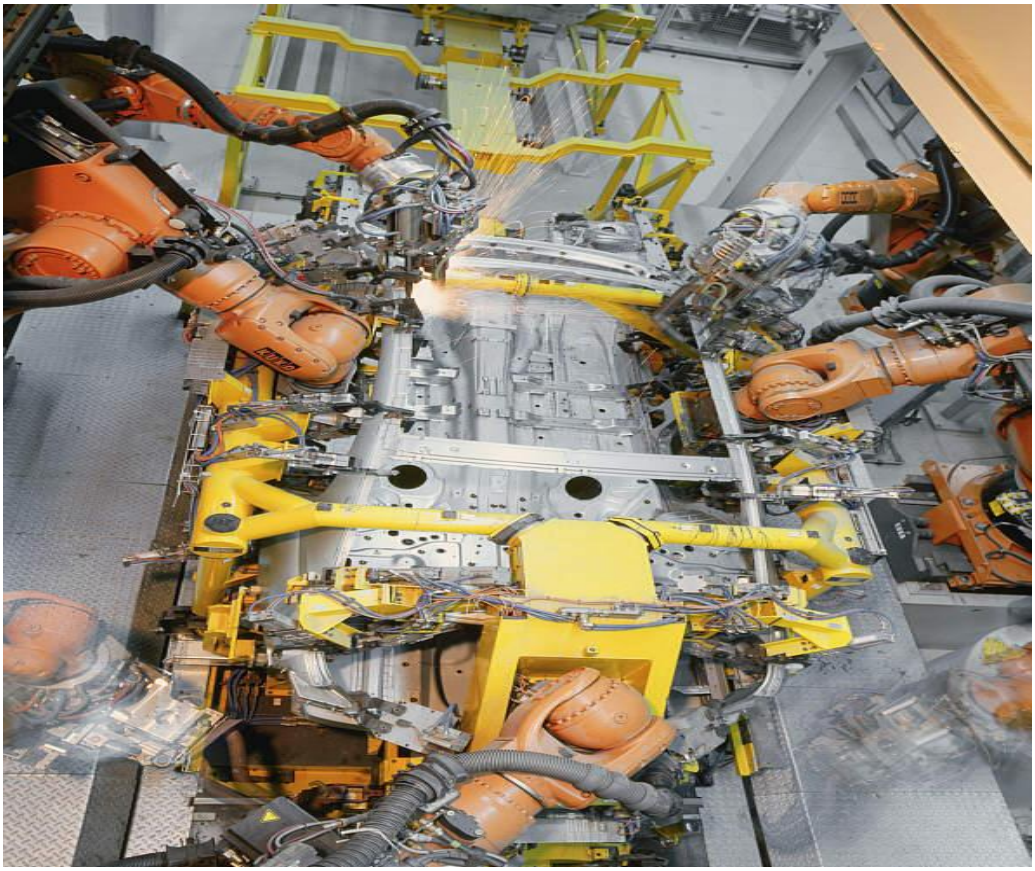

Figure 1.1: Picture of the robot manipulators in operation

This picture is taken in an auto repair factory. The robot manipulators are doing adhesive and welding operations to connect the side frame with the body shell. Typical applications of robot manipulators include welding, painting, assembly, pick and place, and so on. More than 800,000 robot manipulators are in operation in the world, mostly in Japan, the European Union and North America [1].

In this work, robust control is designed for the robot manipulators in the presence of unknown disturbances and uncertainties. The joint variables of each robot manipulator's joint are controlled in order to control the motion. As a case study, a 2-link robot manipulator is studied and simulated. This paper demonstrates the robustness of the sliding mode control with gain adaptation through the case study. The results reveal that the sliding mode control with gain adaptation is an effective method to design a robust control for those multipurpose robot manipulators which perform various tasks.

1.2 Structure of the Thesis

The structure of the thesis is as follows:

Chapter 2 introduces the robot manipulator dynamics and discusses the existent control algorithms. Two control algorithms are presented: one is inverse dynamics and the other is robust inverse dynamics. Components of robot manipulator dynamics are explained briefly.

Chapter 3 reviews concepts and design techniques of sliding mode control and higher-order sliding mode control. The basics of sliding mode control and various sliding mode controls are explicitly explained with simple examples. Then, the sliding mode observers are compared to the super-twisting observers to demonstrate the superior effectiveness of super-twisting observers as measures of the error between estimated and actual values. The design techniques of the gain adaptation are also introduced.

Chapter 4 shows the design process of adaptive sliding mode controls for the robot manipulator. Using the equations from Chapters 2 and 3, the system equation for

the robot manipulator is derived, along with sliding manifolds and sliding surfaces. These are necessary to design the sliding mode control. The design process for the traditional sliding mode control for the robot manipulator is shown along with a gain adaptation designed for each control.

Chapter 5 shows the application of the theories presented in Chapters 2-4 in the specific case of the 2-link robot manipulator. A traditional sliding mode control is applied to the 2-link robot manipulator. A super-twisting observer and a gain adaptation are also applied. The time derivatives of joint variables are estimated using the super-twisting observer. Using the estimation, the sliding variable is then defined. In addition, the auxiliary sliding variable is designed and applied for traditional sliding mode controls. The gain adaptation which was studied in Chapter 4 is applied. The comparative study of the results of the sliding mode control without gain adaptation and the results of the sliding mode control with gain adaptation are analyzed.

Chapter 6 describes the summary of the results of this thesis and draws a conclusion.

In the end of the thesis, the list of references is provided.

CHAPTER 2

ROBOT DYNAMICS AND CONTROL

This chapter introduces the dynamics of robot manipulators and the control algorithms used in those robot manipulators. Since its inception, the field of robot dynamics has presented many issues in refining both theory and operations; one of the most challenging areas of study has been the problem of computational efficiency in the dynamics of mechanisms. Many efficient algorithms in dynamics have been developed to address this problem. In this chapter, using the developed robot dynamics and basic control algorithms, the inverse dynamics of robot manipulators are derived and used to develop a control design.

2.1. Equations of Dynamics

The dynamics of robot manipulators illustrate the relationship between force and motion. The generalized force for a robot manipulator can be described as a second-order nonlinear differential equation. The dynamic equation of robot manipulators is derived using the Lagrangian [1]. The Lagrangian is derived by subtracting potential energy from kinetic energy [1]. The following figure shows a basic model of a 2-link robot manipulator.

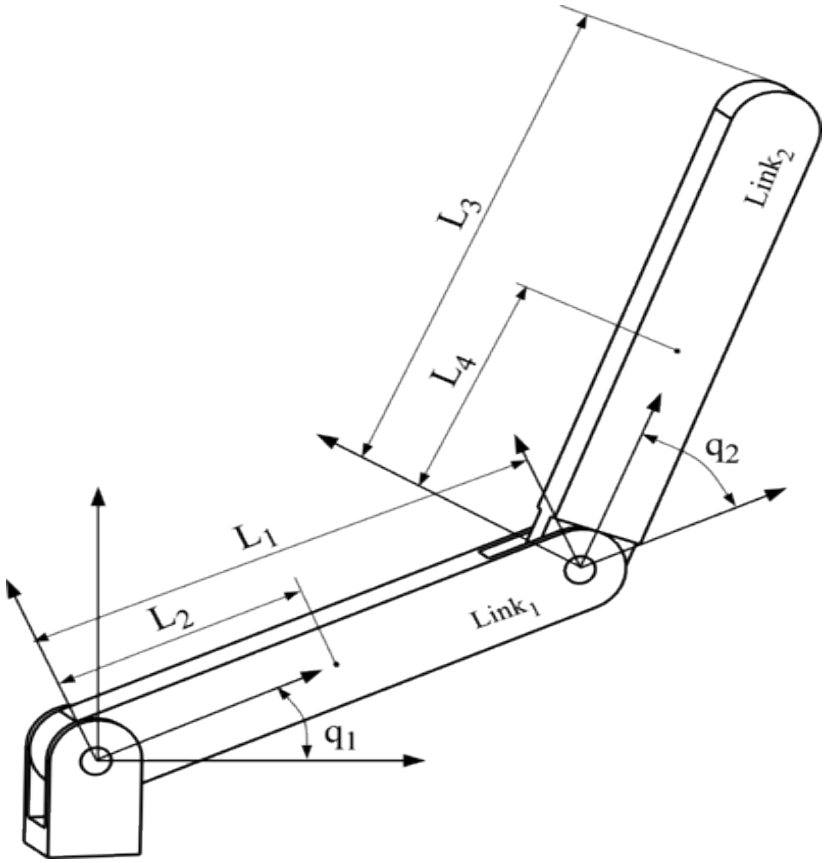

Figure 2.1 :2-link planar manipulator

Lagrangian is defined as [1]:

$$L = K - P \tag{2.1}$$

where *K* is defined as the sum of the kinetic energy for each joint, and *P* is defined as the sum of the potential energy for each joint. Using Lagrangian *L*, Euler-Lagrange Equation is defined as [1]:

$$\frac{d}{dt}\frac{\partial L}{\partial \dot{q}_k} - \frac{\partial L}{\partial q_k} = \tau_k; \;\; k = 1, \dots, n \tag{2.2}$$

where $\dot{q}$ is defined as a joint velocity, q is defined as a joint variable, τ is defined as a generalized force. The equation, which is rewritten Equation (2.2) in matrix form, is the dynamic equation of robot manipulator.

Dynamic equation of robot manipulator is defined as [1],[2],[3]:

$$M(q)\ddot{q} + C(q,\dot{q})\dot{q} + \mathrm{G}(q) = \tau + \tau_d \tag{2.3}$$

$q, \dot{q}, \ddot{q} \in \mathbb{R}^n$, $q - joint\ position,$ $\dot{q} - \ velocity,$ $\ddot{q} - \ acceleration$

$M(q)$: $nxn\ inertial\ Matrix$, should be invertible

$C(q,\dot{q})$: $nxn\ Matrix\ of\ Coriolis\ and\ centrifugal\ forces$

$G(q)$: $nx1\ vector\ of\ gravity\ term$

τ: $control\ force$

τ_d: $disturbances/uncertainties$

Equation (2.3) holds these properties:

Property 1. The matrix *M(q)* is symmetric, positive definite, bounded, and invertible. Its inverse matrix is positive definite and bounded also.

Property 2. The matrix $\dot{M}(q) - 2C(q,\dot{q})$ is skew-symmetric. Therefore, the following condition is satisfied:

$$x^T\left[\dot{M}(q) - 2C(q,\dot{q})\right]x = 0, \qquad \forall\, x \in \mathbb{R}^n \tag{2.4}$$

2.2. Control Algorithms

In this section, two control algorithms for robot manipulators are introduced. The first algorithm is the method of inverse dynamics, and the second algorithm is the method of robust inverse dynamics [1]. The method of inverse dynamics is a special case of the method of feedback linearization [1]. After introducing the basic idea of inverse dynamics, the practical situation of uncertainty in the parameters defining the manipulator dynamics will be discussed.

2.2.1 Inverse dynamics

In this section, the control force τ is designed using the inverse dynamics control theory. The objective of the control force τ is to provide stability and error compensation to the system, which does not include the disturbances and uncertainties. Consider the dynamic equation of an n-link rigid robot without disturbances/uncertainties in matrix form:

$$M(q)\ddot{q} + C(q,\dot{q})\dot{q} + \mathrm{G}(q) = \tau \tag{2.5}$$

Equation (2.5) is derived by using a Euler-Lagrange formulation. The idea of inverse dynamics is to find a nonlinear feedback control law

$$\tau = f(q,\dot{q},t) \tag{2.6}$$

The control τ is chosen as follows [1]:

$$\tau = M(q)a_q + C(q,\dot{q})\dot{q} + \mathrm{G}(q) \tag{2.7}$$

This Equation (2.7) is called the inverse dynamics control [1]. The matrix *M* is invertible. Then the combined system given by Equations (2.5)-(2.7) reduces to [1]:

$$\ddot{q} = a_q \tag{2.8}$$

The term a_q stands for a new input that is yet to be chosen. Equation (2.8) is recognized as the double integrator system. Then the system given by Equation (2.8) is linear. Therefore, a_q can now be designed to control a linear second order system; an obvious choice for a_q is to set [1]:

$$a_q = \ddot{q}^d(t) - K_0\tilde{q} - K_1\dot{\tilde{q}} \tag{2.9}$$

where $\tilde{q} = q - q^d, \dot{\tilde{q}} = \dot{q} - \dot{q}^d$ represents the difference between presence $q, \dot{q}$ and reference $q^d, \dot{q}^d$, where K_0, K_1 are diagonal matrices with diagonal elements consisting of position and velocity gains [1]. The reference trajectory is represented as:

$$t \to (q^d(t), \dot{q}^d(t), \ddot{q}^d(t)) \tag{2.10}$$

Equation (2.10) defines the desired time history of joint positions, velocities, and accelerations. Substituting Equation (2.9) into Equation (2.8), results in:

$$\ddot{\tilde{q}}(\mathrm{t}) + K_1\dot{\tilde{q}}(t) + K_0\tilde{q}(\mathrm{t}) = 0 \tag{2.11}$$

A simple decision for the gain matrices K_0 and K_1 is:

$$K_0 = \begin{bmatrix} \omega_1^2 & 0 & \cdots & 0 \\ 0 & \omega_2^2 & \cdots & 0 \\ \vdots & & \ddots & \vdots \\ 0 & 0 & \cdots & \omega_n^2 \end{bmatrix}, K_1 = \begin{bmatrix} 2\omega_1 & 0 & \cdots & 0 \\ 0 & 2\omega_2 & \cdots & 0 \\ \vdots & & \ddots & \vdots \\ 0 & 0 & \cdots & 2\omega_n \end{bmatrix} \tag{2.12}$$

where ω_i is natural frequency [1]. The natural frequency determines the speed of response of the joint, or equivalently, the rate of decay of the tracking error.

The control u is obtained by substituting (2.9) to (2.7) as follows,

$$\tau = M(q)\{\ddot{q}^d(t) - K_0\tilde{q} - K_1\dot{\tilde{q}}\} + C(q, \dot{q})\dot{q} + \mathrm{G}(q) \tag{2.13}$$

where K_0 and K_1 are shown in Equation (2.12).

However, the designed control force τ can drive the joint variable to the referenced trajectory when the disturbances and uncertainties are not introduced to the robot manipulator dynamics system. The designed control force τ is sensitive to the disturbances and uncertainties.

2.2.2 Robust Inverse Dynamics

In this section, the control force τ is designed to provide stability and compensation to the system, which does include the disturbances and uncertainties. Consider the dynamic equations of a robot manipulator

$$M(q)\ddot{q} + C(q,\dot{q})\dot{q} + \mathrm{G}(q) = \tau + \tau_d \tag{2.14}$$

and assume the inverse dynamics control input τ as [1]:

$$\tau = \hat{M}(q)a_q + \hat{C}(q,\dot{q})\dot{q} + \hat{G}(q) \tag{2.15}$$

where the symbols $\widehat{(\cdot)}$ represent the computed or nominal value of $(\cdot)$ and indicate that the theoretically exact inverse dynamics control cannot be achieved in practice due to the uncertainties in the system. The error $\widetilde{(\cdot)} = (\cdot) - \widehat{(\cdot)}$ is a measure of one's knowledge of the system parameters. Substituting Equation (2.15) into Equation (2.14) results in

$$\ddot{q} = a_q + \eta(q,\dot{q},a_q) \tag{2.16}$$

where

$$\eta\left(q,\dot{q},a_q\right) = M^{-1}(\tilde{M}a_q + \tilde{C}\dot{q} + \tilde{G}) \tag{2.17}$$

is described as the uncertainty. *E* is chosen as [1]:

$$E \coloneqq M^{-1}\tilde{M} = M^{-1}\hat{M} - I \tag{2.18}$$

Then, Equation (2.17) is expressed as [1]:

$$\eta\left(q, \dot{q}, a_q\right) = E a_q + M^{-1}(\tilde{C}\dot{q} + \tilde{G}) \tag{2.19}$$

The System (2.16) is nonlinear and coupled due to the uncertainty $\eta\left(q, \dot{q}, a_q\right)$. Therefore, there is no guarantee that the control given by Equation (2.9) will satisfy desired tracking performance specifications. Using Lyapunov's second method, redesign the control (2.9) to guarantee global convergence of the tracking error for the System (2.16). The control a_q is chosen as [1]:

$$a_q = \ddot{q}^d(t) - K_0\tilde{q} - K_1\dot{\tilde{q}} + \delta a \tag{2.20}$$

where δa is an additional term which is designed. Tracking error is expressed as [1]:

$$\mathrm{e} = \begin{bmatrix}\tilde{q} \\ \dot{\tilde{q}}\end{bmatrix} = \begin{bmatrix}q - q^d \\ \dot{q} - \dot{q}^d\end{bmatrix} \tag{2.21}$$

Using Equations (2.16) and (2.20) as [1]:

$$\dot{e} = Ae + B\{\delta a + \eta\} \tag{2.22}$$

where *A* and *B* are defined as [1]:

$$\mathrm{A} = \begin{bmatrix}0 & I \\ -K_0 & -K_1\end{bmatrix}, \qquad B = \begin{bmatrix}0 \\ I\end{bmatrix} \tag{2.23}$$

At first, the double integrator is stabilized by the linear feedback term $-K_0\tilde{q} - K_1\dot{\tilde{q}}$, and then the additional control term δa should be designed to overcome the potentially destabilizing effect of the uncertainty η. The concept is to assume that the uncertainty is bounded [1]:

$$\|\eta\| \leq \rho(e,t) \geq 0 \tag{2.24}$$

and an additional input δa is designed to guarantee ultimate boundary of the error trajectory in Equation (2.22) [1]. The bound ρ is in general a function of the tracking error and time [1]. Reconsider Equation (2.19), substituting for a_q from Equation (2.20):

$$\eta\left(q,\dot{q},a_q\right) = E\delta a + E\left(\ddot{q}^d(t) - K_0\tilde{q} - K_1\dot{\tilde{q}}\right) + M^{-1}\left(\tilde{C}\dot{q} + \tilde{G}\right) \tag{2.25}$$

The constants are defined as $\alpha < 1$, r_1, and r_2, together with possibly time-varying r_3 such that [1]:

$$\|\eta\| \leq \alpha\|\delta a\| + r_1\|e\| + r_2\|e\|^2 + r_3 \tag{2.26}$$

Keep in mind that the condition $\alpha := \|E\| = \left\|M^{-1}\widehat{M} - I\right\| < 1$ determines how close our estimate $\widehat{M}$ must be to the true inertia matrix. Assume that M^{-1} is bounded [1].

$$\underline{M} \leq \|M^{-1}\| \leq \overline{M} \tag{2.27}$$

The estimated inertia matrix $\widehat{M}$ is defined as [1]:

$$\widehat{M} = \frac{2}{\overline{M} + \underline{M}} I \tag{2.28}$$

Then the following expression can be shown [1]:

$$\left\|M^{-1}\widehat{M} - I\right\| \leq \frac{\overline{M} - \underline{M}}{\overline{M} + \underline{M}} < 1 \tag{2.29}$$

There is always a selection for $\widehat{M}$ that satisfies the condition $\|E\| < 1$. Then assume that $\|\delta a\| \leq \rho(e,t)$, which must be checked. Therefore [1],

$$\|\eta\| \leq \alpha\rho(e,t) + r_1\|e\| + r_2\|e\|^2 + r_3 =: \rho(e,t) \tag{2.30}$$

Since $\alpha < 1$, define ρ as [1]:

$$\rho(e,t) = \frac{1}{1-\alpha}(r_1\|e\| + r_2\|e\|^2 + r_3) \tag{2.31}$$

K_0 and K_1 are selected so that the matrix A in Equation (2.22) is Hurwitz. A Hurwitz matrix is a matrix that has all its eigenvalues in the open left half of the complex plane. $Q > 0$ and $P > 0$ are selected to be the unique symmetric positive definite matrix satisfying the Lyapunov equation [1]

$$A^T P + PA = -Q \tag{2.32}$$

Define the control δa as follows [1]:

$$\delta a = \begin{cases} -\rho(e,t)\dfrac{B^T Pe}{\|B^T Pe\|} & ;\ if\ \ \|B^T Pe\| \neq 0 \\ 0 & ;\ if\ \ \|B^T Pe\| = 0 \end{cases} \tag{2.33}$$

With Equation (2.33), it follows that the Lyapunov function $\mathrm{V} = e^T Pe$ satisfies $\dot{V} < 0$ along solution trajectories of Equation (2.22). To prove this result, compute the following equation [1]:

$$\dot{V} = -e^T Qe + 2e^T PB\{\delta a + \eta\} \tag{2.34}$$

For a simple assumption, set $\omega = B^T Pe$ and consider the second term $\omega^T\{\delta a + \eta\}$ in the above expression. If $\omega = 0$, this term is canceled, and for $\omega \neq 0$, δa becomes [1]:

$$\delta a = -\rho\frac{\omega}{\|\omega\|} \tag{2.35}$$

Thus, using the Cauchy-Schwartz inequality, the following expression is obtained [1]:

$$\omega^T\left(-\rho\frac{\omega}{\|\omega\|} + \eta\right) \leq -\rho\|\omega\| + \|\omega\|\|\eta\| = \|\omega\|(-\rho + \|\eta\|) \tag{2.36}$$

$$\leq 0$$

since $\|n\| \leq \rho$. Therefore [1],

$$\dot{V} \leq -e^T Q e < 0; \text{ where } \|\delta a\| \leq \rho \tag{2.37}$$

The control term δa is discontinuous on the subspace defined by $B^T P e = 0$: therefore, solution trajectories on this subspace are not well defined in the usual sense. In practice, the discontinuous control results in the phenomenon of chattering. The control shown as follows is implemented by a continuous approximation [1]:

$$\delta a = \begin{cases} -\rho(e,t)\dfrac{B^T P e}{\|B^T P e\|} & ; \ if \ \ \|B^T P e\| > \epsilon \\ -\dfrac{\rho(e,t)}{\epsilon} B^T P e & ; \ if \ \ \|B^T P e\| \leq \epsilon \end{cases} \tag{2.38}$$

In this case, since the control given by Equation (2.38) is continuous, a solution to the System (2.22) exists for any initial condition.

As a result, the control a_q is obtained by combining Equations (2.20) and (2.38) [1]:

$$a_q = \ddot{q}^d(t) - K_0 \tilde{q} - K_1 \dot{\tilde{q}} - \ \rho(e,t)\frac{B^T P e}{\|B^T P e\| + \epsilon} \tag{2.39}$$

However, the designed control force τ provides stability and compensation to the system, which has the disturbances and uncertainties. The overestimation of the controller gain, which is introduced as $\rho(e,t)$, introduces a decrease in accuracy. In this control algorithm, the boundary of the disturbances and uncertainties should be known before the design of the control.

2.3. Problem Formulation

The derived control u in (2.38) is similar to a sliding mode control without gain adaptation. In this control design process, we assume the boundary of the disturbance $f(q, \dot{q}, t)$, L is known. We can select a large controller gain value to design the control, when the boundary L of the bounded disturbance is not known. However, the large controller gain also results in chattering, which might damage actual components and cause a loss in accuracy.

Task1: In this thesis, a sliding mode control with gain adaptation is to be used as a solution to the problems caused by chattering in the robot manipulator control problem. The performances of robot manipulator control systems with traditional and adaptive gain sliding mode controller are to be compared via computer simulations.

Task2: Another important component of these control algorithms is joint velocity $\dot{q}$, which is not measurable. Other terms in System Equation (2.5) are assumed to be measurable, except for the disturbances/uncertainties. In order to design a control for System Equation (2.3), $\dot{q}$ should be estimated by means of sliding mode observation techniques. The designed sliding mode observers/differentiators are to be used in a concert with the sliding mode controllers. Their performances are to be verified via computer simulations.

2.4. Summary

In this chapter, robot manipulator dynamics and existent robot manipulator control algorithms have been presented. Dynamics compensated for input-output tracking errors have been derived, and the robot manipulator dynamic equation has been presented. The dynamic inversion and robust dynamic inversion control algorithms have been discussed; in addition, the deficiencies of the mentioned algorithms have been discovered. In order to address these deficiencies, we have proposed the use of an adaptive gain sliding mode control.

CHAPTER 3

FUNDAMENTALS OF SLIDING MODE CONTROL (SMC)

The previous chapter discussed the dynamics of robot manipulator and control algorithms. This chapter introduces the basic concepts of sliding mode control and observation. The main advantage of sliding mode control is the robustness that can be achieved when properly matched to the bounded disturbances. This chapter begins by introducing the concepts of the sliding surface, the sliding mode, and the sliding mode control using a simple example. Then, it demonstrates how to design 1) a sliding mode control and 2) a gain adaptive sliding mode control.

3.1. Concepts of a Sliding Surface, a Sliding Mode, and Sliding Mode Control

Consider a double integrated system as follows:

$$\begin{cases} \dot{x_1} = x_2 & x_1(0) = x_{10} \\ \dot{x_2} = u + f(x_1, x_2, t) & x_2(0) = x_{20} \end{cases} \tag{3.1}$$

where u is the control function, and $f(x_1, x_2, t)$ is the disturbance. The disturbance is assumed to be bounded, i.e. $|f(x_1, x_2, t)| \leq L > 0$. The problem is in designing the control function u that drives $x_1, x_2 \to 0$ as time increases in the presence of the bounded disturbance $f(x_1, x_2, t)$. Let us introduce desired compensated dynamics for the system

as described in Equation (3.1). A good candidate for the desired compensated dynamics is a homogeneous linear time invariant differential equation, such as:

$$\dot{x_1} + cx_1 = 0, \quad c > 0 \tag{3.2}$$

Keep in mind that $\dot{x_1} = x_2$. The general solution of Equation (3.2) is:

$$\begin{aligned} x_1(t) &= x_1(0)\exp(-ct) \\ x_2(t) &= \dot{x_1}(t) = -cx_1(0)\exp(-ct) \end{aligned} \tag{3.3}$$

The solution, obtained in Equation (3.3), converges to 0 asymptotically and the effect of the bounded disturbance $f(x_1, x_2, t)$ on the compensated dynamics is not observed. To achieve these compensated dynamics, let us introduce a variable σ, in the state space of the System Equation (3.1).

$$\sigma = \sigma(x_1, x_2) = x_2 + cx_1, \qquad c > 0 \tag{3.4}$$

The variable σ is called the sliding variable. The first step in designing a sliding mode control is to obtain the following equation, using Equations (3.2) and (3.4):

$$\sigma = \sigma(x_1, x_2) = x_2 + cx_1 = 0, \qquad c > 0 \tag{3.5}$$

Equation (3.5) defines a straight line in the state variable space of the System (3.1). This is called a sliding surface.

Now the problem is reduced to driving the sliding variable $\sigma \to 0$ in finite time, because when σ is equal to 0, $x_2 + cx_1$ is also equal to 0 and $\dot{x_1} + cx_1$ is also equal to 0 Finally state variables x_1, x_2 keep the general solution, which is shown in Equation (3.3). This task can be achieved by applying Lyapunov function techniques to the sliding variable dynamics that are derived using Equations (3.1) and (3.5).

$$\dot{\sigma} = cx_2 + f(x_1, x_2, t) + u, \quad \sigma(0) = \sigma_0 \tag{3.6}$$

For the sliding variable dynamics Equation (3.5), the Lyapunov function is expressed as:

$$V = \frac{1}{2}\sigma^2 \tag{3.7}$$

In order to provide for the asymptotic stability of Equation (3.6) about the equilibrium point $\sigma = 0$, the following conditions must be satisfied:

$$\text{a)}\dot{V} < 0 \tag{3.8}$$

$$\text{b)}\lim_{|\sigma|\to\infty} V = \infty$$

The condition (b) is clearly satisfied. In order to achieve finite time convergence, part a) in Equation (3.8) is modified to:

$$\dot{V} = \sigma\dot{\sigma} \leq -\alpha V^{1/2}, \quad \alpha > 0 \tag{3.9}$$

The condition shown in Equation (3.9) is called the reachability condition in a sliding mode control. System state variables x_1, x_2 are driven towards the sliding surface, as shown in Equation (3.5), and stay on the sliding surface thereafter, when the reachability condition is met. Integrating Equation (3.9) over the time interval $0 \leq \tau \leq t$, the following equation is obtained:

$$V^{\frac{1}{2}}(t) \leq -\frac{1}{2}\alpha t + V^{\frac{1}{2}}(0) \tag{3.10}$$

Since V converges to 0 in finite time t_r, Equation (3.10) can be rewritten as:

$$V^{\frac{1}{2}}(t_r) = 0 \leq -\frac{1}{2}\alpha t_r + V^{\frac{1}{2}}(0) \tag{3.11}$$

t_r is called the reaching time. Solving Equation (3.11), the equation for t_r is obtained:

$$t_r \leq \frac{2V^{\frac{1}{2}}(0)}{\alpha} \tag{3.12}$$

The control u, which is designed to satisfy Inequality (3.8), drives the sliding variable to 0 in finite time and keeps the sliding variable at 0 thereafter. The next part introduces the method of design for control u.

The control u must satisfy Equation (3.8) to drive the sliding variable to 0 in finite time and keep it at 0 thereafter. The derivative of V is expressed as follows:

$$\dot{V} = \sigma\dot{\sigma} = \sigma(cx_2 + f(x_1, x_2, t) + u) \tag{3.13}$$

The choice of the control u is expressed by the following equation:

$$u = -cx_2 - \rho \cdot sign(\sigma), \qquad \rho > 0 \tag{3.14}$$

Substituting Equation (3.14) into Equation (3.13), Equation (3.13) can be rewritten as follows:

$$\dot{V} = \sigma(f(x_1, x_2, t) - \rho \cdot sign(\sigma)) \tag{3.15}$$

$f(x_1, x_2, t)$ is bounded by L. Therefore, Equation (3.15) can be rewritten as:

$$\dot{V} = \sigma(f(x_1, x_2, t) - \rho \cdot sign(\sigma)) \leq |\sigma|(L - \rho) \tag{3.16}$$

Using Equation (3.7) and Inequality (3.9), the boundary of the derivative of V is derived as follows:

$$\dot{V} \leq -\alpha V^{1/2} = -\frac{\alpha}{\sqrt{2}}|\sigma|, \;\; \alpha > 0 \tag{3.17}$$

Comparing Equations (3.15 and (3.16), the following expression is obtained:

$$\dot{V} \leq -|\sigma|(\rho - L) = -\frac{\alpha}{\sqrt{2}}|\sigma| \tag{3.18}$$

Solve the Equation (3.18) for controller gain ρ.

$$\rho = L + \frac{\alpha}{\sqrt{2}} \tag{3.19}$$

Finally the control u is:

$$u = -cx_2 - \rho \cdot sign(\sigma), \qquad \rho = L + \frac{\alpha}{\sqrt{2}} \tag{3.20}$$

The control u drives the sliding variable to 0 in finite time and keeps it at 0 thereafter; state variables x_1, x_2 are driven to 0 asymptotically in the presence of the bounded disturbance. This type of control is called a sliding mode control, which has now been proven to be robust to the bounded disturbances [4]. The control which is given in (3.20) is called a traditional sliding mode control.

Example 1:

Consider System (3.1) with given parameters as follows:

$$\begin{cases} \dot{x_1} = x_2 & x_1(0) = 2 \\ \dot{x_2} = u + f(t) & x_2(0) = -1 \end{cases}, \qquad f(t) = sin2t$$

The bounded disturbance $f(t)$ is defined as $2t$. The objective of this example is to design a sufficiently robust control to be insensitive to the bounded disturbance, using the traditional sliding mode control design technique. The sliding variable is selected as:

$$\sigma = x_2 + 2x_1$$

The traditional sliding mode control is designed as follows:

$$u = -2x_2 - \rho \cdot sign(\sigma), \qquad \rho > 1 = |sin2t|$$

The Figures 3.1-3 show the results of the simulation with $\rho = 3$ (no overestimation), and time increment is 10^{-4}.

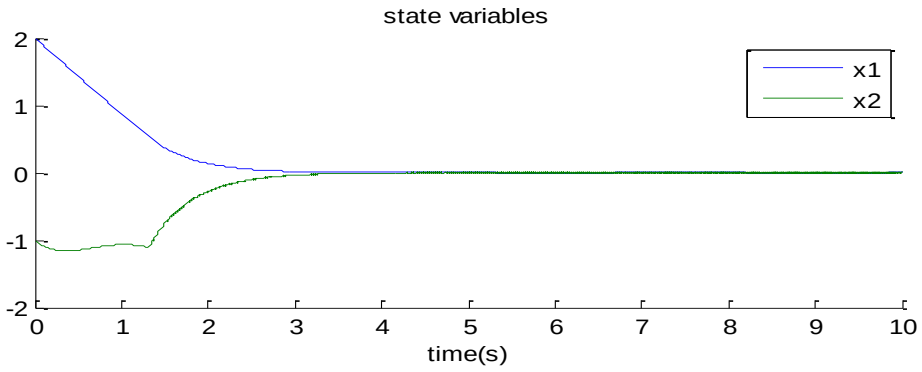

Figure 3.1: State variables of Example 1

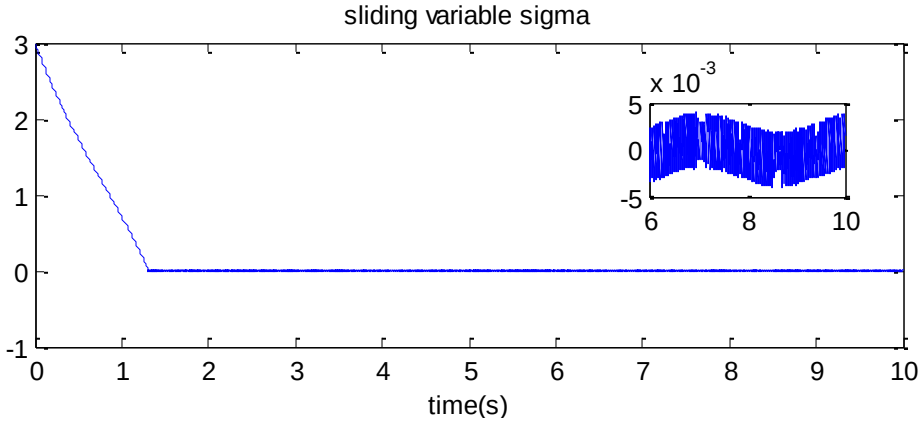

Figure 3.2: Sliding variable tracking of Example 1

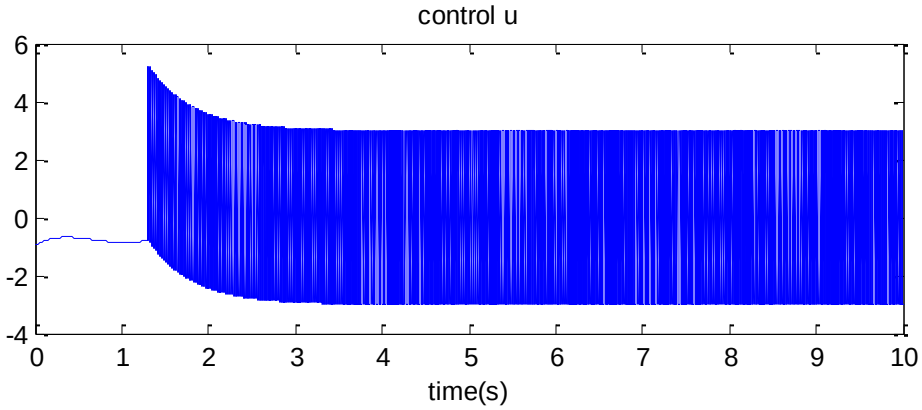

Figure 3.3: Control *u* of Example 1 ($\rho = 3$)

The Figures 3.4-6 show the results of the simulation with $\rho = 30$ (overestimation), and time increment is 10^{-4}.

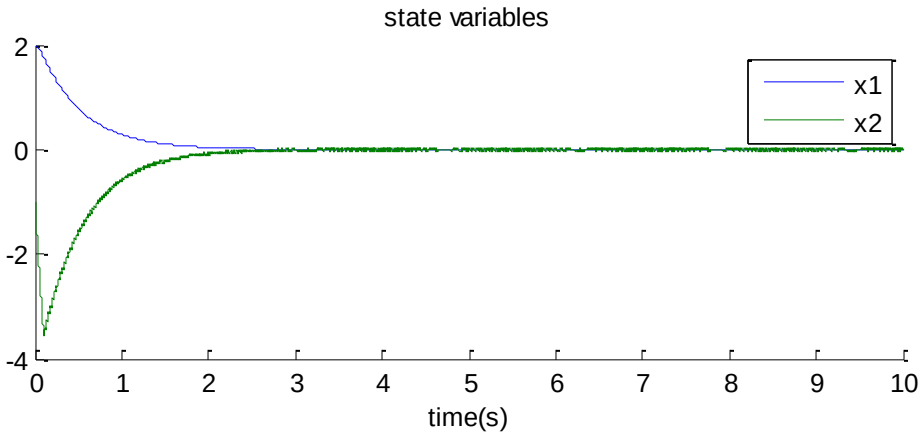

Figure 3.4: State variables of Example 1

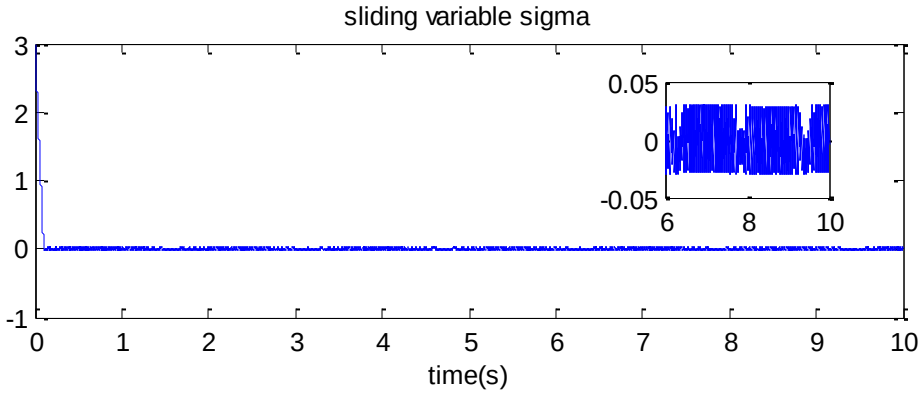

Figure 3.5: Sliding variable tracking of Example 1

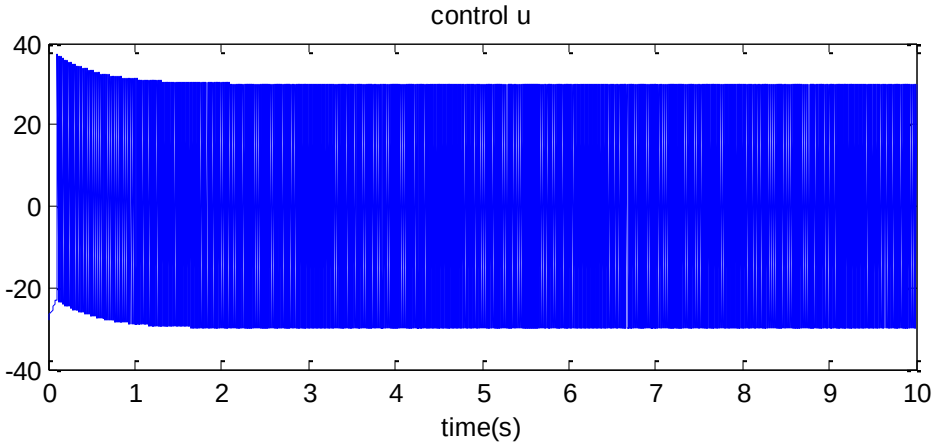

Figure 3.6: Control *u* of Example 1 ($\rho = 30$)

State variables converge to 0 in finite time for both simulations. The oscillations in Figures 3.2 and 3.5 clearly show the chattering that appears in the control system. Comparing the Figures 3.2 and 3.5, the sliding variable converges to 0 but retains some oscillation, and the oscillation becomes larger when the controller gain is overestimated. The high frequency switching control would produce a chattering motion in output. The chattering effect prevents the sliding variable from converging to 0 exactly; in addition, a high frequency switching control is not acceptable for actual components. The control might cause serious damage to the actual material if it is applied. The following section introduces the chattering attenuation procedure.

3.1.1. Chattering Attenuation using a Sigmoid Function

In this section a sigmoid function is introduced as a response to the need to attenuate chattering.

The sigmoid function is an approximation of a sign function. That is introduced as:

$$sign(\sigma) \approx \frac{\sigma}{|\sigma| + \varepsilon}, \quad \varepsilon \; is \; a \; very \; small \; numb\text{er} \tag{3.21}$$

Eliminating the sign function in control *u* using Equation (3.21), discontinuous control *u* becomes continuous. However, robustness of control and accuracy are lost.

Example 2:

In this example, we simulate Example 1 with a sigmoid function instead of a sign function.

Consider System (3.1) with given parameters as follows:

$$\begin{cases} \dot{x_1} = x_2 & x_1(0) = 2 \\ \dot{x_2} = u + f(t) & x_2(0) = -1 \end{cases}, \qquad f(t) = sin2t$$

The sliding variable is selected as:

$$\sigma = x_2 + 2x_1$$

The traditional sliding mode control with sigmoid function is designed as follows:

$$u = -2x_2 - \rho \cdot \frac{\sigma}{|\sigma| + \varepsilon}, \qquad \rho > 1 = |sin2t|, \qquad \varepsilon = 0.1$$

Assume the controller gain $\rho = 5$, and time increment is 10^{-4}.

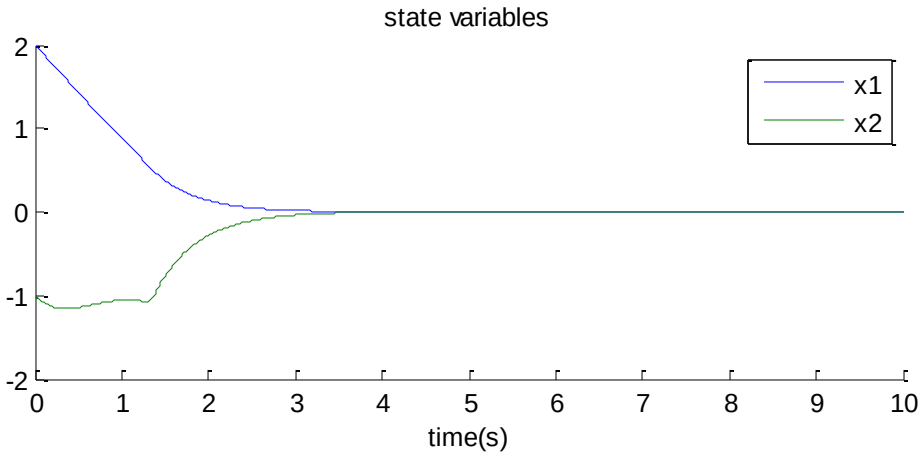

Figure 3.7: State variables versus time(s)

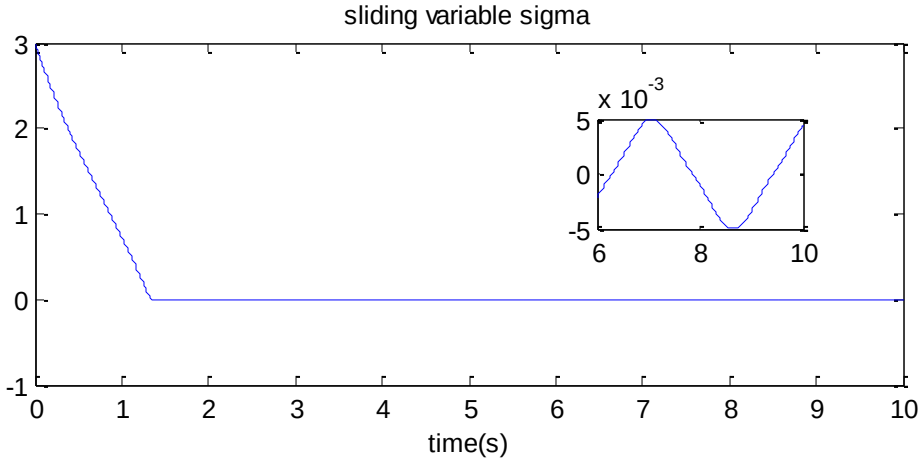

Figure 3.8: Sliding variable versus time(s)

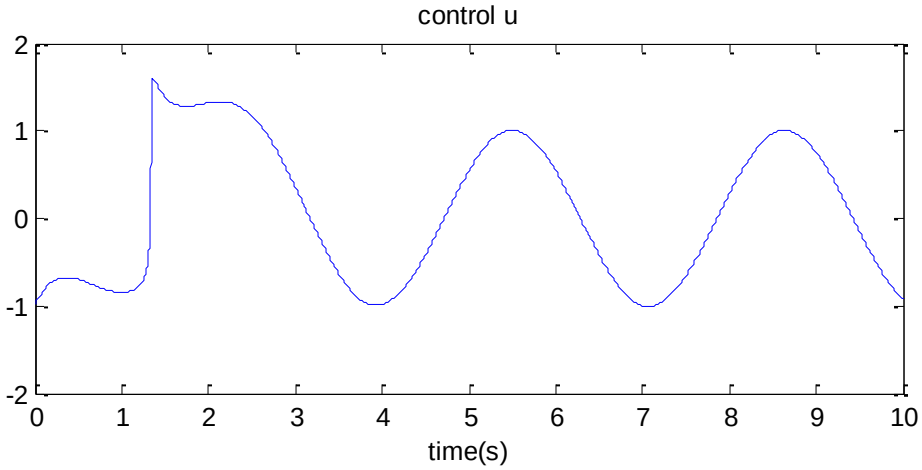

Figure 3.9: Control u versus time(s)

In looking at the results, the sigmoid function succeeds in eliminating the chattering, but the sliding variable oscillates. It is obvious that the sigmoid function results in a loss of accuracy.

3.1.2. Chattering Attenuation: Asymptotic Sliding Mode

In this section, chattering is attenuated in the design of a derivative of control by means of an asymptotic sliding variable. Consider System (3.1) again, and keep in mind that the sliding variable given in Equation (3.4) converges to 0 in finite time, while state variables x_1, x_2 converge to 0 asymptotically in finite time in the presence of the bounded disturbance. In addition to $|f(x_1, x_2, t)| \leq L > 0$, it is necessary to satisfy the following condition.

$$\left|\dot{f}(x_1, x_2, t)\right| \leq \bar{L} > 0 \tag{3.22}$$

An auxiliary sliding variable *S* is introduced as follows:

$$S = \dot{\sigma} + \bar{c}\sigma, \qquad \bar{c} > 0 \tag{3.23}$$

The control *u* exists in this auxiliary sliding variable *S*, thereby driving *S* to 0 in finite time and keeping the auxiliary sliding variable *S* at 0 thereafter. The ideal sliding mode occurs in the sliding surface of *S=0*. Therefore, the sliding surface of *S* is expressed as follows:

$$S = \dot{\sigma} + \bar{c}\sigma = 0 \tag{3.24}$$

The sliding variable σ and state variables x_1, x_2 converge to 0 as time increases in the presence of the bounded disturbance. Combining Inequalities (3.9) and (3.17), the following expression is obtained:

$$S\dot{S} \leq -\frac{\alpha}{\sqrt{2}}|S| \tag{3.25}$$

where $S\dot{S}$ is expressed as:

$$S\dot{S} = S(\ddot{\sigma} + \bar{c}\dot{\sigma}) \tag{3.26}$$

$$= \mathrm{S}[\dot{u} + \dot{f}(x_1, x_2, t) + (c + \bar{c})\{u + f(x_1, x_2, t)\} + c\bar{c}x_2]$$

Now assume the derivative of control *u* is:

$$\dot{u} = -(c + \bar{c})u - c\bar{c}x_2 - \rho \cdot sign(S), \qquad \rho > 0 \tag{3.27}$$

the following inequality is obtained:

$$S\dot{S} = \mathrm{S}[\dot{u} + \dot{f}(x_1, x_2, t) + (c + \bar{c})\{u + f(x_1, x_2, t)\} + c\bar{c}x_2] \tag{3.28}$$

$$\leq |S|[-\rho + \bar{L} + (c + \bar{c})L]$$

Applying the same procedure as shown in Equation (3.18), the following expression is obtained:

$$S\dot{S} \leq |S|[-\rho + \bar{L} + (c + \bar{c})L] = -\frac{\alpha}{\sqrt{2}}|S| \tag{3.29}$$

Then the controller gain ρ is obtained.

$$\rho = \bar{L} + (c + \bar{c})L + \frac{\alpha}{\sqrt{2}} \tag{3.30}$$

Finally the control *u* is expressed as:

$$\dot{u} = -(c + \bar{c})u - c\bar{c}x_2 - \rho \cdot sign(S), \qquad \rho = \bar{L} + (c + \bar{c})L + \frac{\alpha}{\sqrt{2}} \tag{3.31}$$

Example 3:

In this example, we design a control for the system shown in Example 1 to attenuate chattering using an auxiliary sliding variable. Consider System (3.1) with given parameters as follows:

$$\begin{cases} \dot{x_1} = x_2 & x_1(0) = 2 \\ \dot{x_2} = u + f(t) & x_2(0) = -1 \end{cases}, \qquad f(t) = sin2t$$

The sliding variable is selected as:

$$\sigma = x_2 + 2x_1$$

The auxiliary sliding variable is chosen as follows:

$$S = \dot{\sigma} + 2\sigma$$

The traditional sliding mode control is designed as follows:

$$\dot{u} = -4u - 4x_2 - \rho \cdot sign(S), \qquad \rho > 6 = |\dot{sin}2t| + 4|sin2t|$$

Assume the controller gain $\rho = 10$, and time increment is 10^{-4}.

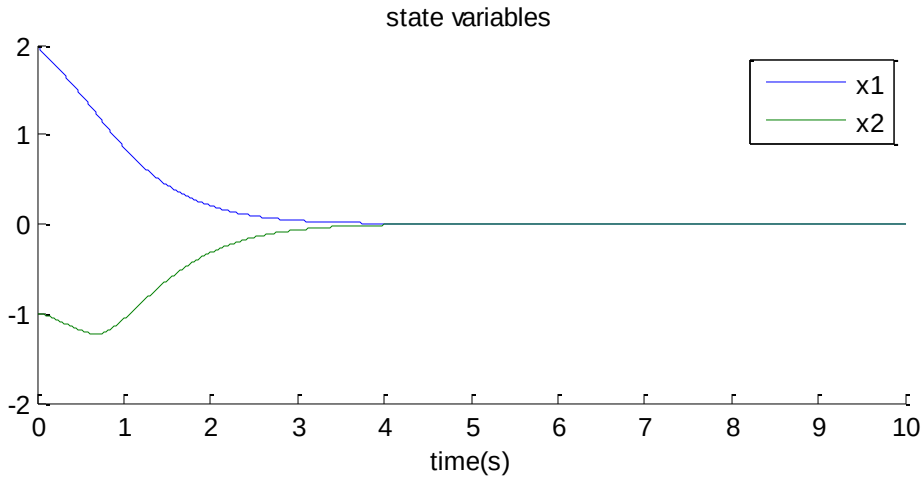

Figure 3.10: State variables versus time

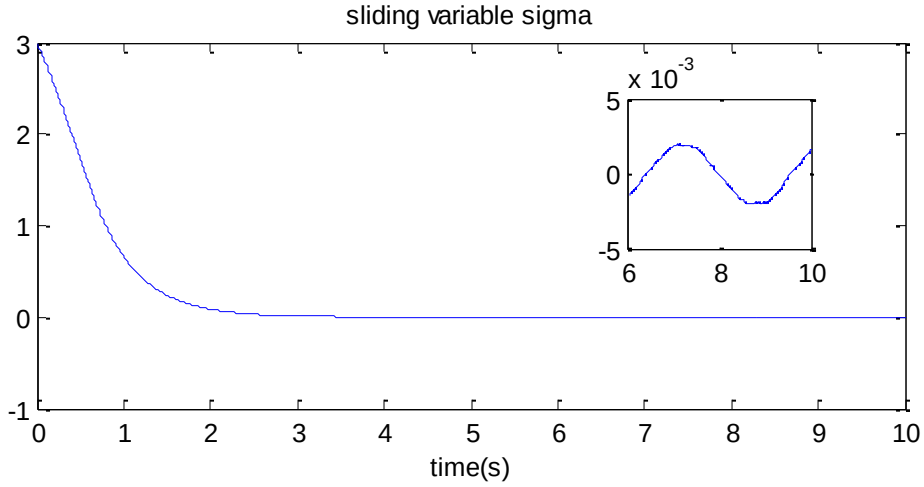

Figure 3.11: Sliding variable versus time

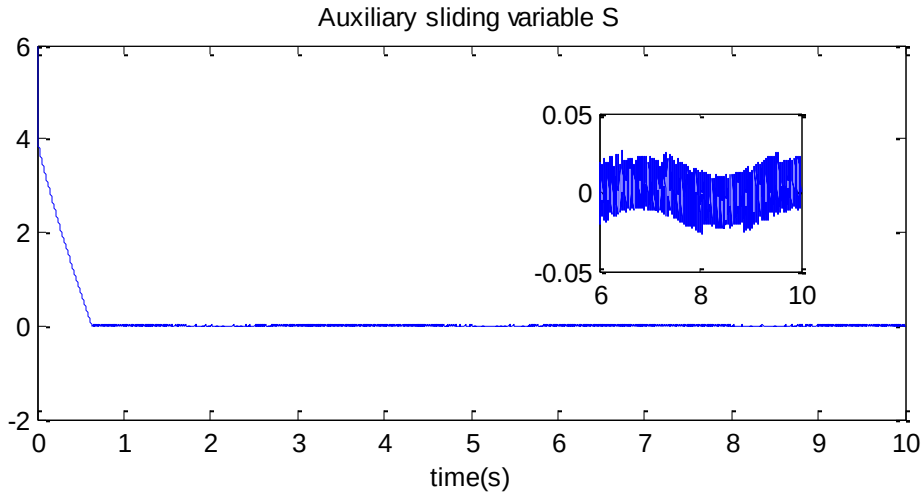

Figure 3.12: Auxiliary sliding variable versus time(s)

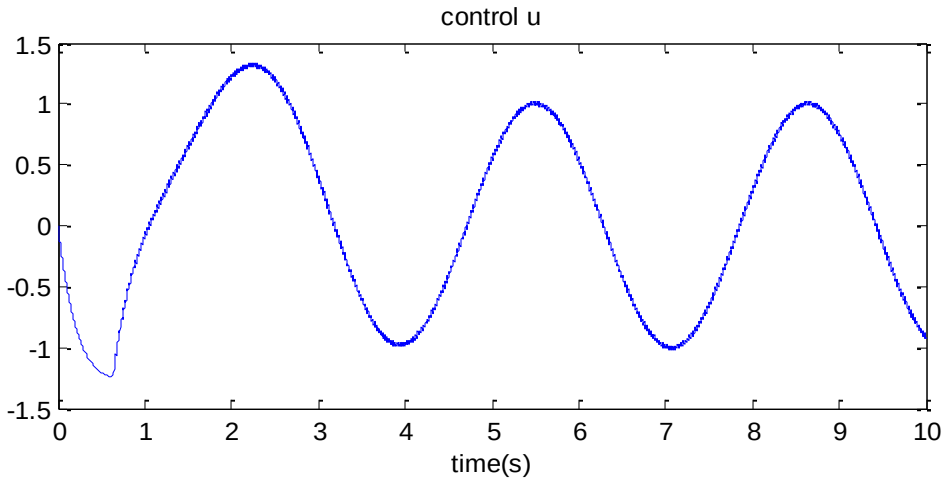

Figure 3.13: Control u versus time(s)

When the sliding variable is compared to the sigmoid function, the asymptotic sliding mode is more accurate. The control function becomes continuous.

3.2 Higher-Order Sliding Mode Control and Second-Order Sliding Mode Control

In the previous section, the concept of the sliding mode control has been introduced. The control u is obtained in Equation (3.20), thereby driving sliding variable σ for System (3.1) to 0 in finite time and keeping the sliding variable at 0 thereafter in the presence of the bounded disturbance. The higher-order sliding mode control drives the sliding variable and the r-times derivative of the sliding variable of a system to 0 in finite time and keeps them at 0 thereafter in the presence of a disturbance. Only the following condition is satisfied:

$$\sigma = \dot{\sigma} = \cdots = \sigma^{(r-1)} = 0, \qquad \text{in finite time.} \tag{3.32}$$

An r-th order sliding mode control exists in Equation (3.32). Then the r-th derivative of the sliding variable is defined as:

$$\sigma^{(r)} = \varphi + gu, \qquad |\varphi| \leq L, \qquad g \in [K_m, K_M] \tag{3.33}$$

The control function u that drives $\sigma, \dot{\sigma}, \cdots, \sigma^{(r-1)}$ in System (3.33) to zero in finite time and keeps them there is called the higher-order sliding mode control (HOSM). Advantages in using the higher-order sliding mode include the possibility for continuity, the capacity to obtain observable chattering attenuation, the ability to control an arbitrary higher-order system, and the enhanced accuracy: $|\sigma| \sim \tau^r$ where τ is defined as time increment. A higher-order sliding mode for which the relative degree is 2 is called a second-order sliding mode. Fundamentals of the second-order sliding mode control and the super-twisting control are introduced in the following subsections.

3.2.1. Fundamentals of Second-order Sliding Mode Control

Consider (3.33) for r=2:

$$\sigma^{(2)} = \varphi + gu, \tag{3.34}$$

The following conditions for Equation (3.34) are assumed to be met:

$$0 < K_m \leq \frac{\partial}{\partial u}\ddot{\sigma} \leq K_M, \qquad |\ddot{\sigma}|_{u=0} \leq C \tag{3.35}$$

where $K_m, K_M \; and \; C$ are certain positive constants, where u is a second-order sliding mode control, and where σ is a sliding variable. Then Equation (3.35) can be rewritten in terms of differential inclusions:

$$\ddot{\sigma} \in [-C, C] + [K_m, \; K_M]u \tag{3.36}$$

Second-order sliding mode controls are considered as a control which drives the sliding variable and its first derivative to 0 in finite time and keeps them at 0 thereafter in the

presence of the bounded disturbance. As a result, the second-order sliding mode control is robust in cases where disturbances are bounded, and the size of the boundary layer of the sliding manifold is $|\sigma| \sim \tau^2$.

3.2.2. Super-twisting Control (STW)

A super-twisting control is a continuous second-order sliding mode control. This approach is effective for relative degree 1. The advantage of this control technique is that it eliminates chattering. In other words, a super-twisting control stabilizes the sliding variables robustly at 0 in finite time for any bounded disturbance.

The sliding variable dynamics for a super-twisting control is given to be as follows:

$$\dot{\sigma} = \varphi + gu \tag{3.37}$$

where $|\dot{\varphi}| \leq C,\ 0 \leq K_m \leq g \leq K_M$.

For the sliding variable dynamics given in Equation (3.37), the super-twisting control is introduced as:

$$\begin{cases} u = -c|\sigma|^{\frac{1}{2}} sign(\sigma) + \omega \\ \dot{\omega} = -b \cdot sign(\sigma) \end{cases} \tag{3.38}$$

where

$$c = 1.5\sqrt{C}, \qquad b = 1.1C, \qquad |\dot{\varphi}| \leq C \tag{3.39}$$

This super-twisting control creates the compensated dynamics of sliding variables as follows:

$$\dot{\sigma} + \ c|\sigma|^{\frac{1}{2}} sign(\sigma) + b \int sign(\sigma)\, dt = \varphi \tag{3.40}$$

In sliding mode, $b\int sign(\sigma)\,dt$ is equal to φ. In order to achieve asymptotic convergence of the state variables, the super-twisting control drives both sigma and the first derivative of sigma to zero in finite time and keeps them at 0 thereafter.

Example 4:

In this example, we design a super-twisting control for the system shown in Example 1. The objective is to design a robust and continuous control for the system. Consider System (3.1) with given parameters as follows:

$$\begin{cases} \dot{x_1} = x_2 & x_1(0) = 2 \\ \dot{x_2} = u + f(t) & x_2(0) = -1 \end{cases}, \qquad f(t) = sin2t$$

The sliding variable is selected as:

$$\sigma = x_2 + 2x_1$$

The sliding variable dynamics is derived as:

$$\dot{\sigma} = 2x_2 + f(t) + u$$

The super-twisting control is designed as follows:

$$\begin{cases} u = -2x_2 - c|\sigma|^{\frac{1}{2}} sign(\sigma) + \omega \\ \dot{\omega} = -b \cdot sign(\sigma) \end{cases}, \qquad c = 1.5\sqrt{C}, \qquad b = 1.1C,$$

$$C = \left|f(\dot{t})\right| = \left|s\dot{\imath}n2t\right| \rightarrow C = 2$$

The time increment of this simulation is 10^{-4}.

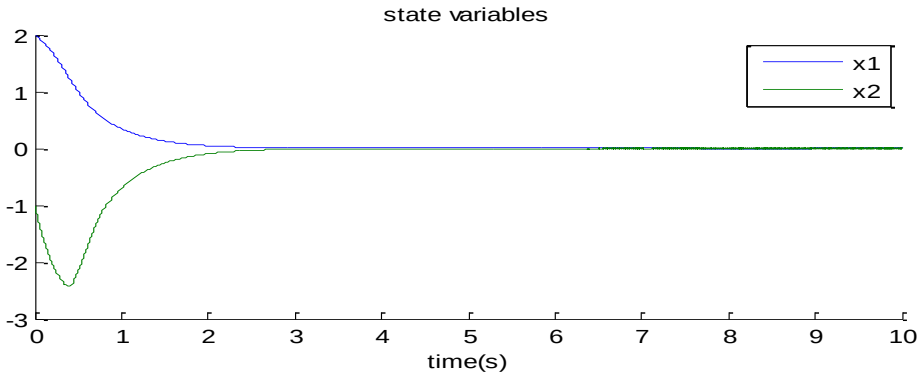

Figure 3.14: State variables versus time with STW

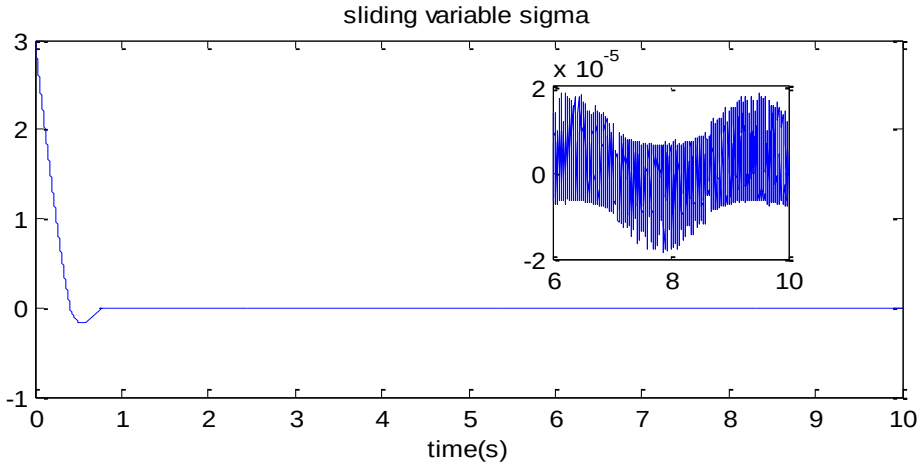

Figure 3.15: Sliding variable versus time(s) with STW

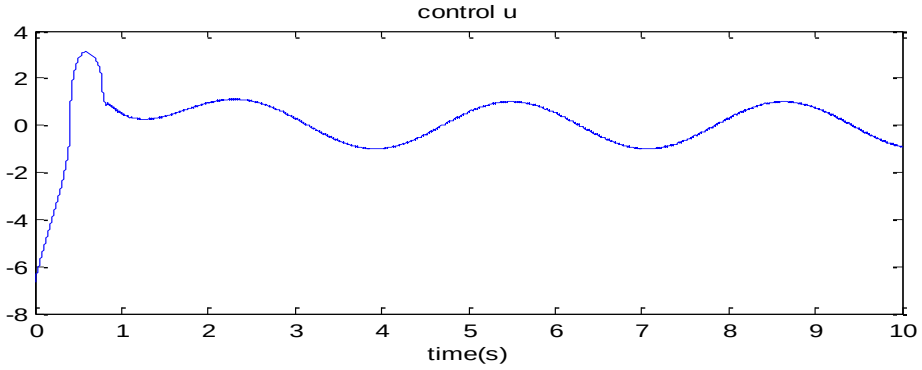

Figure 3.16: Control *u* versus time(s)

Comparing the results of this example and the results of traditional sliding mode control (Example 1), the super-twisting control function is continuous and the sliding variable is less chattering.

3.3 Sliding Mode Observer/Differentiator

In previous sections, state variables are assumed as measurable. But, in some cases, only x_1 is measurable and x_2 is estimated. In this section, the state variables are estimated using sliding mode observers. The traditional sliding mode observer and the super-twisting observer are the two types of the sliding mode observer. This section introduces a sliding mode observer using System (3.1).

3.3.1. Traditional Sliding Mode Observer Design

Consider System (3.1),

$$\begin{cases} \dot{x_1} = x_2 & x_1(0) = x_{10} \\ \dot{x_2} = u + f(x_1, x_2, t) & x_2(0) = x_{20} \end{cases}$$

Assume state variable x_1 is measurable, x_2 is not measurable, and disturbance $f(x_1, x_2, t)$ is bounded. The first step in the design of a sliding mode control is to design a sliding variable. In the beginning of this chapter, a sliding mode control has been designed using sliding variable dynamics (3.4). However, the sliding variable dynamics always include the term x_2, which is a state variable Since x_2 is not measurable, x_2 must be estimated. To estimate x_2, let us assume:

$$\dot{\widehat{x_1}} = \nu \tag{3.41}$$

where $\widehat{x_1}$ is the estimated value of x_1 and where ν is an observer injection term. v is designed so that $\widehat{x_1}, \widehat{x_2} \rightarrow x_1, x_2$. Keep in mind that $\dot{\widehat{x_1}} = \widehat{x_2}$ since $\dot{x_1} = x_2$. The auxiliary sliding variable for the sliding mode observer is defined as:

$$z_1 = \widehat{x_1} - x_1 \tag{3.42}$$

Then the derivative of Equation (3.42) is derived:

$$\dot{z_1} = -x_2 + \nu \tag{3.43}$$

The choice of the injection term ν that drives $z_1 = \widehat{x_1} - x_1 \rightarrow 0$ in finite time is:

$$\nu = -\rho \cdot sign(z_1), \qquad \rho > |x_2| + \beta, \qquad \beta > 0 \tag{3.44}$$

Then the reachable condition is expressed as follows:

$$z_1 \dot{z_1} = z_1\big(-x_2 - \rho \cdot sign(z_1)\big) \leq |z_1|(|x_2| - \rho) \leq -\beta|z_1| \tag{3.45}$$

Equation (3.45) proves the finite time convergence of z_1. The reaching time is obtained as follows:

$$t_r \leq \frac{|z_1(0)|}{\beta} \tag{3.46}$$

This equation is obtained by deriving the dynamics of the sliding mode observer equation:

$$\dot{z_1} = -x_2 + \nu_{eq} = 0 \tag{3.47}$$

The concept of equivalent control is defined as the average effect of the high frequency switching control. Equivalent control is obtained by low-pass filtering of the high frequency switching term, i.e. $sign(x)$, of the control.

Equation (3.54) can be rewritten as:

$$x_2 = \nu_{eq}, \qquad t \geq t_r \tag{3.48}$$

Then the injection term ν_{eq} is estimated by low-pass filtering of ν.

$$\widehat{v_{eq}} = \frac{1}{\tau s + 1} v, \qquad \tau \text{ is a small positive constant.} \tag{3.49}$$

Then x_2 is estimated after reaching time t_r.

$$x_2 \approx \widehat{x_2} = \widehat{v_{eq}}, \qquad t \geq t_r \tag{3.50}$$

Example 5:

Using the system in Example 1,

$$\begin{cases} \dot{x_1} = x_2 & x_1(0) = 2 \\ \dot{x_2} = u + f(t) & x_2(0) = -1 \end{cases}, \qquad f(t) = sin2t$$

assume that x_2 should be estimated. In this example, using a sliding mode observer, estimate x_2, then drive the state variable to 0 in finite time in the presence of the bounded disturbance, using the traditional sliding mode control, $u = -2\widehat{x_2} - 5 \cdot sign(\sigma)$. The variable x_2 is estimated using the sliding mode observer (3.41), (3.44), (3.49) and (3.50) with $\rho = 10$ and the time increment $\tau = 10^{-5}$.

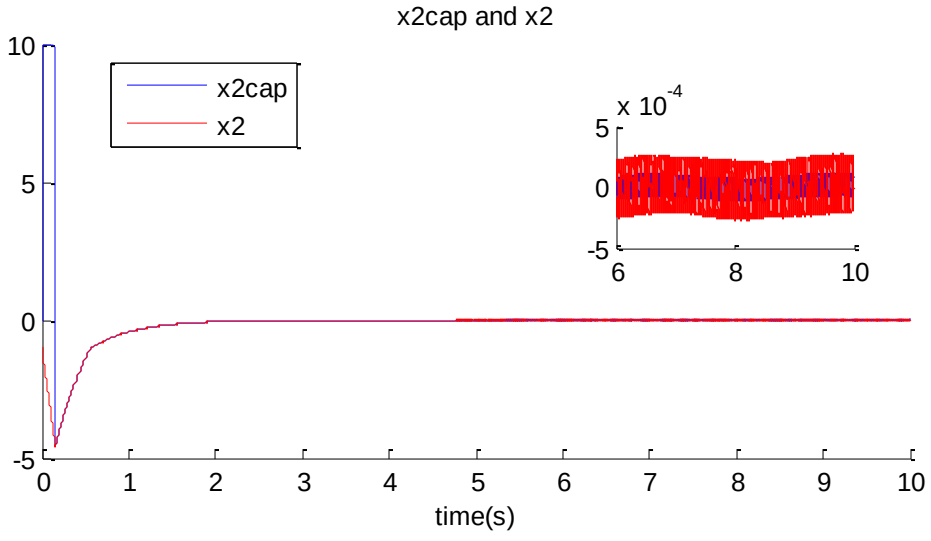

Figure 3.17: x_2 and estimated x_2 versus time

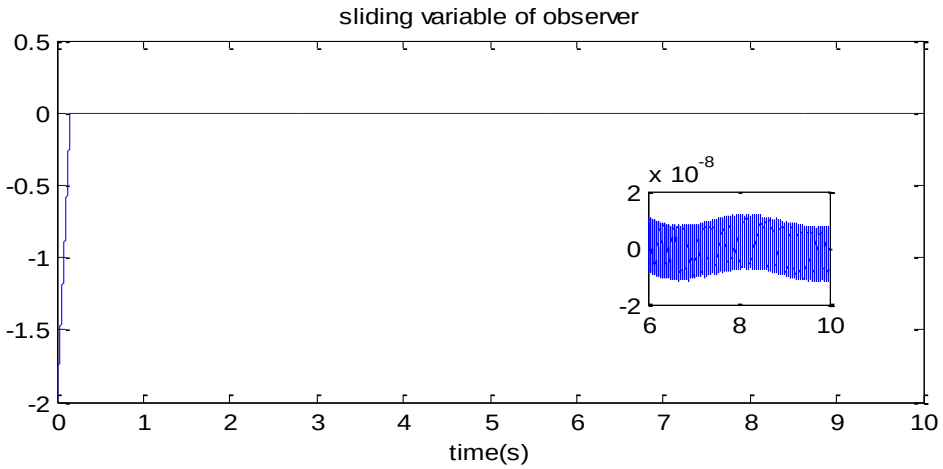

Figure 3.18: Sliding variable of observer versus time

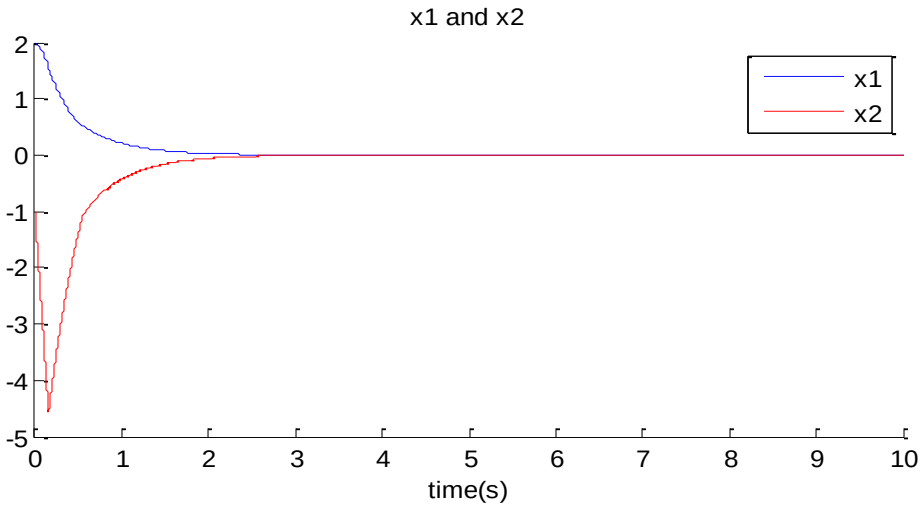

Figure 3.19: State variables x_1 and x_2 versus time

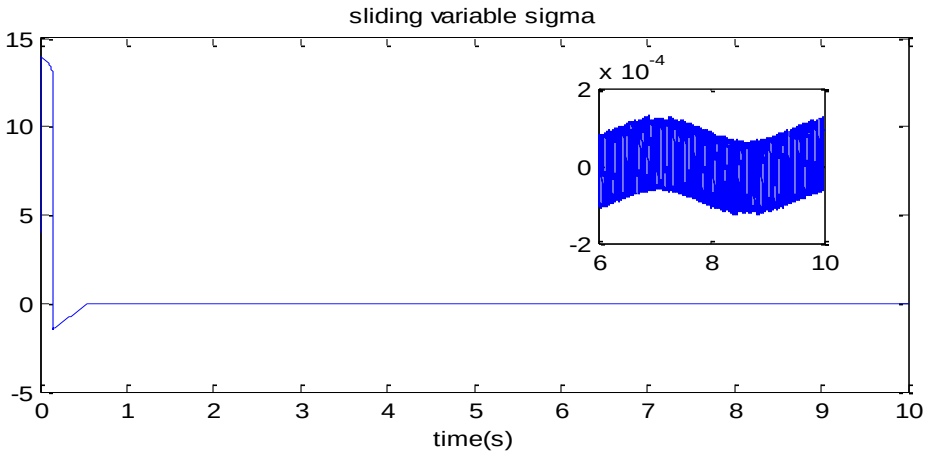

Figure 3.20: Sliding variable σ versus time

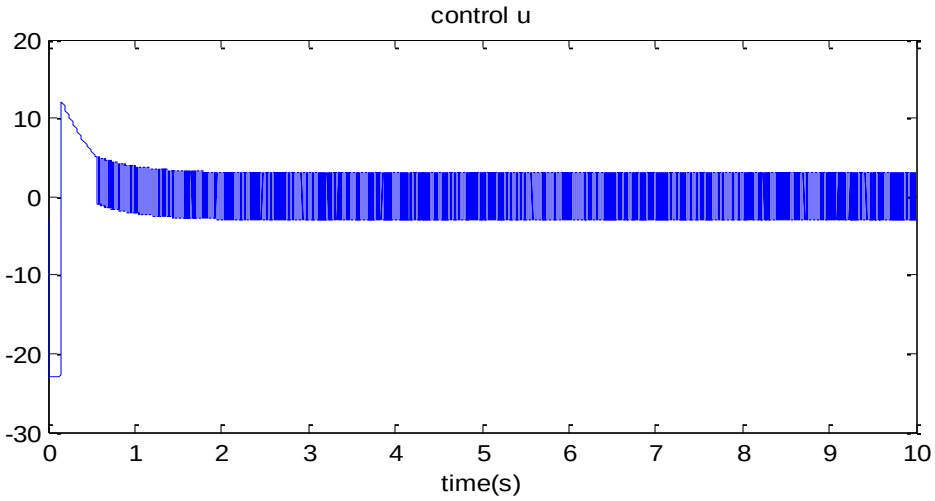

Figure 3.21: Control u versus time

Figure 3.17 shows clearly that the state variable x_2 is estimated by means of the sliding mode observer. Then the sliding variable is driven to 0 in finite time and keeps 0 in the presence of the bounded disturbance, by means of the control which is designed with the estimated state variable.

3.3.2. Super-twisting Observer/Differentiator

In this section, estimate the state variables for the system by using super-twisting observer. The system is given as:

$$\begin{cases} \dot{x_1} = x_2 & x_1(0) = x_{10} \\ \dot{x_2} = u + f(x_1, x_2, t) & x_2(0) = x_{20} \end{cases}$$

Using a super-twisting control law, we design ν to drive the z_1 dynamics $z_1 = \widehat{x_1} - x_1$ which is given in Equation (3.43) to 0 in finite time. As presented in Section (3.2.3), the super-twisting control law is defined as:

$$\nu = -c|z_1|^{\frac{1}{2}} sign(z_1) - \omega, \tag{3.51}$$

$$\dot{\omega} = bsign(z_1)$$

Let us assume that the gain value for the sliding mode observer is as follow:

$$c = 1.5\sqrt{C}, \qquad b = 1.1C, \qquad C > |\dot{x_2}|, \tag{3.52}$$

The super-twisting control law is a continuous function as explained in Section (3.2.3); the Equation (3.51) estimates x_2 accurately. Therefore,

$$x_2 \approx \widehat{x_2} = \nu, \qquad t \geq t_r \tag{3.53}$$

Then, z_1 converges to 0 in finite time, and $\widehat{x_1} \rightarrow x_1$.

Example 6:

Consider Example 1,

$$\begin{cases} \dot{x_1} = x_2 & x_1(0) = 2 \\ \dot{x_2} = u + f(t) & x_2(0) = -1 \end{cases}, \qquad f(t) = sin2t$$

and assume x_2 should be estimated. In this example, using the super-twisting sliding mode observer, estimate x_2, then drive the state variable to 0 in finite time in the presence of the bounded disturbance, using the traditional sliding mode control, $u = -2\widehat{x_2} - 5 \cdot sign(\sigma)$ and the super-twisting observer $\nu = -c|z_1|^{\frac{1}{2}}sign(z_1) - b\int sign(z_1)dt$, where $c = 1.5\sqrt{C},\ b = 1.1C,\ C = 5$. The time increment is 10^{-5}.

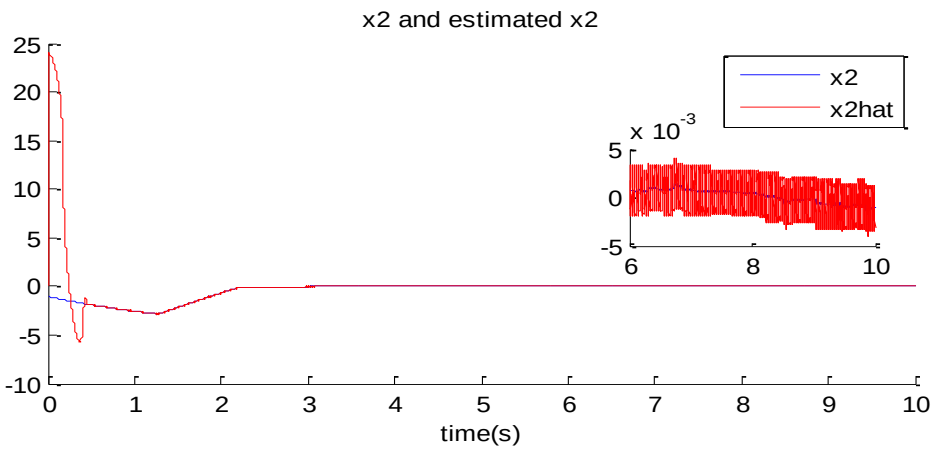

Figure 3.22: x_2 and estimated x_2 versus time

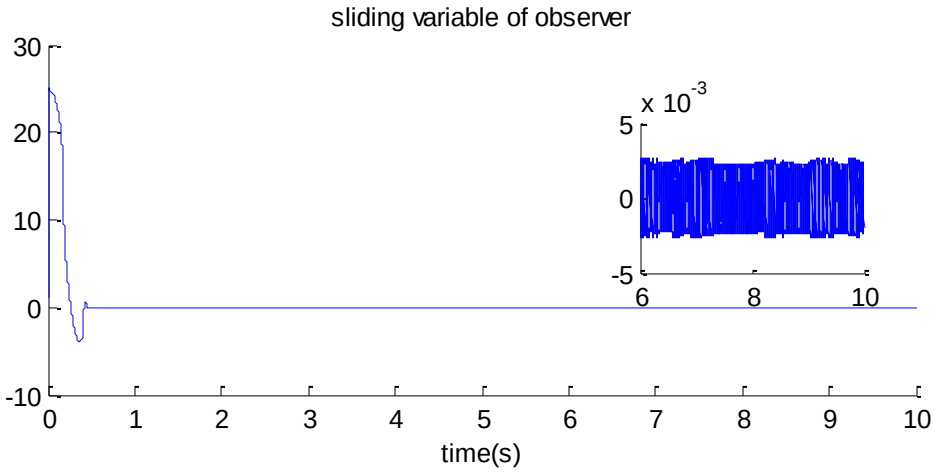

Figure 3.23: Sliding variable for observer

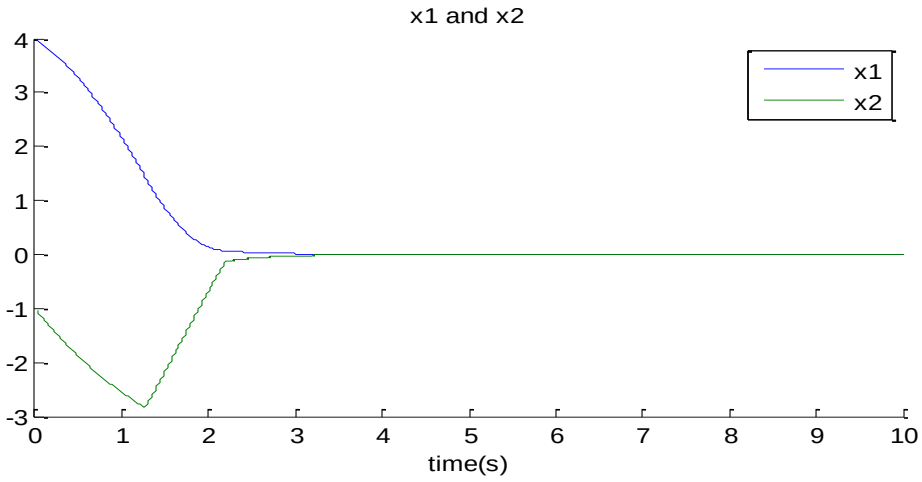

Figure 3.24: State variables versus time

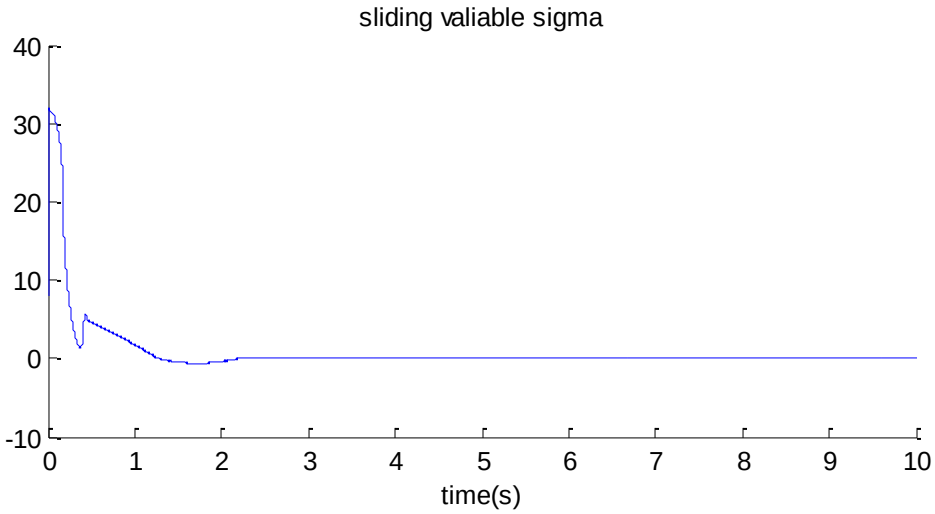

Figure 3.25: Sliding variable σ

The sliding variable for the observer is defined as the error between the actual x_2 and the estimated x_2. The super-twisting observer succeeds in estimating the state variable x_2 accurately in finite time.

3.4 Adaptive Sliding Mode Control

The previous sections have discussed the sliding mode control design of a certain system with bounded disturbances where those boundaries are known. In this section, a sliding mode control design used when the boundary of the disturbances in a system is unknown is discussed. Actually, it is possible to design a sliding mode control with a large controller gain; however, overestimating the sliding mode controller gain results in chattering, which, as we have seen, causes loss of accuracy and possible damage to components of the system. Gain adaptation is one way to fix overestimation by adjusting the controller gain dynamically. When the sliding mode occurs, a magnitude of the disturbance is recovered via estimating equivalent control. The equation of gain adaptation is designed for each system.

Consider a System

$$\begin{cases} \dot{x_1} = x_2 \\ \dot{x_2} = u + f(x_1, x_2, t) \end{cases} \tag{3.54}$$

where x_1, x_2 are state variables. $f(x_1, x_2, t)$ is the disturbance bounded by a certain positive constant *D*, but *D* is unknown.

3.4.1. Adaptive Traditional Sliding Mode Control (ATSMC)

In this section, the concept and design process of gain adaptation for a traditional sliding mode control are introduced.

Two adaptive sliding mode controls have been proposed in Lee and Utkin [6] and Huang et al [5]. The difference between these adaptive sliding mode controls is that the first does not require knowledge of the boundary of the uncertainties/disturbances and increases the controller gain until the sliding mode is established; the sliding variable becomes a very small number. In contrast, the second one requires knowledge of the boundary of the uncertainties/disturbances and uses the equivalent control concept in order both to evaluate and to minimize the controller gain. The same objective, dynamic gain adaptation in order to counteract disturbances and uncertainties, is claimed by both types of controls.

The first gain adaptation algorithm is introduced as follows [5]:

The nonlinear uncertain system is defined as [5]:

$$\dot{x} = f(x) + g(x)u \tag{3.55}$$

with $x \in \mathbb{R}^n$ the state vector and $u \in \mathbb{R}$ the control. Functions $f(x)$ and $g(x)$ are uncertain functions and bounded. The control objective is to drive the sliding variable to 0. The sliding variable is defined as [5]:

$$\dot{\sigma} = \Psi(x,t) + \Gamma(x,t)u, \qquad \sigma \in \mathbb{R} \tag{3.56}$$

where $\Psi(x,t)$ and $\Gamma(x,t)$ are bounded. The boundaries are not known.

The System (3.55) with the sliding variable dynamics (3.56) is controlled by [5]:

$$u = -K(t) \cdot sign(\sigma(x,t)) \tag{3.57}$$

with the gain adaptation $K(t)$ given by [5]:

$$\dot{K} = \overline{K} \cdot |\sigma(x,t)| \tag{3.58}$$

where $\overline{K} > 0$ and $K(0) > 0$; then the state variable converges to 0 in finite time in the presence of the bounded uncertainties/disturbances.

The main advantage of this approach is that it does not require knowledge of the boundary of the uncertainties/disturbances. However, there is a great risk of the controller gain being overestimated by the gain adaptation (3.58); as a result, chattering is caused.

The Second gain adaptation algorithm is introduced following the work [6]:

The given System (3.55) with the sliding variable dynamics (3.56) is controlled by [6]:

$$u = -K(t) \cdot sign(\sigma(x,t)) \tag{3.59}$$

with the gain adaptation $K(t)$ given by [6]:

$$K(t) = \bar{K} \cdot |\eta| + \alpha \tag{3.60}$$

where $\bar{K} \geq \frac{\Psi}{\Gamma}$, $\alpha > 0$ and η is the average of $sign(\sigma(x,t))$ obtained through a low-pass filter. The sliding mode is established in finite time.

The main advantage of this adaptive sliding mode control is the adjustment of the control given by using the low-pass filter, which results in a decrease in chattering. However, the gain adaptation does require knowledge of the boundary of the uncertainties/disturbances.

Two adaptive sliding mode control laws with non-overestimating gains in systems with bounded disturbances with unknown bounds

Two interesting gain adaptations for traditional sliding mode control are proposed in Plestan, Shtessel et al [7][8]. The two algorithms of the adaptive sliding mode control allow establishment of the sliding mode via the sliding mode control with the gain adaptation without a priori knowledge of uncertainties/disturbances bounds, as long as the adaptive-gain values are not overestimated. One of these adaptive sliding mode controls is established using two adaptive sliding mode control theorems proposed in Lee and Utkin, and Huang et al, but requires estimation of parameters for the gain adaptation. The second type of gain adaption is simpler to design due to fewer parameters but actually performs just as well as the first.

First Plestan and Shtessel adaptive sliding mode control law

Consider the control as follows [8]:

$$u = -K(t) \cdot sign(\sigma(x,t)) \tag{3.61}$$

with the gain $K(t)$ defined as follows [8]:

$$\dot{K} = \bar{K}_1 \cdot |\sigma(x,t)| \quad \text{when } |\sigma(x,t)| \neq 0 \tag{3.62}$$

$$K(t) = \bar{K}_2 \cdot |\eta| + \bar{K}_3 \text{ when } |\sigma(x,t)| = 0$$

$$\tau\dot{\eta} + \eta = sign(\sigma(x,t))$$

with $\bar{K}_1$, $\bar{K}_3$, and $K(0)$ as positive constants, where η is the low-pass filtering output of $sign(\sigma(x,t))$, and where $\bar{K}_2$ is $K(t^*)$. t^* is the largest time value before $|\sigma(x,t)| = 0$.

The adaptive sliding mode control law (3.61)-(3.62) works as follows:

- The gain $K(t)$ increases enough to counteract the bounded disturbances/uncertainties with unknown bounds in System (3.55) until the sliding mode occurs, due to the adaptation law (3.62).
- As the sliding mode starts, $K(t)$ follows the gain adaptation law (3.62). The gain $K(t)$ decreases to adjust the gain with respect to the current uncertainties/disturbances.
- When the sliding mode is destroyed by means of the gain adaptation, the gain $K(t)$ increases until the sliding mode occurs again.

Theorem of gain adaptation of traditional sliding mode control (3.61)-(3.62)

Given the nonlinear uncertain System (3.55) with the sliding variable $\sigma(x_1, x_2, t)$ dynamics (3.56) controlled by (3.61) with the adaptation law (3.62) with $\bar{K} > 0$ and

$K(0) > 0$, then there exists a finite time $t_F \geq 0$ so that a sliding mode is established in the system for all $t \geq t_F$; in other words, $\sigma(x_1, x_2, t) = 0$ for $t \geq t_F$ [8].

The first adaptive sliding mode control algorithm (3.61)-(3.62) is not ready for practical implementation. It is impossible to reach the objective $\sigma(x, t) = 0$ due to sampled computation, noisy measurements, or other non-idealities. The adaptive sliding mode control is modified as:

$$u = -K(t) \cdot sign(\sigma(x, t)) \tag{3.63}$$

with the gain $K(t)$ defined as follows: [8]

$$\begin{aligned} \dot{K} &= \bar{K}_1 \cdot |\sigma(x, t)| \quad \text{when } |\sigma(x, t)| > \epsilon \\ K(t) &= \bar{K}_2 \cdot |\eta| + \bar{K}_3 \quad \text{when } |\sigma(x, t)| \leq \epsilon \end{aligned} \tag{3.64}$$

with $\bar{K}_1$, $\bar{K}_3$, and $K(0)$ as positive constants, where η is low-pass filtering output of $sign(\sigma(x, t))$, and where $\bar{K}_2$ is $K(t^*)$. t^* is the largest time value before $|\sigma(x, t)| \leq 0$.

Second Plestan and Shtessel adaptive sliding mode control law

The first adaptive sliding mode control law uses the concept of equivalent control, which introduces low-pass filter dynamics with the parameter τ. The parameter τ is not easy to tune [8]. The control introduced as the second adaptive sliding mode control does not estimate the boundary of disturbances/uncertainties.

Consider the following control [8]:

$$u = -K(t) \cdot sign(\sigma(x, t)) \tag{3.65}$$

with the gain $K(t)$ defined such that [8]:

$$\dot{K} = \begin{cases} \bar{K}|\sigma(x,t)|sign(|\sigma(x,t)| - \epsilon) & if\ K > \mu \\ \mu & if\ K \leq \mu \end{cases} \quad (3.66)$$

where *K(0)>0*, $\bar{K} > 0, \epsilon > 0\ and\ \mu > 0$. μ is a very small constant. The parameter μ is introduced in order to keep positive values for *K*.

When σ is a large value, $\dot{K}$ becomes large, thereby increasing *K* rapidly. Similarly, when $|\sigma|$ becomes smaller than the ϵ value, $\dot{K}$ is a negative, and therefore *K* decreases slowly. The gain adaptation function changes the sign, and the slope of *K* changes from positive to negative and vice-versa, on the boundary of $|\sigma| - \epsilon = 0$. When *K* is smaller than μ, *K* increases in the slope of μ.

Theorem of gain adaptation of traditional sliding mode control [8]

Given the nonlinear uncertain System (3.55) with the sliding variable $\sigma(x_1, x_2, t)$ dynamics (3.56) controlled by (3.65) with the adaptation law (3.66) with $\bar{K} > 0$ and $K(0) > 0$, then there exists a finite time $t_F \geq 0$ so that a sliding mode is established in the system for all $t \geq t_F$: in other words, $\sigma(x_1, x_2, t) < \delta$ for $t \geq t_F$, with $\delta = \sqrt{\epsilon^2 + \frac{\Psi_M^2}{\bar{K}\Gamma_m}}$.

Example 7

The challenge is to design a control without knowledge of the boundary of the disturbance. In this example, an adaptive traditional sliding mode control is designed without knowledge of the boundary of the disturbances. Consider the System (3.1) with given parameters as follows:

$$\begin{cases} \dot{x_1} = x_2 & x_1(0) = 2 \\ \dot{x_2} = u + f(t) & x_2(0) = -1 \end{cases}, \quad f(t) = sin2t$$

Assume the boundary of the disturbance is not known. The sliding variable is selected as:

$$\sigma = x_2 + 2x_1$$

The traditional sliding mode control is designed as follows:

$$u = -2x_2 - K \cdot sign(\sigma)$$

where *K* is defined as follows:

$$\dot{K} = \begin{cases} \bar{K}|\sigma(x,t)|sign(|\sigma(x,t)| - \epsilon) & if\ K > \mu \\ \mu & if\ K \leq \mu \end{cases}$$

where $\mu = 0.1$, $\epsilon = 0.1$, $\bar{K} = 5$. The time increment is 10^{-4}. As a result, the state variables and the sliding variable converge to 0 in finite time in the presence of the disturbance, and the controller gain decreases.

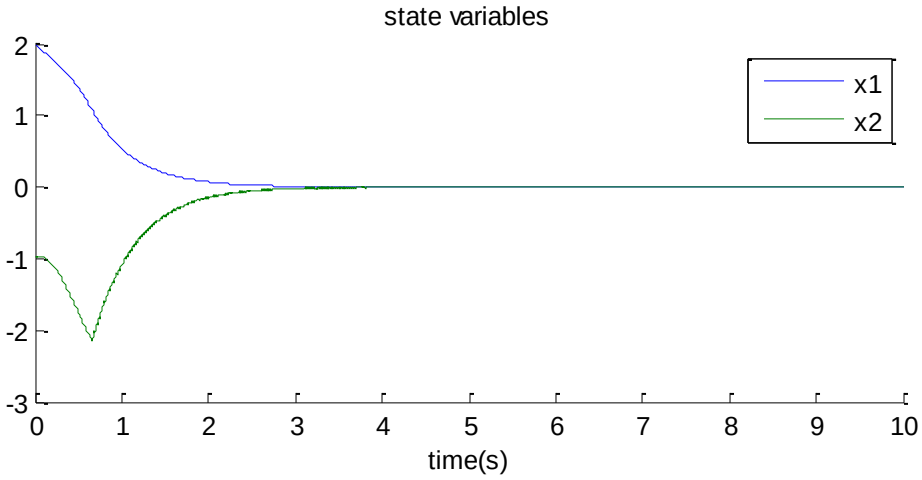

Figure 3.26: Depiction of state variables versus time using ATSMC

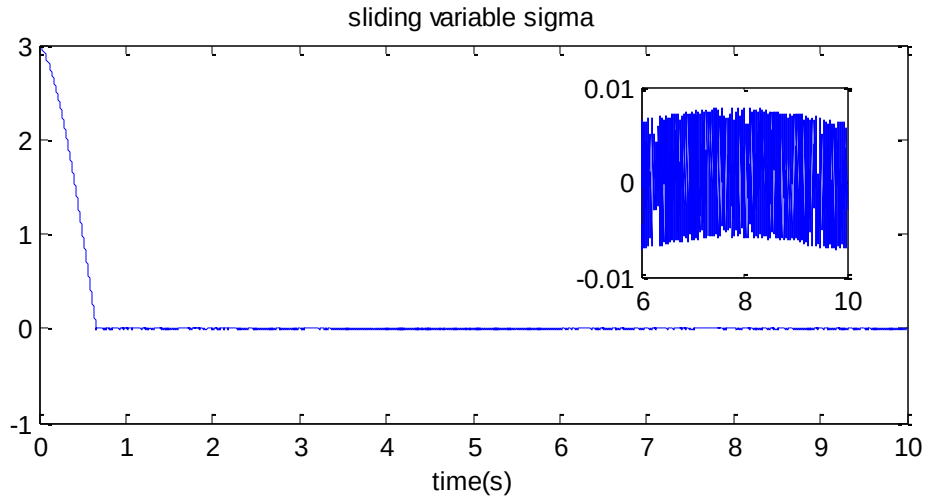

Figure 3.27: Plot of sliding variable versus time using ATSMC

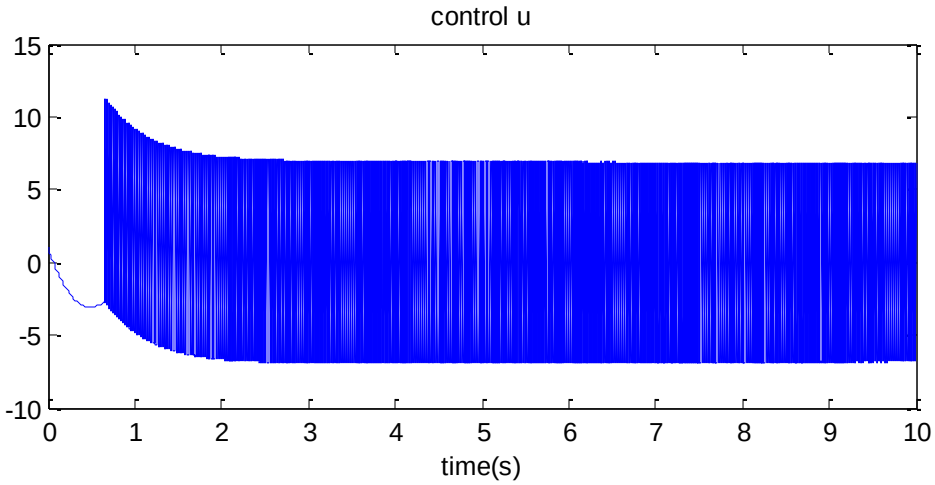

Figure 3.28: Control *u* versus time using ATSMC

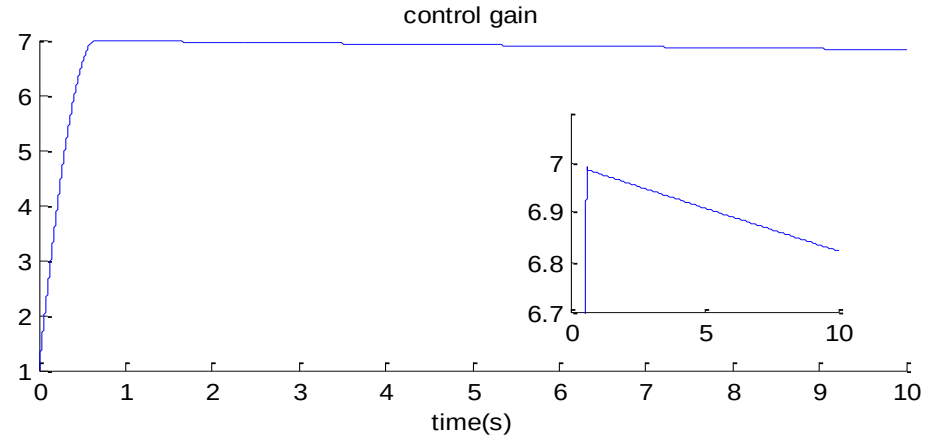

Figure 3.29: Controller gain versus time using ATSMC

The simulation results show that the adaptive traditional sliding mode control does not produce overestimation, and decreases the controller gain slowly. As a result, the adaptive sliding mode control is a robust control for the unknown bounded disturbance.

3.5 Summary

In this chapter, the concepts of the sliding mode control have been introduced. The control problem in the system with disturbances is reduced to stabilization of the sliding variable. The method of design of a sliding variable has been presented, along with a computation corresponding to the control function. In combination, the control function drives the sliding variable to 0 in finite time in the presence of a bounded disturbance. The concepts of higher-order sliding mode and second-order sliding mode control have been studied and applied. A particular second-order sliding mode control algorithm namely a super-twisting control that is used for second-order sliding mode observer has been discussed. A gain adaptation of a sliding mode control has been presented. The gain decreases slowly. The other adaptive-gain sliding mode control that provides faster gain-adaptation is proposed and tested in Chapter 4.

CHAPTER 4

SLIDING MODE CONTROL AND GAIN ADAPTATION DESIGN FOR A ROBOT MANIPULATOR

The fundamentals of sliding mode control and robot manipulator dynamics have been elucidated in previous chapters. In this chapter, the robot manipulator control system is designed using the gain adaptation of the sliding mode control. A review of the robot manipulator system dynamics has been conducted before considering the adaptive sliding mode control design. Robot manipulator dynamic equation is presented as a second order derivative. All the values in the robot manipulator dynamic equation are known or measurable, except for the boundary of the bounded disturbances and uncertainties and joint velocities. The robot manipulator is controlled via joint variables, and the commands are given as joint variables.

The goal of the adaptive sliding mode control for the robot manipulator is to drive the joint variables to the desired or command values in finite time and keep them thereafter in the presence of the bounded disturbances, without overestimation of controller gains. The following is the design procedure for the control system for the robot:

- Estimate joint velocities using a super-twisting observer.
- Design sliding variables of the robot manipulator control system for each control.
- Derive control u.
- Design a gain adaptation for each control.

4.1. Estimation of Joint Velocities using a Super-twisting Observer

In this section, the estimate for the i-th row of the joint velocity $\dot{q}$ is obtained using the super-twisting observer presented in Chapter 3. Henceforth, we derive the i-th row of the sliding variable for super-twisting observer z_i as follows:

$$z_i = \hat{q}_i - q_i \tag{4.1}$$

The derivative of the i-th row of the sliding variable z is a term of estimated value.

$$\dot{z}_i = \dot{\hat{q}}_i - \dot{q}_i \tag{4.2}$$

Therefore, the estimated value of the i-th row of the joint velocities $\dot{q}$ is expressed as:

$$\dot{\hat{q}}_i = -\alpha_i |z_i|^{\frac{1}{2}} sign(z_i) - \omega_i \tag{4.3}$$

$$\dot{\omega}_\iota = \beta_i sign(z_i)$$

where $\alpha_i = 1.5\sqrt{C_i}$, $\beta_i = 1.1C_i$, and $C_i \geq |\dot{q}_\iota|$. This observer drives $\dot{z}_i$ and z_i to 0 in finite time and keeps them at 0 thereafter in the presence of the bounded disturbance. Then, $\dot{\hat{q}}_i \to \dot{q}_i, \hat{q}_i \to q_i$ in finite time.

4.2. State Variable System for Robot Manipulator

The dynamic equation of robot manipulators is given as follows:

$$M(q)\ddot{q} + C(q,\dot{q})\dot{q} + \mathrm{G}(q) = \tau + \tau_d \tag{4.4}$$

$$q, \tau, \tau_d \in \mathbb{R}^n, M \in \mathbb{R}^{n\times n}, C \in \mathbb{R}^{n\times n}, G \in \mathbb{R}^n$$

Assume that the matrices M, C, and G are nominal values and known, while τ_d represents the bounded disturbances and uncertainties. Solving (4.4) for $\ddot{q}$, the following equation is obtained:

$$\ddot{q} = M(q)^{-1}\tau + M(q)^{-1}(\tau_d - C(q,\dot{q})\dot{q} - G(q)) \tag{4.5}$$

$$M(q)^{-1}\tau = u$$

$$M(q)^{-1}\tau_d = d(q,\dot{q},t)$$

$$M(q)^{-1}\big(-C(q,\dot{q})\dot{q} - G(q)\big) = f(q,\dot{q},t)$$

Assume the command trajectory is given as q_c. The tracking error is obtained as follows:

$$e = q_c - q \tag{4.6}$$

$$\dot{e} = \dot{q}_c - \dot{q}$$

$$\ddot{e} = \ddot{q}_c - \ddot{q}$$

$$e, q_c \in \mathbb{R}^n$$

The i-th row of the input-output tracking of the compensated error dynamic equation for the robot manipulator is given as,

$$\ddot{e}_i = \ddot{q_{ci}} - u_i - f_i(q,\dot{q},t) - d_i(q,\dot{q},t) \tag{4.7}$$

where $e_i = q_{ci} - q_i$, and where $d_i(q,\dot{q},t)$ is the i-th row of the bounded disturbance such as:

$$|d_i(q, \dot{q}, t)| \leq L_i \tag{4.8}$$

The objective of the control is to drive the joint position q to the command position q_c, which means the error is driven to 0 in finite time, and is kept at 0 thereafter in the presence of the bounded disturbance. In the following section, the design process of the adaptive traditional control is introduced.

4.3. Traditional Sliding Mode Control of Robot Manipulator

As presented in Chapter 2, the traditional sliding mode control is a first-order sliding mode control. Therefore, the sliding variables are selected such that they have relative degree one with respect to the control u. It is now necessary to design a sliding variable for the traditional sliding mode control of the robot manipulator. So $\sigma_i = \dot{e}_i + \lambda_i e_i$ and $s_i = \dot{\sigma}_i + \omega_i \sigma_i$ are selected as sliding variables for each simulation.

Let the i-th row of the sliding variables be:

$$\sigma_i = \dot{e}_i + \lambda_i e_i, \qquad \lambda > 0 \tag{4.9}$$

Then the derivative of the i-th row of the sliding variables is expressed as:

$$\dot{\sigma}_i = \ddot{e}_i + \lambda_i \dot{e}_i = \ddot{q_{c_i}} - \ddot{q}_i + \lambda_i(\dot{e}_i) \tag{4.10}$$

$$= \ddot{q_{c_i}} - f_i(q, \dot{q}, t) - d_i(q, \dot{q}, t) + \lambda_i(\dot{e}_i) - u_i$$

Therefore, using the Lyapunov function, the following inequality is derived:

$$\sigma_i \dot{\sigma}_i = \sigma_i(\ddot{q_{c_i}} - f_i(q, \dot{q}, t) - d_i(q, \dot{q}, t) + \lambda_i(\dot{e}_i) - u_i) \tag{4.11}$$

To provide stability and convergence to the system in finite time, Equation (4.11) should be negative at all times. Then the i-th row of control function u is designed as follows:

$$u_i = \ddot{q_{c_i}} - f_i(q, \dot{q}, t) + \lambda_i(\dot{e}_i) + K_i \cdot sign(\sigma_i), \tag{4.12}$$

$$K_i > L_i$$

The control u_i derived in Equation (4.12) is a high frequency switching function which causes chattering. It is necessary to design control u_i using an asymptotic sliding variable to eliminate chattering. The asymptotic sliding variable is described in Section (3.1.2).

The i-th row of the auxiliary sliding variable is introduced as:

$$s_i = \dot{\sigma}_i + \omega_i \sigma_i, \qquad \omega_i > 0 \tag{4.13}$$

The derivative of the i-th row of the asymptotic sliding variable is expressed as:

$$\begin{aligned} \dot{s}_i = \ddot{\sigma}_i + \omega_i \dot{\sigma}_i &= \dddot{e}_i + \lambda_i \ddot{e}_i + \omega_i (\ddot{e}_i + \lambda_i \dot{e}_i) = \dddot{e}_i + (\lambda_i + \omega_i)\ddot{e}_i + \omega_i \lambda_i \dot{e}_i \\ &= \dddot{q}_{c_i} - \dddot{q}_i + (\lambda_i + \omega_i)\{\ddot{q}_{c_i} - u_i - f_i(q, \dot{q}, t) - d_i(q, \dot{q}, t)\} \\ &+ \omega_i \lambda_i \dot{e}_i \\ &= \ddot{q}_{c_i} - \dot{u}_i - \dot{f}_i(q, \dot{q}, t) - \dot{d}_i(q, \dot{q}, t) \\ &+ (\lambda_i + \omega_i)\{\ddot{q}_{c_i} - u_i - f_i(q, \dot{q}, t) - d_i(q, \dot{q}, t)\} + \omega_i \lambda_i \dot{e}_i \end{aligned} \tag{4.14}$$

Thus $\dot{s} = \ddot{\sigma} + \lambda \dot{\sigma}$ is in terms of the derivative of control u_i. The derivative of the control u_i is expressed as:

$$\begin{aligned} \dot{u}_\iota = \dddot{q}_{c_i} - \dot{f}_i(q, \dot{q}, t) + (\lambda_i + \omega_i)\{\ddot{q}_{c_i} - u_i - f_i(q, \dot{q}, t)\} \\ + \omega_i \lambda_i \dot{e}_i + K_i \cdot sign(s_i) \end{aligned} \tag{4.15}$$

The controller gain K_i is necessary to satisfy the following condition:

$$\left|\dot{d}_i(q, \dot{q}, t) + (\lambda_i + \omega_i) d_i(q, \dot{q}, t)\right| < K_i \tag{4.16}$$

to provide the finite time convergence.

4.4. The First Gain Adaptation Design for a Traditional Sliding Mode Control

Type 1: This sliding mode control with gain adaptation provides discontinuous control function without overestimating the boundary of the disturbances/uncertainties. Chattering can be observed in the output. For the i-th row, a traditional sliding mode control is defined as follows:

$$u_i = \ddot{q_{c_i}} - f_i(q, \dot{q}, t) + \lambda_i(\dot{e}_i) + K_i \cdot sign(\sigma_i) \tag{4.17}$$

The following gain adaptation function is applied to the traditional sliding mode control:

$$\dot{K}_i = \begin{cases} \overline{K}_i |\sigma_i| sign(|\sigma_i| - \varepsilon_i) & K_i > \mu_i \\ \mu_i & K_i \leq \mu_i \end{cases} \tag{4.18}$$

Type 2: This sliding mode control with gain adaptation provides continuous control function without overestimating the boundary of the disturbances/uncertainties. Auxiliary sliding variables are used to design this controller. Chattering is attenuated. For the i-th row, the traditional sliding mode control with an auxiliary sliding variable is defined as follows:

$$\begin{aligned} \dot{u_i} = \dddot{q}_{c_i} - \dot{f}_i(q, \dot{q}, t) + (\lambda_i + \omega_i)\{\ddot{q}_{c_i} - u_i - f_i(q, \dot{q}, t)\} \\ + \omega_i \lambda_i \dot{e}_i + K_i \cdot sign(s_i) \end{aligned} \tag{4.19}$$

K_i is defined as follows:

$$\dot{K}_i = \begin{cases} \overline{K}_i |s_i| sign(|s_i| - \varepsilon_i) & K_i > \mu_i \\ \mu_i & K_i \leq \mu_i \end{cases} \tag{4.20}$$

At first, K_i is strictly positive. So if K_i is less than a certain small positive number, K_i should be increased. Consequently, ε_i should be a certain positive number. The ε_i should be tuned for each system. If the control for the system needs a large controller

gain, μ_i can be a large number. $\overline{K}_i$ is a positive constant. If $\overline{K}_i$ is a large number, K_i increases or decreases rapidly; conversely, if it is a small number, K_i increases or decreases gradually. The magnitude of the i-th row of the sliding variable is also a gain for gain adaptation. As the sliding variable gets larger, the gain value increases quickly. $sign(|\sigma_i \; or \; s_i| - \mu_i)$ is defined as: if $|\sigma_i \; or \; s_i|$ is less than μ_i, the gain decreases, and if $|\sigma_i or \; s_i|$ is larger than μ_i, the gain increases.

4.5. The Second Gain Adaptation Design for a Traditional Sliding Mode Control

An adaptive traditional sliding mode control is proposed using the gain adaptation theorems introduced in Chapter 3. The objective of the second gain adaptation is to accelerate the decrease of the controller gains. As seen in the example of the adaptive traditional sliding mode control, the first gain adaptation law (4.17-4.20) decreases the controller gain slowly (Figure 3.29). This means that if the first gain adaptation has overestimated the controller gain, it would take a long time to reach the appropriate controller gain. The second gain adaptation is formulated as follows;

$$\dot{K}_i = \begin{cases} A_i + B_i sign(|\sigma_i or \; s_i| - \varepsilon_i) & K_i > \mu_i \\ \mu_i & K_i \leq \mu_i \end{cases} \qquad (4.21)$$

for each control (4.17 and 4.19), where A_i and B_i are positive and condition $A_i < B_i$ is satisfied. Other parameters are set due to the design of the first gain adaptation law. If $K_i \leq \mu_i$, then K_i increases with a slope of μ_i. If $K_i > \mu_i$ and $|\sigma_i or \; s_i| > \varepsilon_i$, then K_i increases with a slope of $A_i + B_i$. If $K_i > \mu$ and $|\sigma_i or \; s_i| < \varepsilon$, then K_i decreases with a slope of $A_i - B_i$.

4.6. Summary

In this chapter, all of the procedures of the simulation have been presented. A super-twisting observer for robot manipulators has been presented. Adaptive traditional sliding mode control designs for the robot manipulator have been presented. Those presented adaptive controls are simulated in Chapter 5.

CHAPTER 5

SIMULATION RESULTS

In this chapter, the 2-link planar robot manipulator is studied and simulated implementing the sliding mode observer and the adaptive sliding mode control. In Figure 5.1, the plant model of the adaptive sliding mode control design for the robot manipulators is shown.

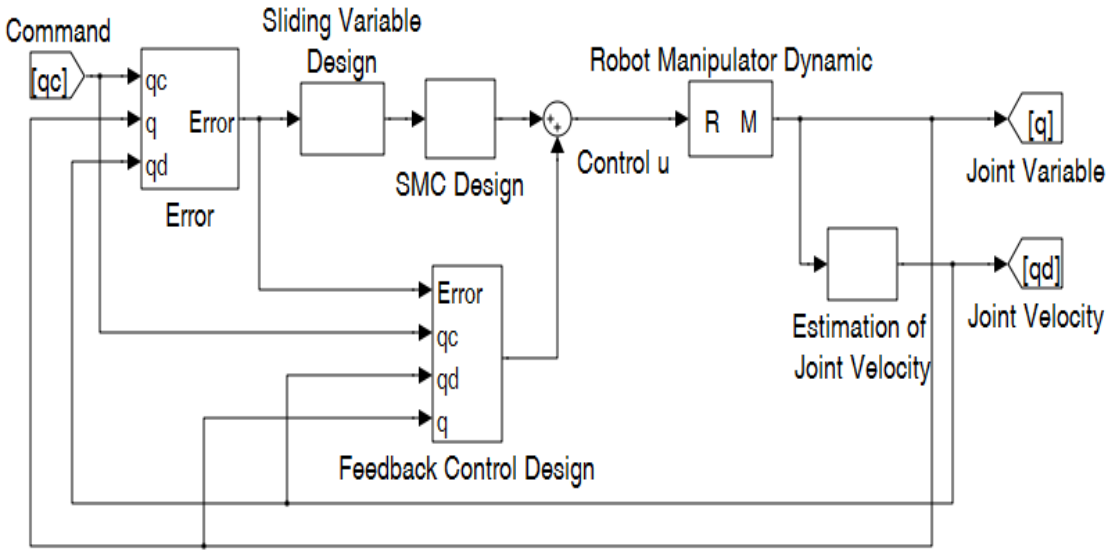

Figure 5.1: Plant model of the adaptive sliding mode control for the robot manipulators

The following simulations scenarios have been executed and the results of the simulations have been analyzed.

Scenario 1: **(TSMC1)** The position tracking using traditional sliding mode control without gain adaptation. It assumes that the boundary of the disturbances is known. The controller gain is estimated from the knowledge of the boundary of the disturbances.

Scenario 2: **(TSMC1-2)** The position tracking using traditional sliding mode control without gain adaptation. It assumes that the boundary of the disturbances is not known. The controller gain is overestimated.

Scenario 3: **(ATSMC1)** The position tracking using traditional sliding mode control with 1^{st} gain adaptation. It assumes that the boundary of the disturbances is not known.

Scenario 4: **(ATSMC1-2)** The position tracking using traditional sliding mode control with 2^{nd} gain adaptation. It assumes that the boundary of the disturbances is not known.

Scenario 5: **(TSMC2)** The position tracking using traditional sliding mode control without gain adaptation. The auxiliary sliding variable is designed to attenuate chattering. It assumes that the boundary of the disturbances is known. The controller gain is estimated from the boundary of the disturbances.

Scenario 6: **(TSMC2-2)** The position tracking using traditional sliding mode control without gain adaptation. The auxiliary sliding variable is designed to attenuate

chattering. It assumes that the boundary of the disturbances is not known. The controller is overestimated.

Scenario 7: **(ATSMC2)** The position tracking using traditional sliding mode control with 1st gain adaptation. It assumes that the boundary of the disturbances is not known. The auxiliary sliding variable is designed to attenuate chattering.

Scenario 8: **(ATSMC2-2)** The position tracking using traditional sliding mode control with 2nd gain adaptation. It assumes that the boundary of the disturbances is not known. The auxiliary sliding variable is designed to attenuate chattering.

5.1. Robot Manipulator Description

In this section, parameter values for robot manipulator dynamic equation, disturbances, and command of the joint variables are given as follows:

2-link Robot Manipulator Parameters:

$$q = \begin{bmatrix} q_1 \\ q_2 \end{bmatrix}$$

$$\tau = \begin{bmatrix} \tau_1 \\ \tau_2 \end{bmatrix}$$

$$\tau_d = \begin{bmatrix} \tau_{1d} \\ \tau_{2d} \end{bmatrix} = \begin{bmatrix} 20 \cdot \sin(10t) \\ 30 \cdot \sin(20t) \end{bmatrix}$$

$$M = \begin{bmatrix} (m_1 + m_2)a_1^2 + m_2 a_2^2 + 2m_2 a_1 a_2 \cos(q_2) & m_2 a_2^2 + m_2 a_1 a_2 \cos(q_2) \\ m_2 a_2^2 + m_2 a_1 a_2 \cos(q_2) & m_2 a_2^2 \end{bmatrix}$$

$$C(q, \dot{q})\dot{q} = \begin{bmatrix} -m_2 a_1 a_2 (2\dot{q}_1 \dot{q}_2 + \dot{q}_2^2) \sin(q_2) \\ m_2 a_1 a_2 \dot{q}_1^2 \sin(q_2) \end{bmatrix}$$

$$G(q) = \begin{bmatrix} (m_1 + m_2) g a_1 \cos(q_1) + m_2 g a_2 \cos(q_1 + q_2) \\ m_2 g a_2 \cos(q_1 + q_2) \end{bmatrix}$$

$$m_1 = 1Kg, \quad m_2 = 2Kg, \quad a_1 = 1m, \quad a_2 = 2m, \quad g = 9.81 m/s^2$$

Command position: $q_c = \begin{bmatrix} q_{1c} \\ q_{2c} \end{bmatrix}$ $q_{1c} = \sin(3t),\ q_{2c} = \sin(5t)$

Time increment is 10^{-5} in the simulations.

Simulink model of robot manipulator

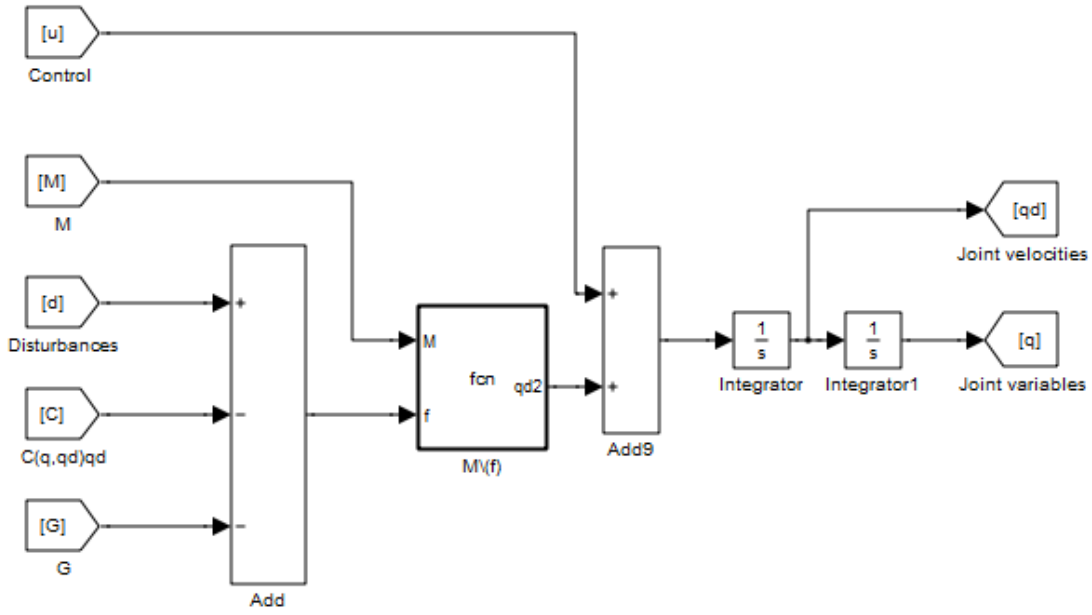

Figure 5.2: Simulink model of robot manipulator dynamics

This implemented model expresses the joint variables dynamic equation as follows:

$$\ddot{q} = M(q)^{-1}\tau + M(q)^{-1}(\tau_d - C(q,\dot{q})\dot{q} - G(q))$$

u is defined as the vector of control $\mathrm{M}^{-1} \cdot \tau$. M, C, and G are defined as the matrices in the robot manipulator dynamic equation. d is defined as the vector of the sum of the disturbances and uncertainties τ_d. q is the vector of the joint variables, while $\dot{q}$ is the vector of the derivatives of the joint variables, in other words, the vector of the joint velocities. The control u is designed for each simulation.

Super-twisting observer design:

$$z_i = \hat{q}_i - q_i$$

$$\dot{\hat{q}}_i = -1.5\sqrt{C_i}|z_i|^{\frac{1}{2}} sign(z_i) - \omega_i$$

$$\dot{\omega}_i = 1.1 C_i \cdot sign(z_i)$$

$$C_i = 200, \qquad for\ i = 1, 2$$

For the simulation with the auxiliary sliding variable, transfer function $\frac{s}{0.0001s+1}$ is used for 1 seconds at the beginning of the simulations, to estimate the vector of the joint velocities $\dot{q}$.

Simulink model of super-twisting differentiator

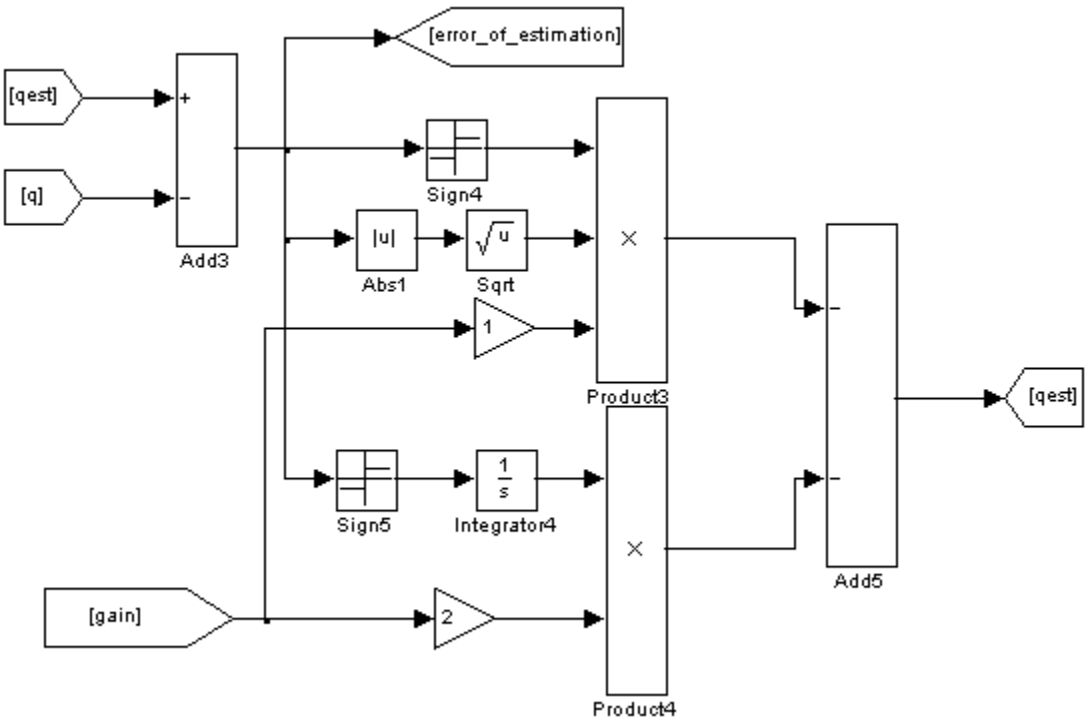

Figure 5.3: Simulink model of super-twisting observer

5.2. Adaptive Traditional Sliding Mode Control for 2-link Robot Manipulator

5.2.1. Parameters of Simulation for Sliding Variable $\sigma = \dot{e} + \lambda e$

1) Traditional sliding mode control design (TSMC1), (TSMC1-2)

The controller gain K_i is constant in this controller design. The controller gain K_i is to be estimated by using the information which is given in the simulation parameters.

$$\sigma_i = \dot{e}_i + 10e_i$$

$$u_i = \ddot{q_{c_i}} - f_i(q, \dot{q}, t) + 10(\dot{e}_i) + K_i \cdot sign(\sigma_i)$$

2) The first adaptive-gain traditional sliding mode control design (ATSMC1)

The controller gain K_i is to be defined by the first gain adaptation algorithm in this controller design. This adaptive-gain traditional sliding mode control does not overestimate the boundary of the disturbances/uncertainties. The gain adaptation mitigates chattering by means of the decrease of the controller gain. The speed of decrease is very slow.

$$\sigma_i = \dot{e}_i + 10e_i$$

$$u_i = \ddot{q_{c_i}} - f_i(q, \dot{q}, t) + 10(\dot{e}_i) + K_i \cdot sign(\sigma_i)$$

$$\text{for } \dot{K}_i = \begin{cases} \overline{K}_i |\sigma_i| sign(|\sigma_i| - \varepsilon_i) & K_i > \mu_i \\ \mu_i & K_i \leq \mu_i \end{cases}$$

$$\varepsilon_i = 0.1, \qquad \mu_i = 0.1, \qquad \overline{K}_i = 10 \quad for\ i = 1, 2$$

$$K_i(0) = 30\ for\ i = 1, 2$$

3) The second adaptive-gain traditional sliding mode control design (ATSMC1-2)

The controller gain K_i is to be defined by the second gain adaptation algorithm in this controller design. This adaptive-gain traditional sliding mode control decreases the

controller gain much faster than the first adaptive-gain traditional sliding mode control does.

$$\sigma_i = \dot{e}_i + 10e_i$$

$$u_i = \ddot{q_{c_i}} - f_i(q, \dot{q}, t) + 10(\dot{e}_i) + K_i \cdot sign(\sigma_i)$$

$$\text{for } \dot{K}_i = \begin{cases} A_i + B_i sign(|\sigma_i| - \varepsilon_i) & K_i > \mu_i \\ \mu_i & K_i \leq \mu_i \end{cases}$$

$$\varepsilon_i = 0.1, \qquad \mu_i = 0.1, \qquad A_i = 20 \; for \; i = 1, 2 \;, \qquad B_i = 30 \; for \; i = 1, 2$$

$$K_i(0) = 30 \; for \; i = 1, 2$$

5.2.2.Simulations for TSMC (TSMC1), (TSMC1-2), (ATSMC1), (ATSMC1-2)

These four control designs will be simulated in order to test their ability to limit the chattering that is a major cause of loss of accuracy. The goal of this simulation is to show that the adaptive traditional sliding mode controls mitigate the chattering on the sliding variables.

Simulation without gain adaptation (TSMC1)

It assumed that the boundary of the disturbance is known, and the controller gain K_i is estimated from the given parameters in this simulation. The controller gain K_i is estimated as follows by using Inequality (4.8):

$$K_i > L_i, \qquad L_i = |d_i| = \left|M^{-1}\tau_{d_i}\right|$$

where $\tau_d = \begin{bmatrix} 20 \cdot \sin(10t) \\ 30 \cdot \sin(20t) \end{bmatrix}$. The controller gain K_i is estimated as 50 for i=1, 2.

$$u_i = \ddot{q_{c_i}} - f_i(q, \dot{q}, t) + \lambda_i(\dot{e}_i) + K_i \cdot sign(\sigma_i)$$

$$\lambda_i = 10 \; for \; i = 1, 2, \qquad K_i = 50 \; for \; i = 1, 2$$

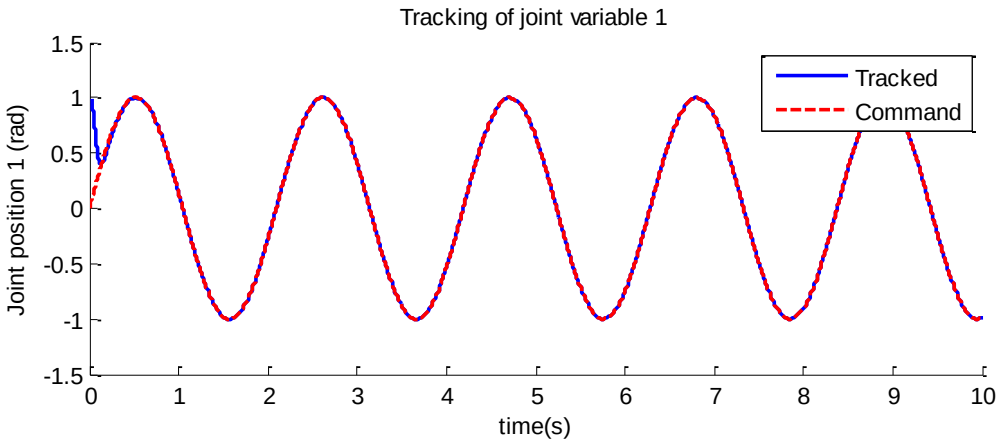

Figure 5.4: (TSMC1) The actual joint variable and the command joint variable versus time 1

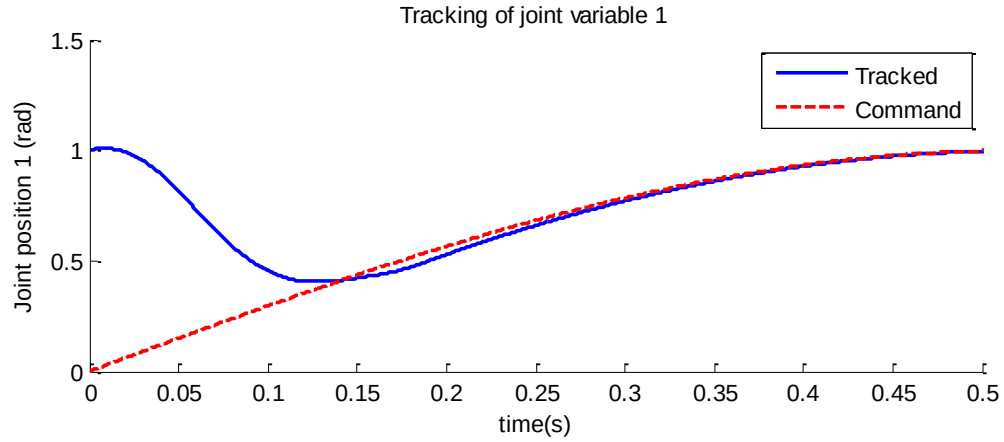

Figure 5.5: (TSMC1) Zoom of the actual joint variable and the command joint variable versus time 1

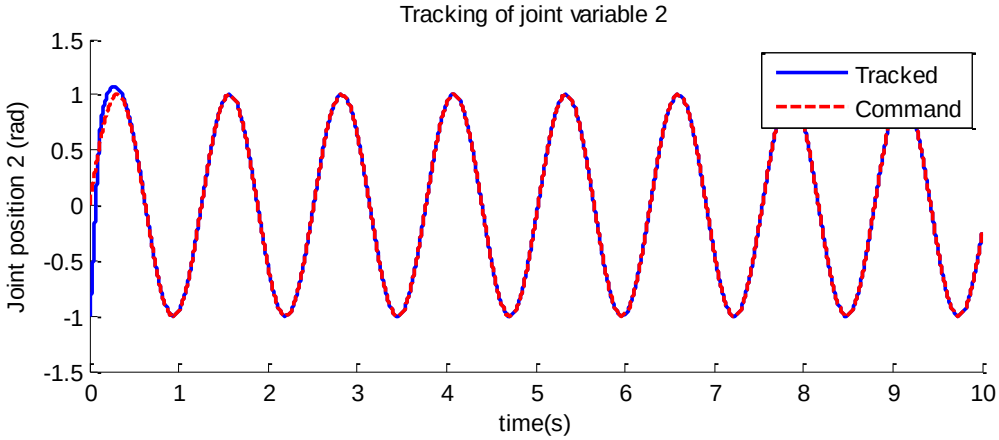

Figure 5.6: (TSMC1) The actual joint variable and the command joint variable versus time 2

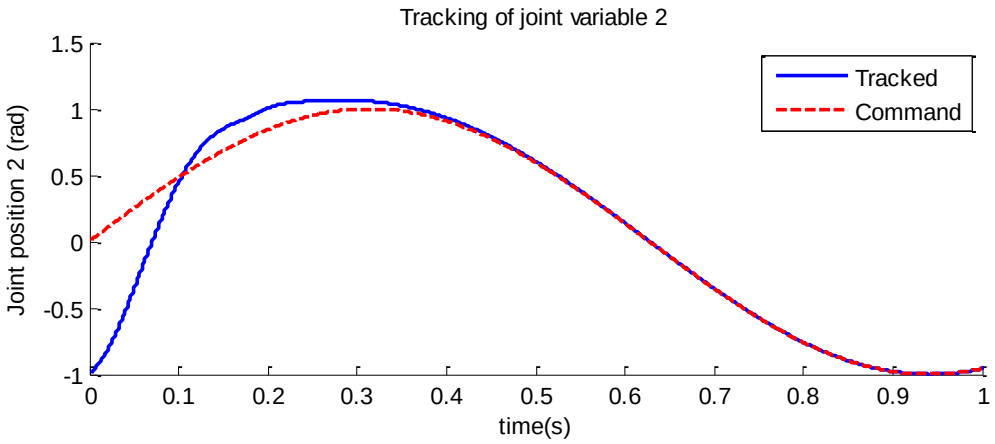

Figure 5.7: (TSMC1) Zoom of the actual joint variable and the command joint variable versus time 2

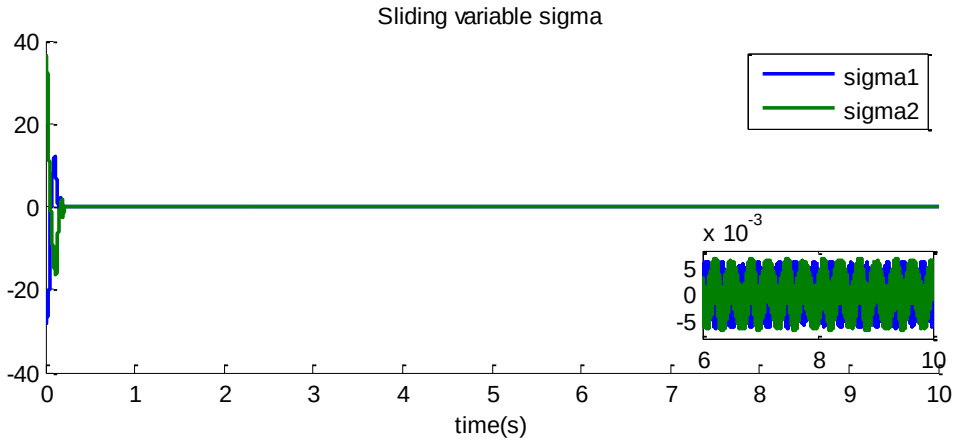

Figure 5.8: (TSMC1) Sliding variable σ versus time

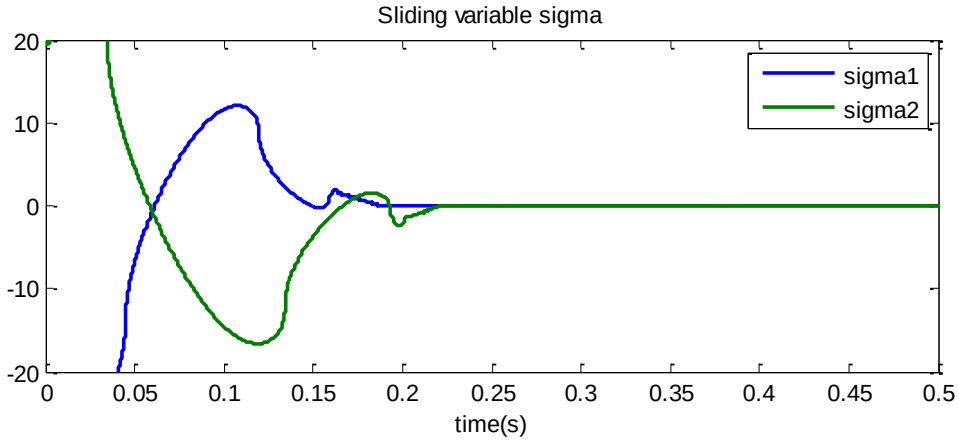

Figure 5.9 : (TSMC1) Zoom of the sliding variable σ versus time

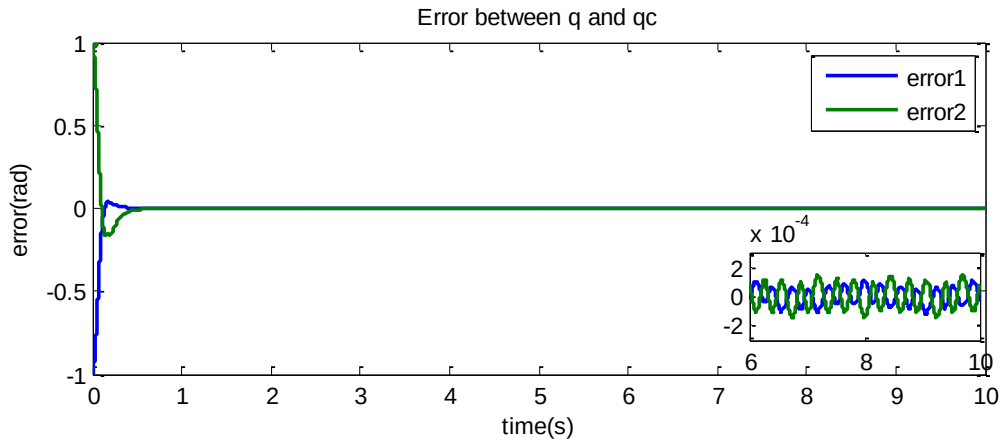

Figure 5.10: (TSMC1) Error between the actual joint variables and the command joint variables versus time

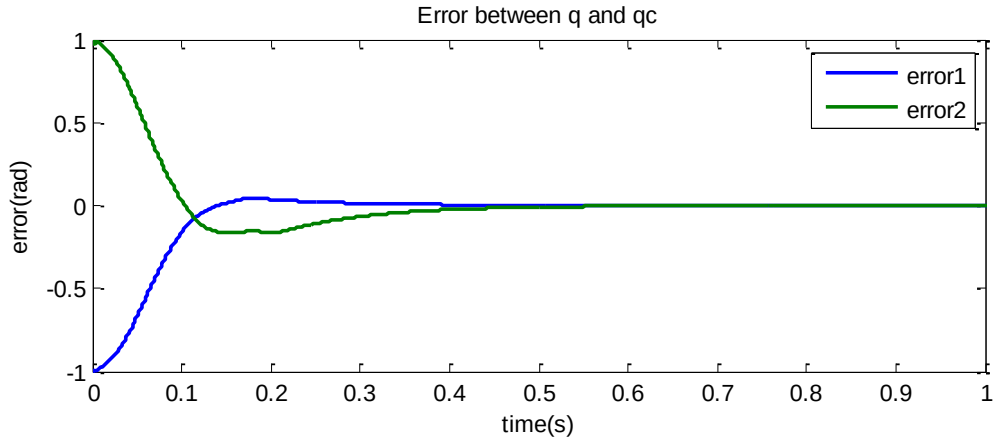

Figure 5.11: (TSMC1) Zoom of the error between the actual joint variables and the command joint variables versus time

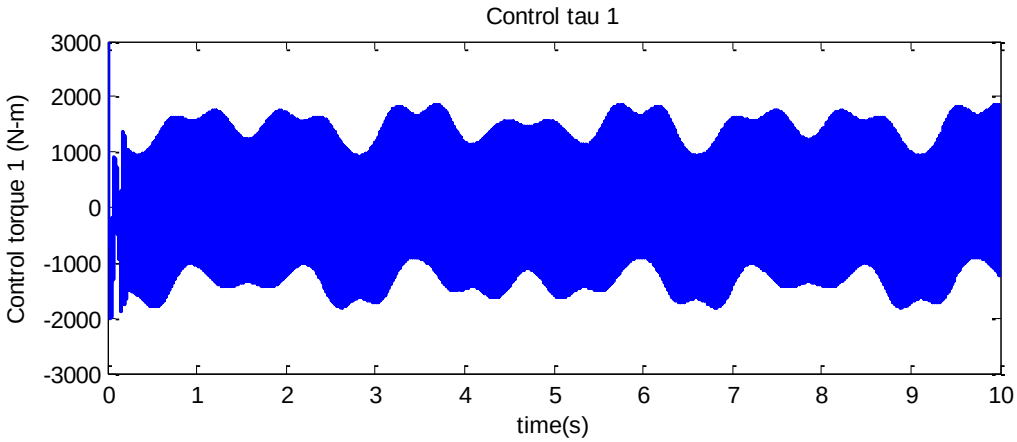

Figure 5.12: (TSMC1) The control τ versus time 1

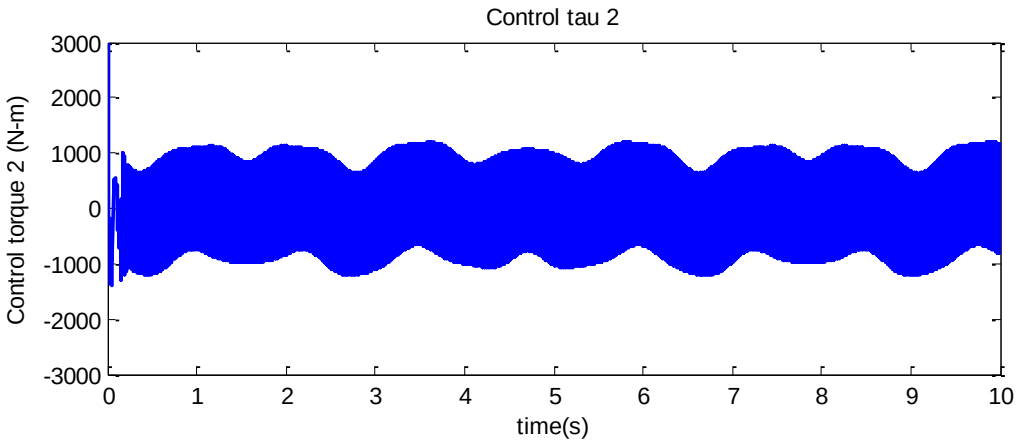

Figure 5.13: (TSMC1) The control τ versus time 2

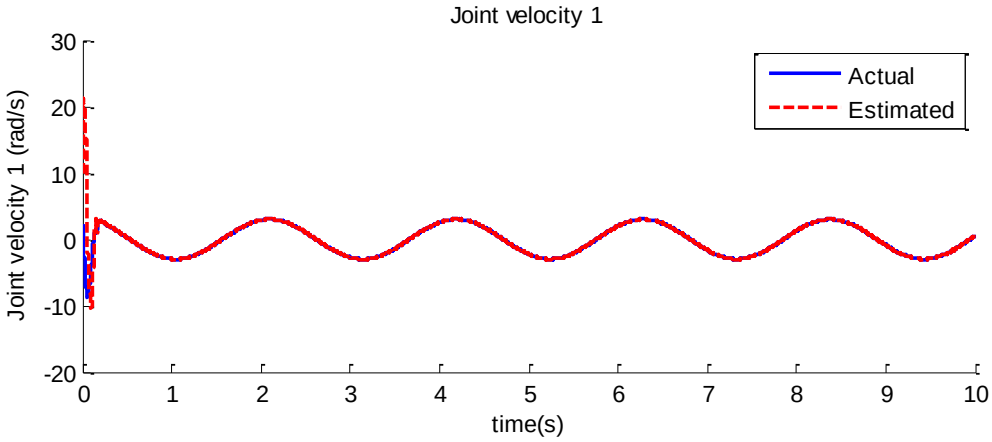

Figure 5.14: (TSMC1) The actual joint velocity and the estimated joint velocity versus time 1

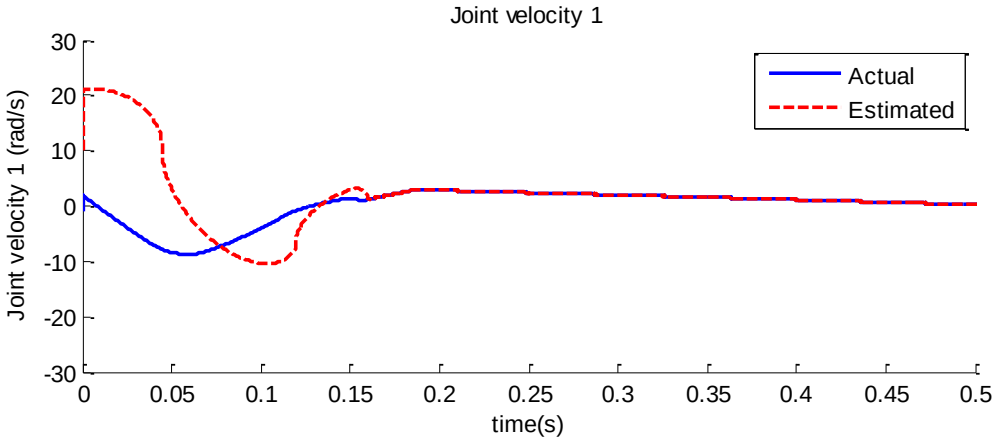

Figure 5.15: (TSMC1) Zoom of the actual joint velocity and the estimated joint velocity versus time 1

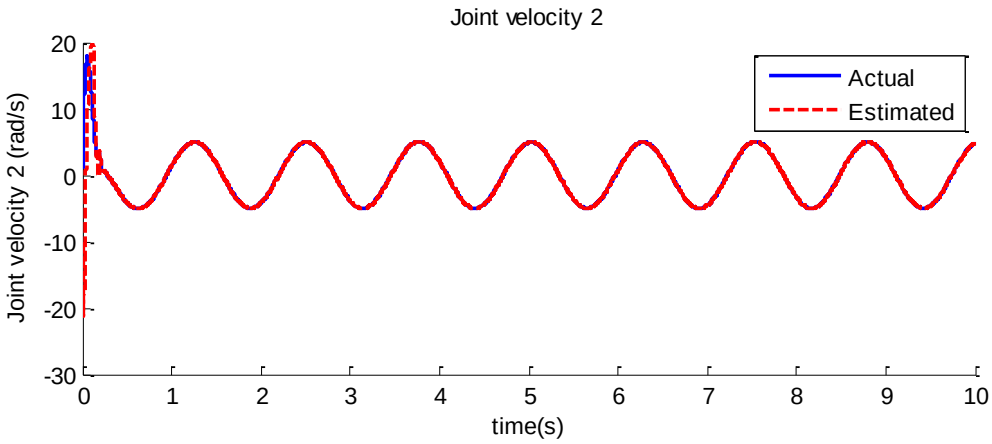

Figure 5.16: (TSMC1) The actual joint velocity and the estimated joint velocity versus time 2

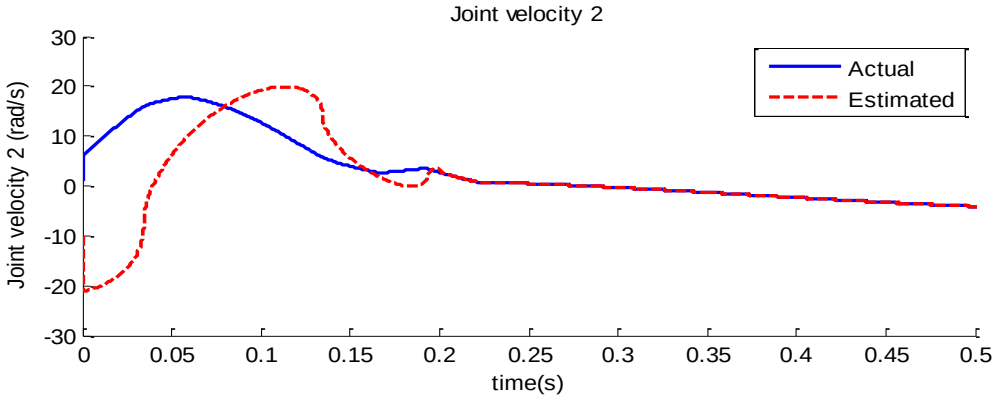

Figure 5.17: (TSMC1) Zoom of the actual joint velocity and the estimated joint velocity versus time 2

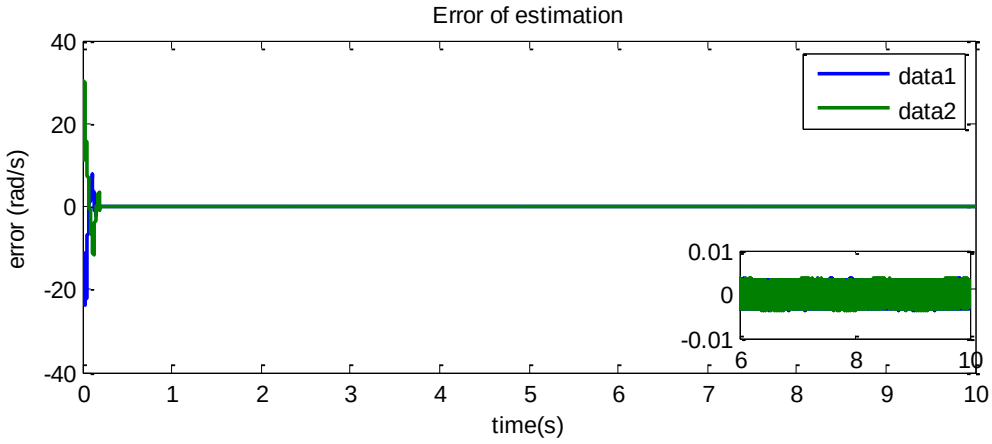

Figure 5.18: (TSMC1) Error between the actual joint velocity and the estimated joint velocity versus time

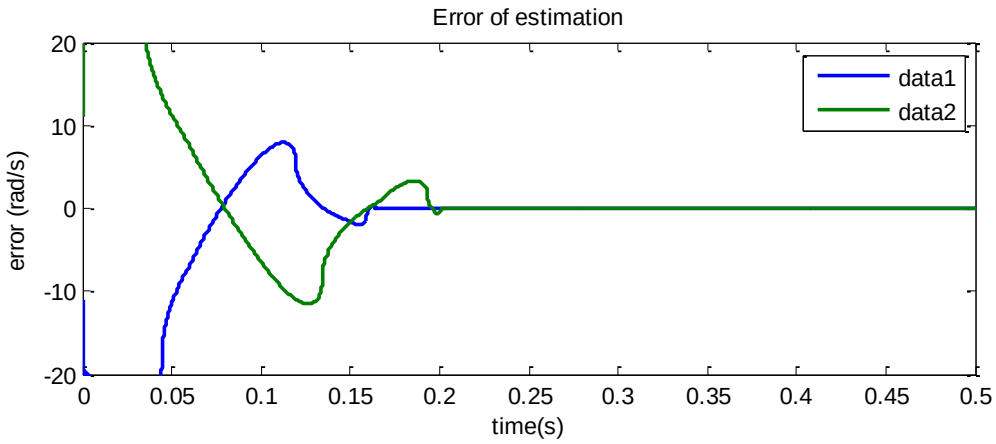

Figure 5.19: (TSMC1) Zoom of the error between the actual joint velocity and the estimated joint velocity versus time

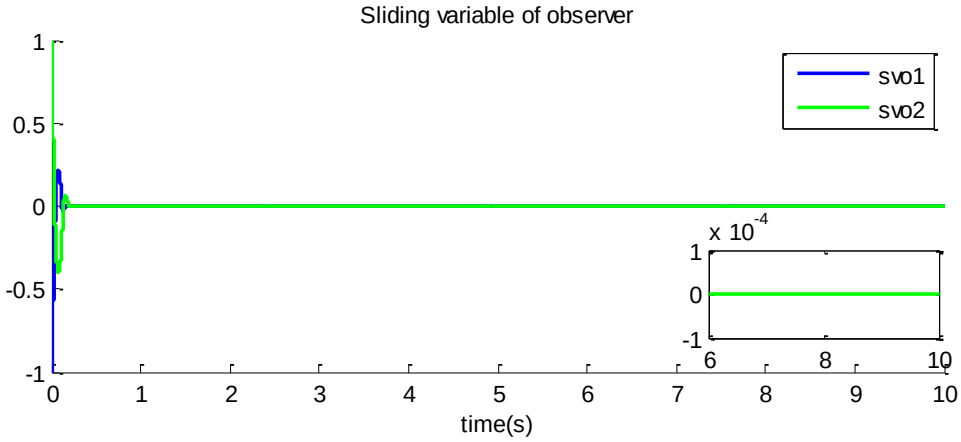

Figure 5.20: (TSMC1) Sliding variable of observer versus time

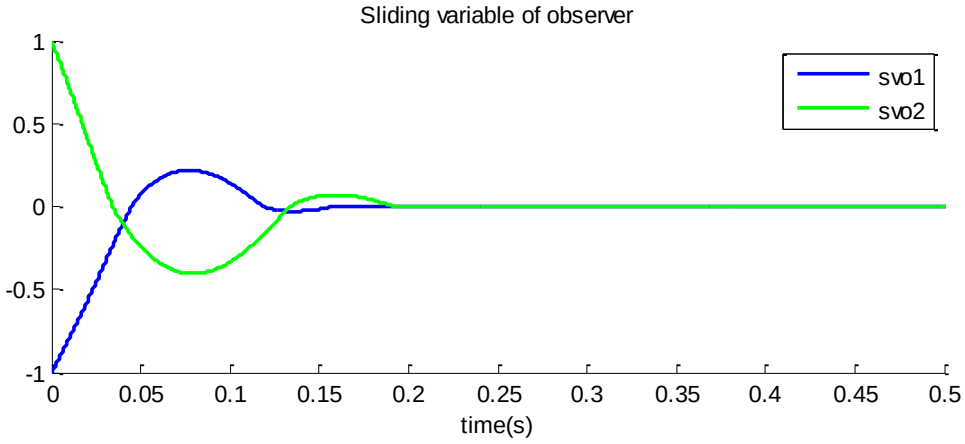

Figure 5.21: (TSMC1) Zoom of the sliding variable of observer versus time

Figures 5.4-5.21 show the results of the simulation of the traditional sliding mode control with each element of the vector of the controller gain equal to 50. In the corresponding row, the controller gain is estimated from the boundary of the bounded disturbance, while the actual joint variable tracks the command joint variable in finite time (Figures 5.4-5.7). The sliding variables converge to 0 in finite time (Figure 5.8). The controls are high frequency switching functions (Figures 5.12-5.13). The chattering effect is very small (Figure 5.8).

Simulation with the large controller gain (TSMC1-2)

It assumed that the boundary of the disturbance is not known, and the controller gain K_i is overestimated in this simulation. Chattering must be observed in output.

$$u_i = \ddot{q_{c_i}} - f_i(q, \dot{q}, t) + \lambda_i(\dot{e}_i) + K_i \cdot sign(\sigma_i), \qquad K_i = 1000 \; for \; i = 1, 2$$

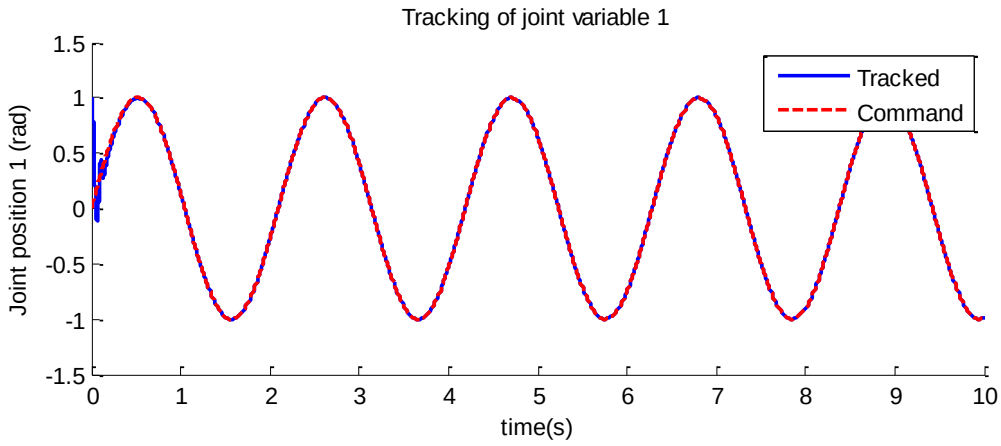

Figure 5.22: (TSMC1-2) The actual joint variable and the command joint variable versus time 1

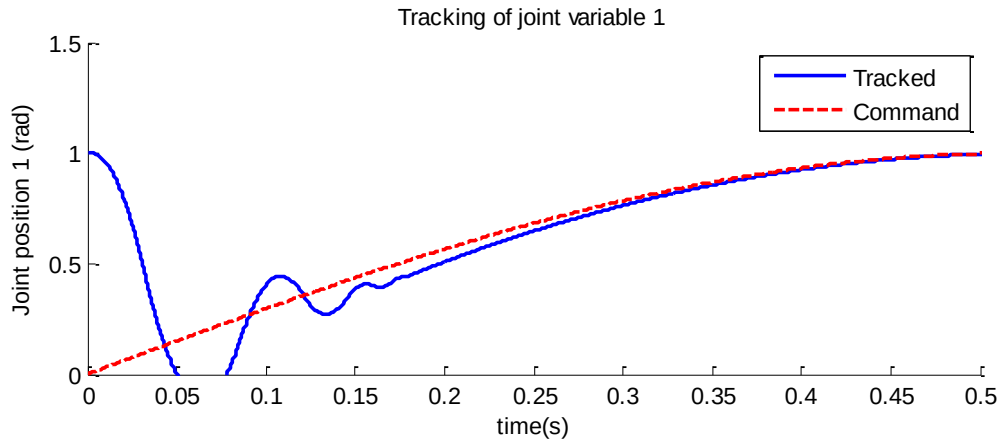

Figure 5.23: (TSMC1-2) Zoom of the actual joint variable and the command joint variable versus time 1

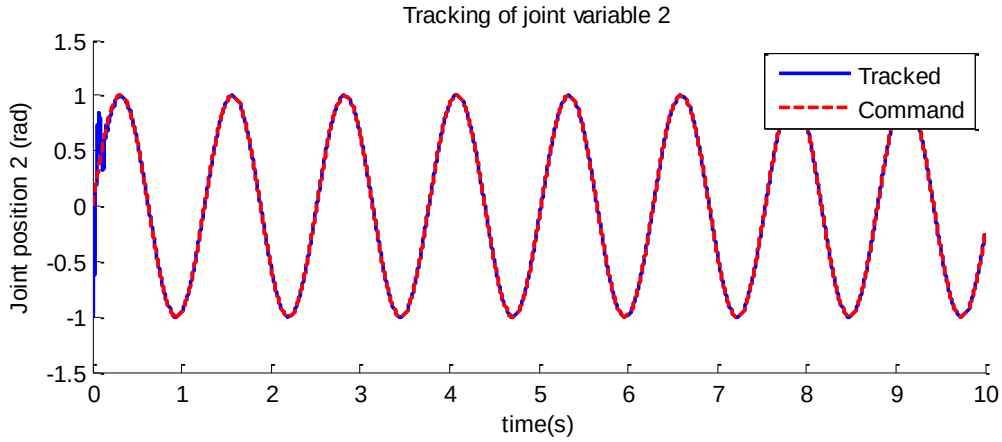

Figure 5.24: (TSMC1-2) The actual joint variable and the command joint variable versus time 2

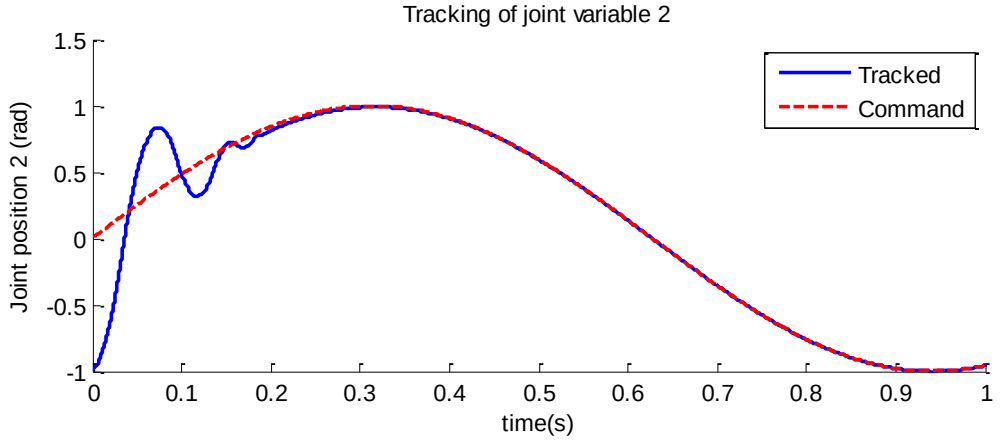

Figure 5.25: (TSMC1-2) Zoom of the actual joint variable and the command joint variable versus time 2

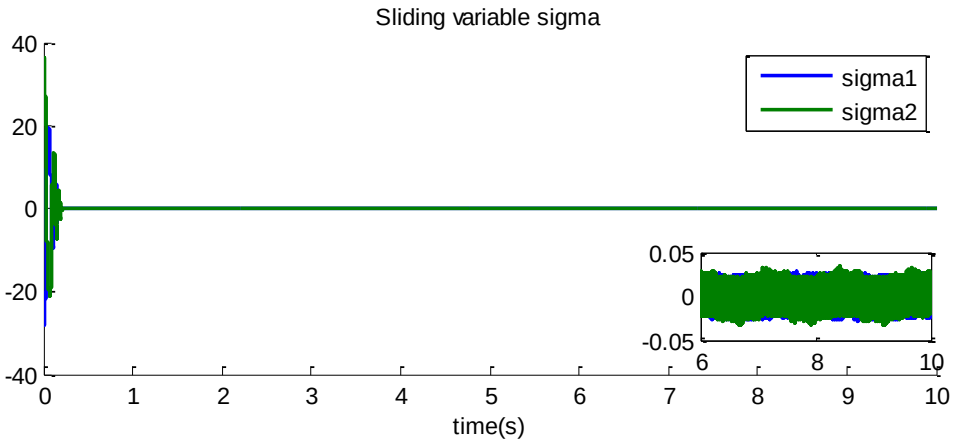

Figure 5.26: (TSMC1-2) Sliding variable σ versus time

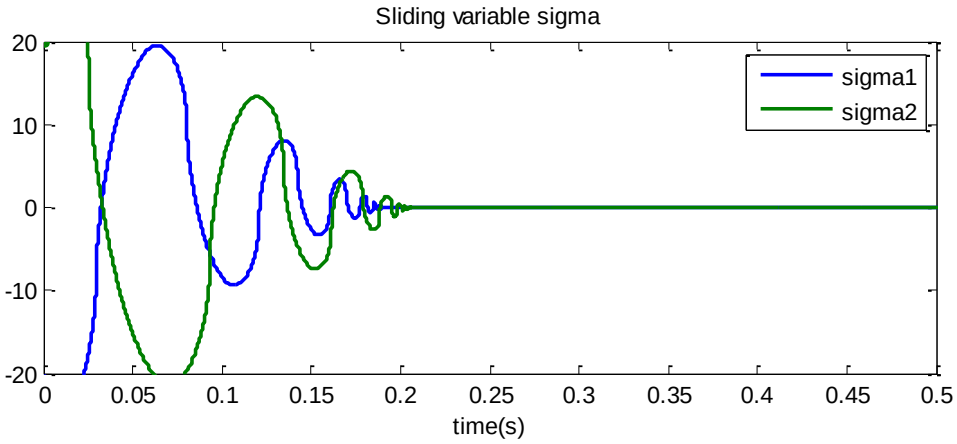

Figure 5.27: (TSMC1-2) Zoom of the sliding variable sigma versus time

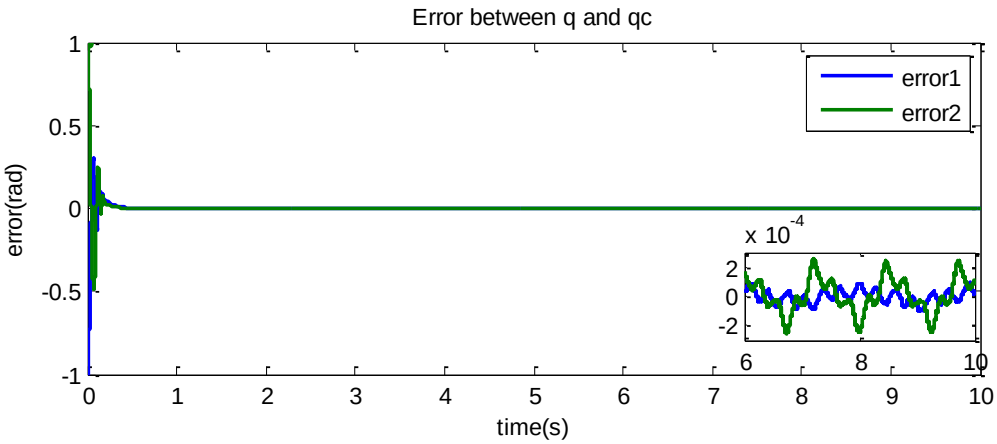

Figure 5.28: (TSMC1-2) Error between the actual joint variable and the command joint variable versus time

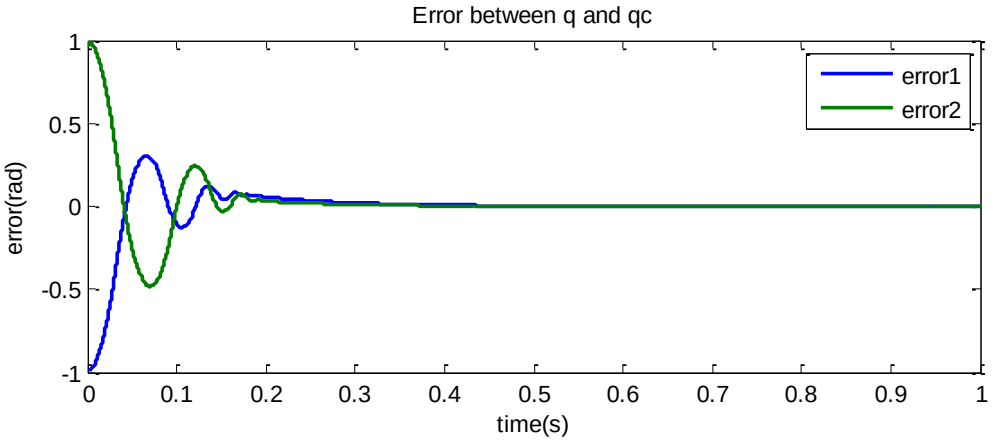

Figure 5.29: (TSMC1-2) Zoom of the error between the actual joint variable and the command joint variable versus time

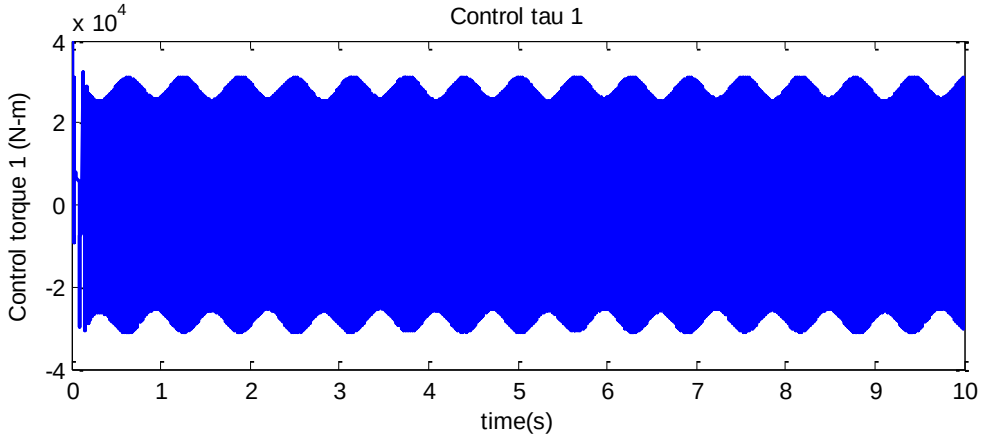

Figure 5.30: (TSMC1-2) The control τ versus time 1

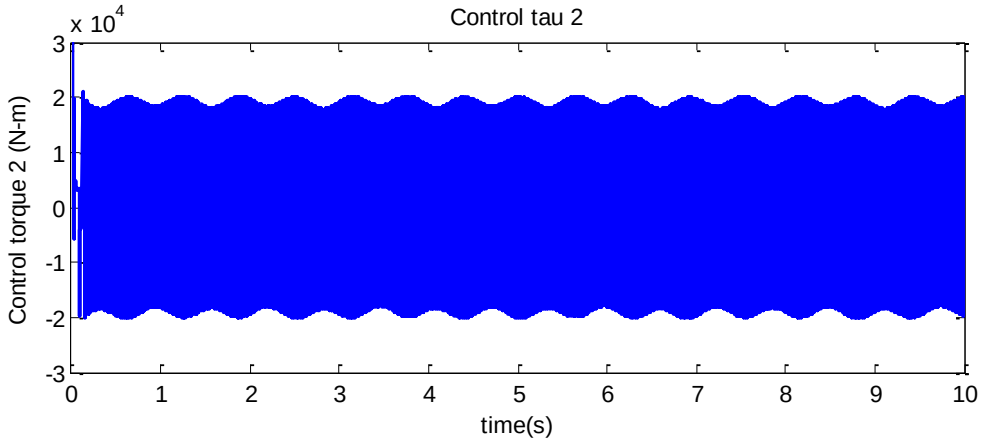

Figure 5.31: (TSMC1-2) The control τ versus time 2

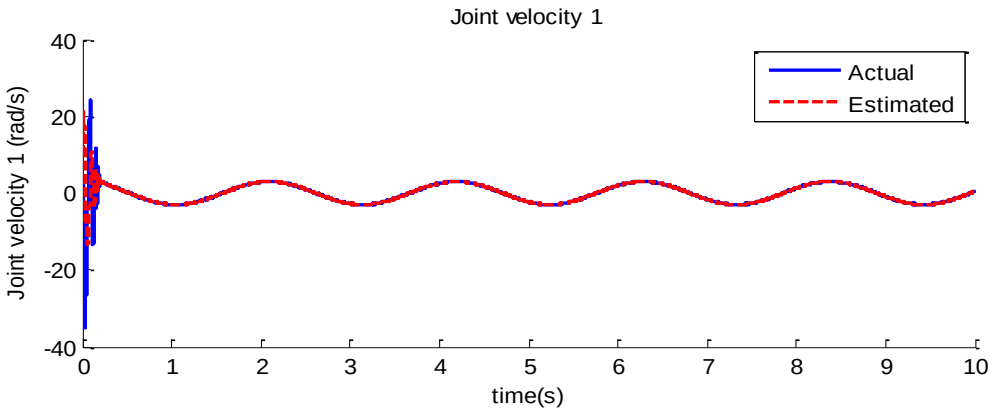

Figure 5.32: (TSMC1-2) The actual joint velocity and the estimated joint velocity versus time 1

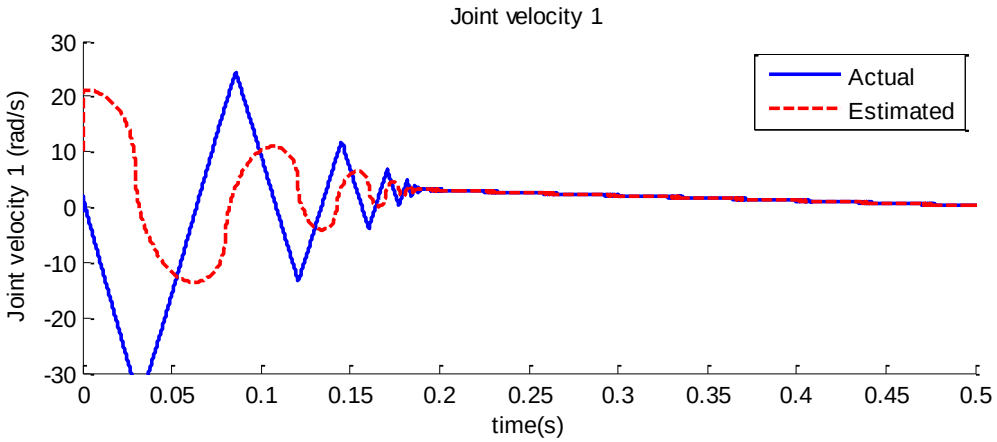

Figure 5.33: (TSMC1-2) Zoom of the actual joint velocity and the estimated joint velocity versus time 1

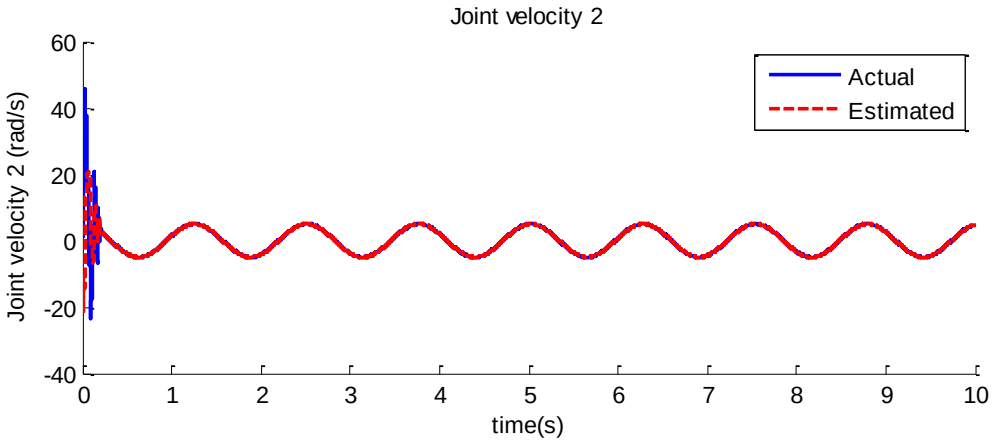

Figure 5.34: (TSMC1-2) The actual joint velocity and the estimated joint velocity versus time 2

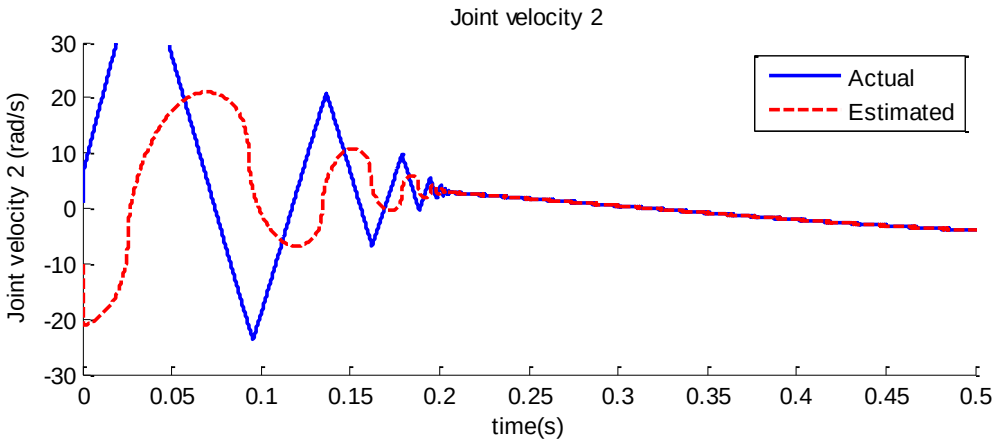

Figure 5.35: (TSMC1-2) Zoom of the actual joint velocity and the estimated joint velocity versus time 2

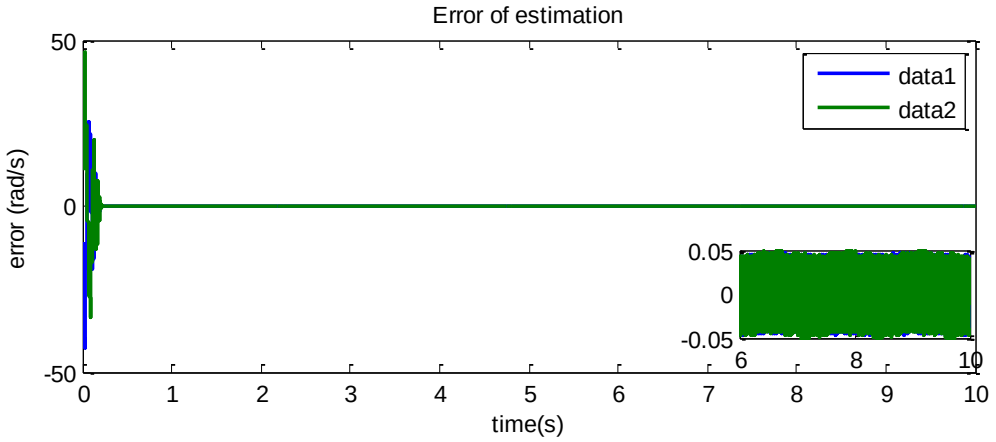

Figure 5.36: (TSMC1-2) Error between the actual joint velocity and the estimated joint velocity versus time

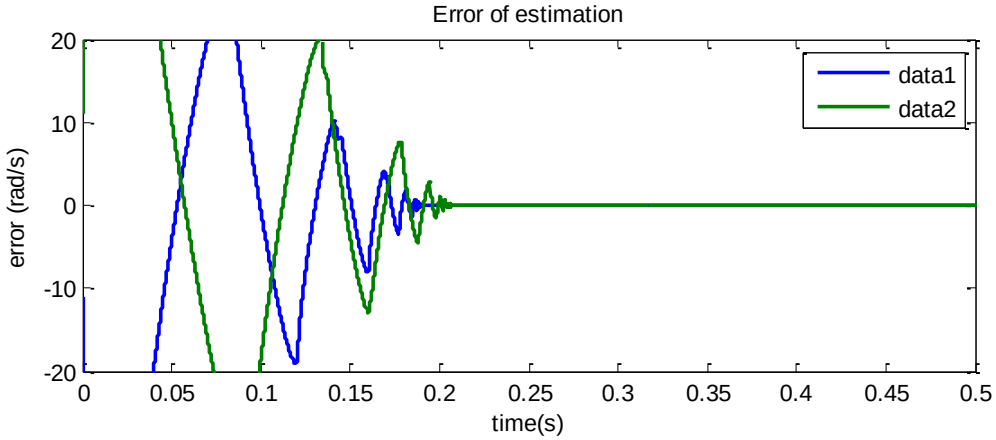

Figure 5.37: (TSMC1-2) Zoom of the error between the actual joint velocity and the estimated joint velocity versus time

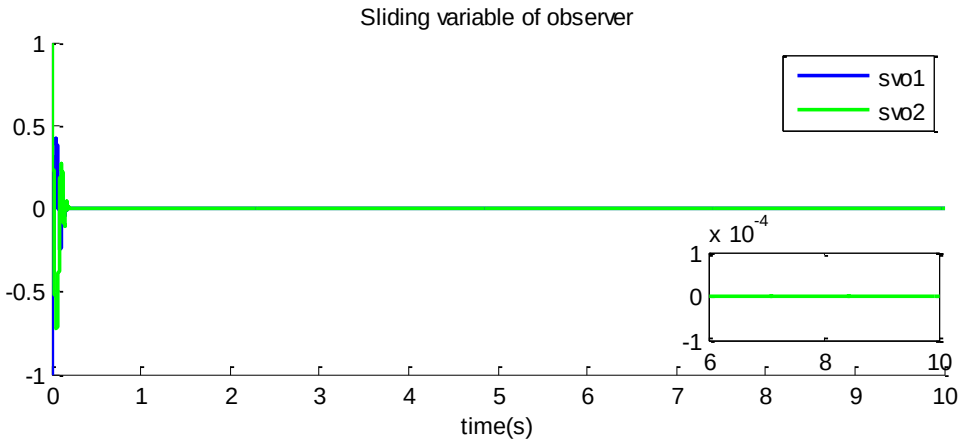

Figure 5.38: (TSMC1-2) Sliding variable of observer versus time

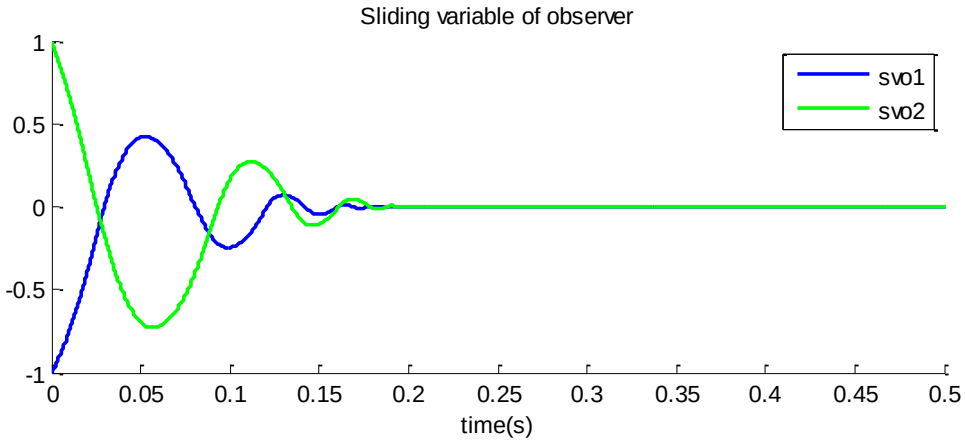

Figure 5.39: (TSMC1-2) Zoom of the sliding variable of observer versus time

Figures 5.22-5.39 show the results of the simulation of the traditional sliding mode control with overestimated controller gains. Compared with the results of (TSMC1), it is obvious that chattering is increased when the controller gain is large (Figure 5.26). Comparing the results between TSMC1 and TSMC1-2, the amplitude of the control functions in TSMC1-2 become much larger than those of TSMC1, and the chattering of output becomes larger than that of TSMC1. Therefore, we can conclude that the loss of energy and the loss of accuracy are caused by the overestimated controller gains.

Simulation with the First Adaptive-Gain TSMC (ATSMC1)

It is assumed that the boundary of the disturbance is not known. The controller gain K_i is defined by the first gain adaptation algorithm. The controller gain K_i increases much fast when the absolute value of sliding variable σ_i is larger than a certain defined value ε_i: $|\sigma_i| > \varepsilon_i$. On the other hand the controller gain K_i decreases much slow when the absolute value of sliding variable σ_i is smaller than a certain defined value ε_i: $|\sigma_i| < \varepsilon_i$.

$$u_i = \ddot{q_{c_i}} - f_i(q, \dot{q}, t) + \lambda_i(\dot{e}_i) + K_i \cdot sign(\sigma_i)$$

$$\text{for } \dot{K}_i = \begin{cases} \overline{K}_i |\sigma_i| sign(|\sigma_i| - \varepsilon_i) & K_i > \mu_i \\ \mu_i & K_i \leq \mu_i \end{cases}$$

$$\varepsilon_i = 0.1, \qquad \mu_i = 0.1, \qquad \overline{K}_i = 10 \; for \; i = 1, 2$$

$$K_i(0) = 30 \; for \; i = 1, 2$$

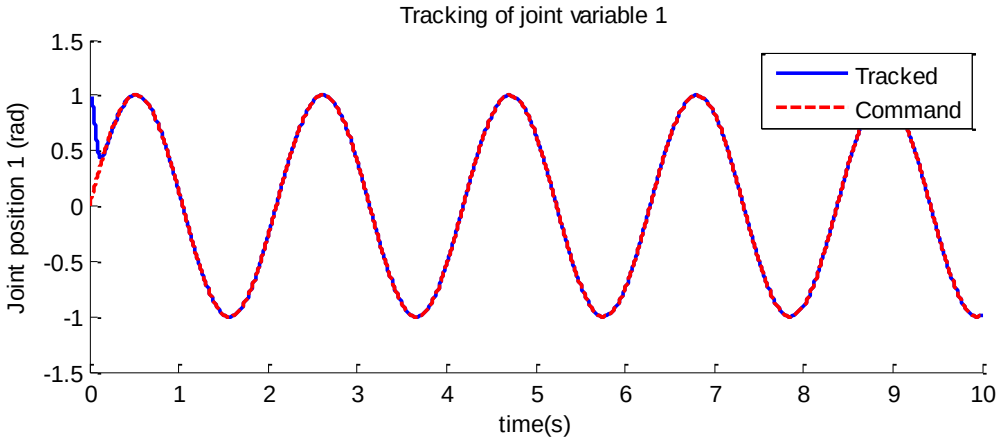

Figure 5.40:(ATSMC1) The actual joint variable and the command joint variable versus time 1

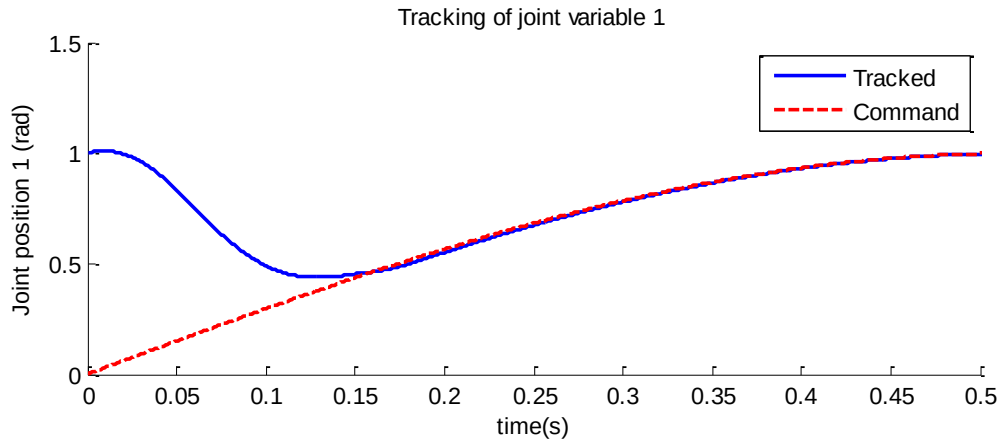

Figure 5.41:(ATSMC1) Zoom of the actual joint variable and the command joint variable versus time 1

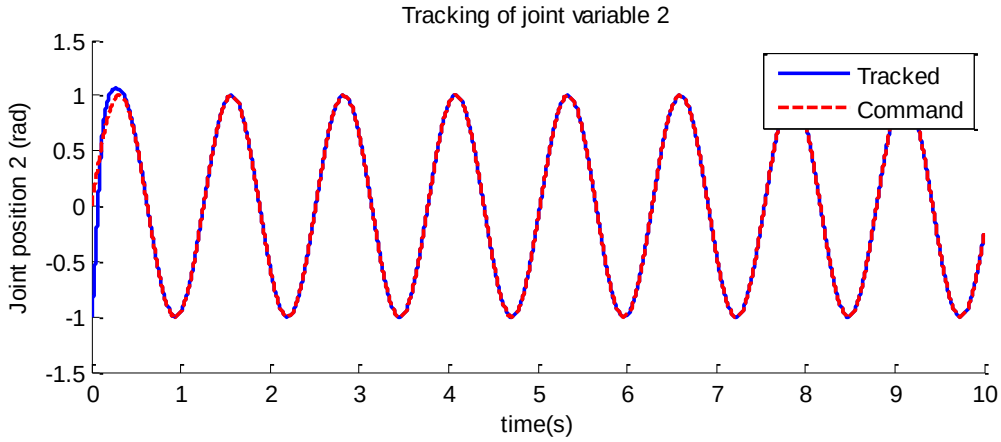

Figure 5.42: (ATSMC1) The actual joint variable and the command joint variable versus time 2

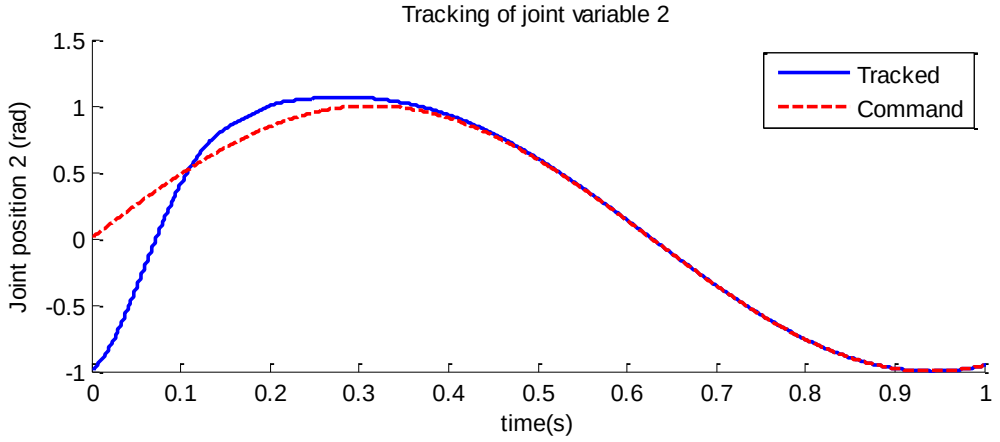

Figure 5.43: (ATSMC1) Zoom of the actual joint variable and the command joint variable versus time 2

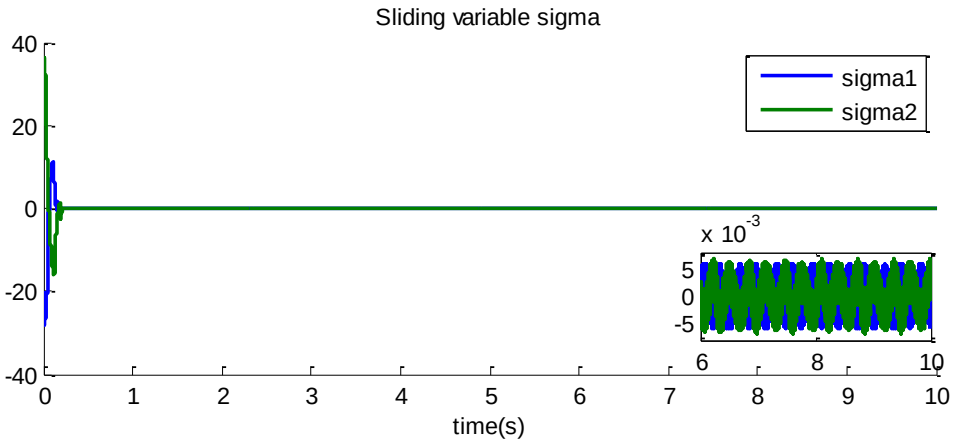

Figure 5.44: (ATSMC1) Sliding variables σ versus time

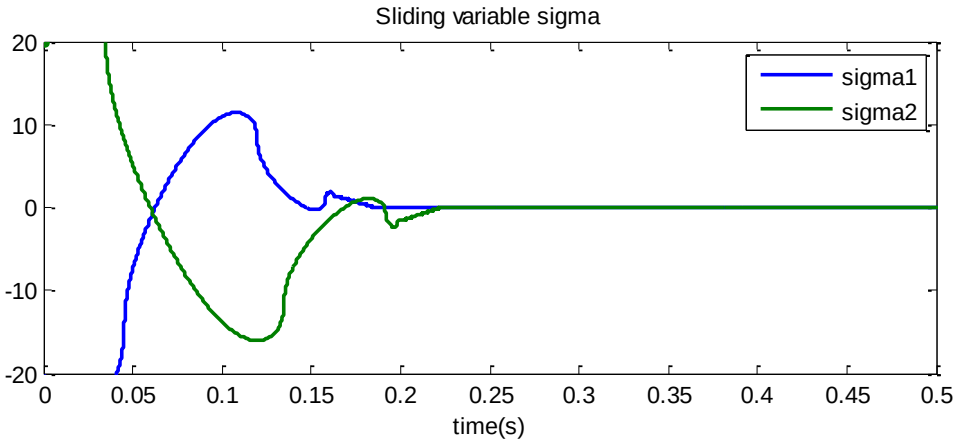

Figure 5.45: (ATSMC1) Zoom of the sliding variables σ versus time

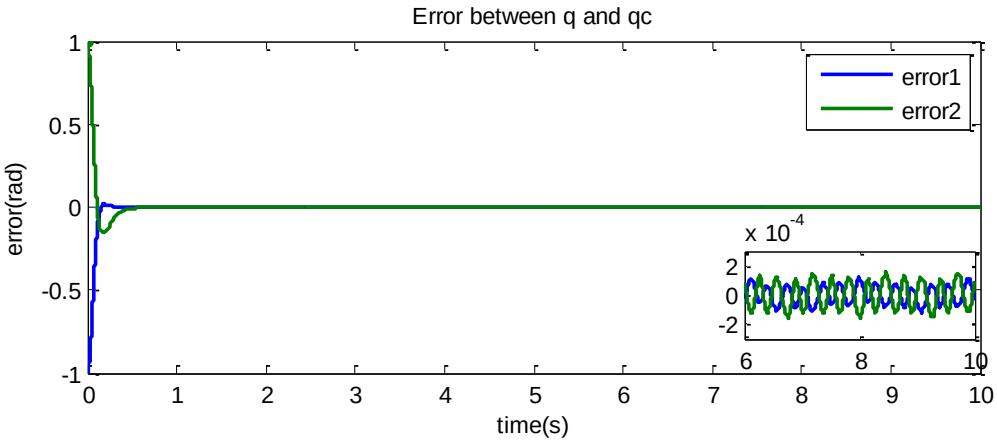

Figure 5.46: (ATSMC1) Error between the actual joint variables and the command joint variables versus time

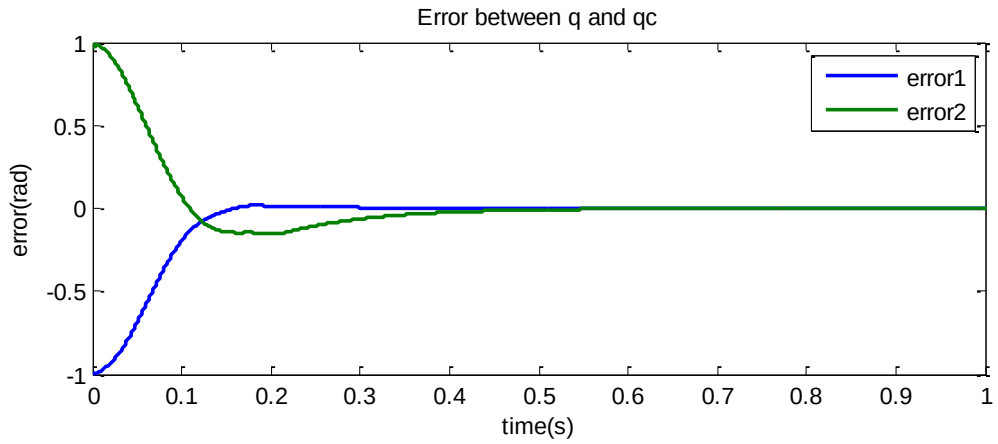

Figure 5.47: (ATSMC1) Zoom of the error between the actual joint variables and the command joint variables versus time

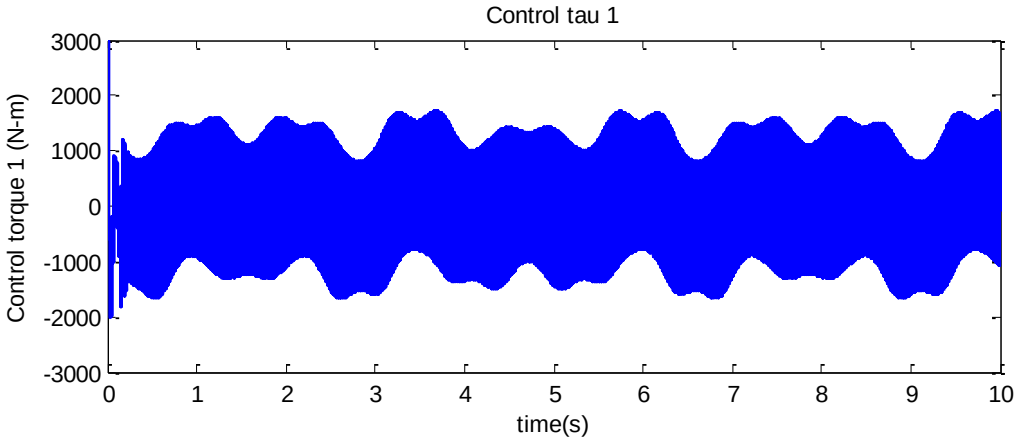

Figure 5.48: (ATSMC1) The control τ versus time 1

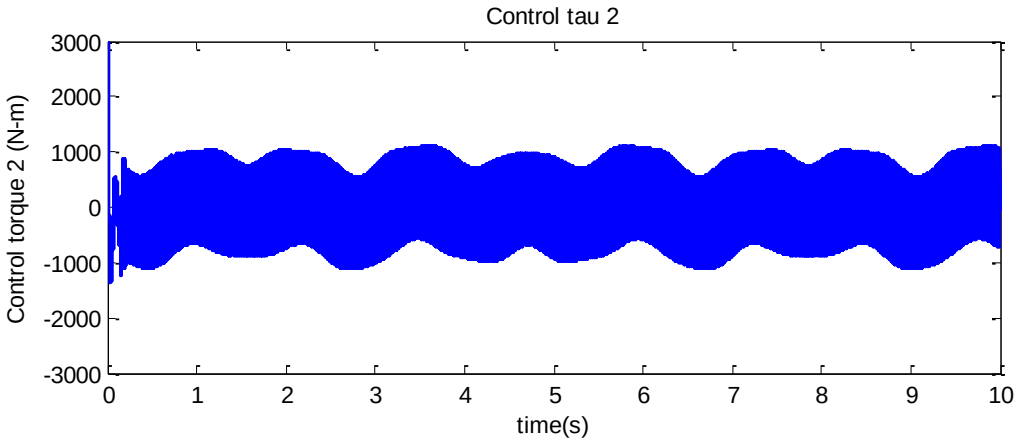

Figure 5.49: (ATSMC1) The control τ versus time 2

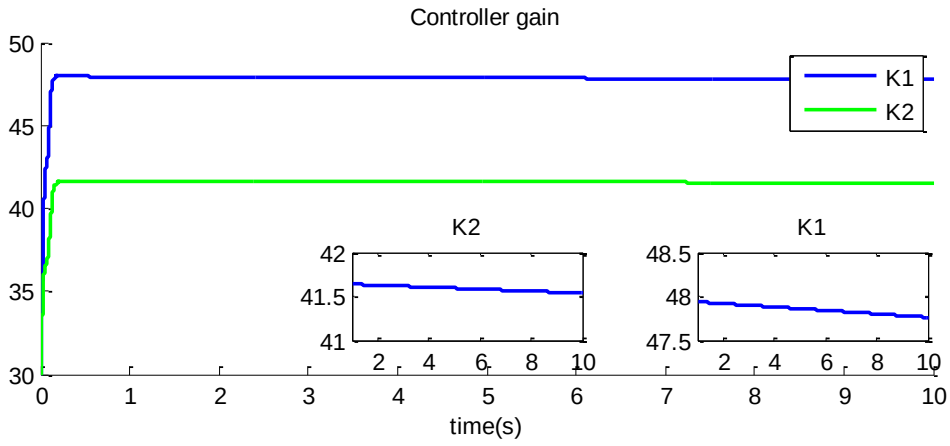

Figure 5.50: (ATSMC1) Controller gains versus time

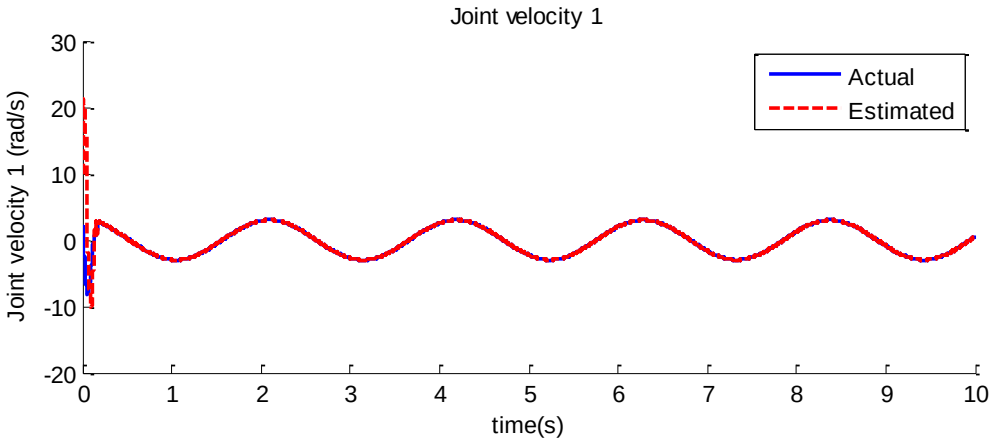

Figure 5.51: (ATSMC1) The actual joint velocity and the estimated joint velocity versus time 1

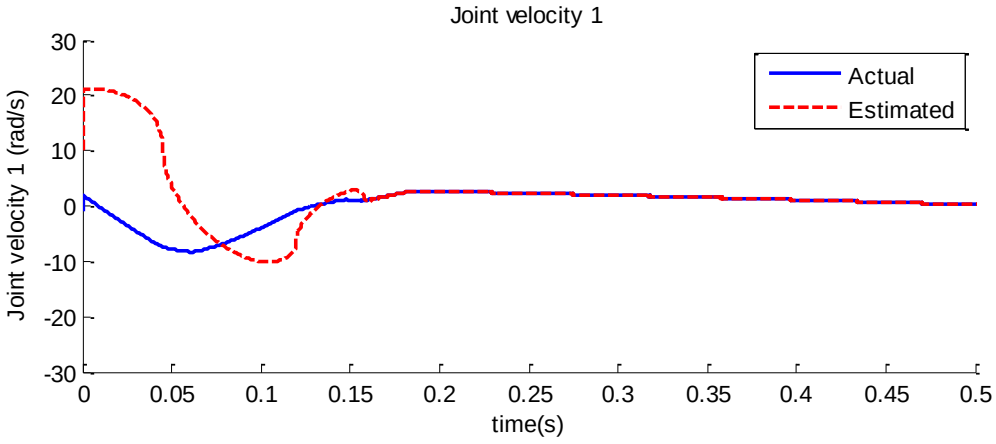

Figure 5.52: (ATSMC1) Zoom of the actual joint velocity and the estimated joint velocity versus time 1

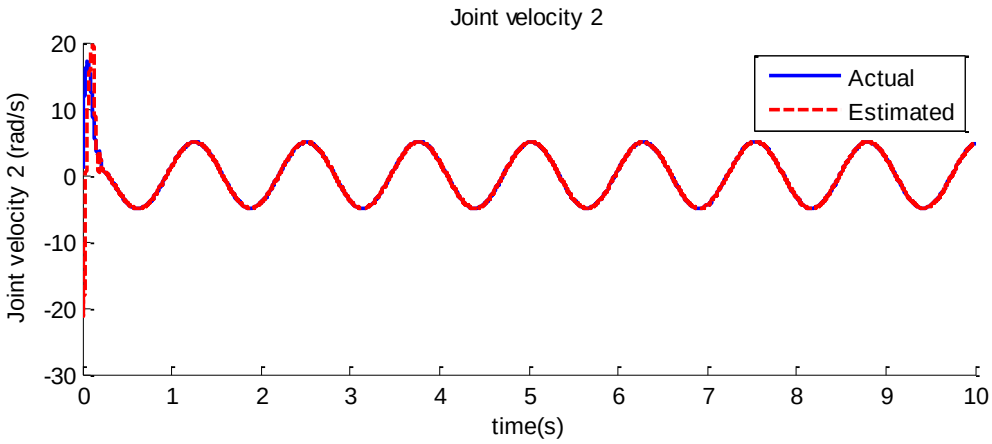

Figure 5.53: (ATSMC1) The actual joint velocity and the estimated joint velocity versus time 2

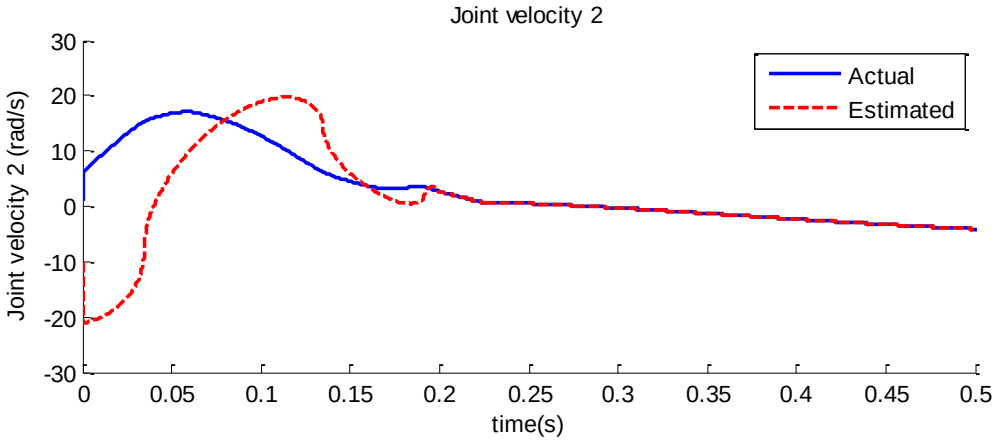

Figure 5.54: (ATSMC1) Zoom of the actual joint velocity and the estimated joint velocity versus time 2

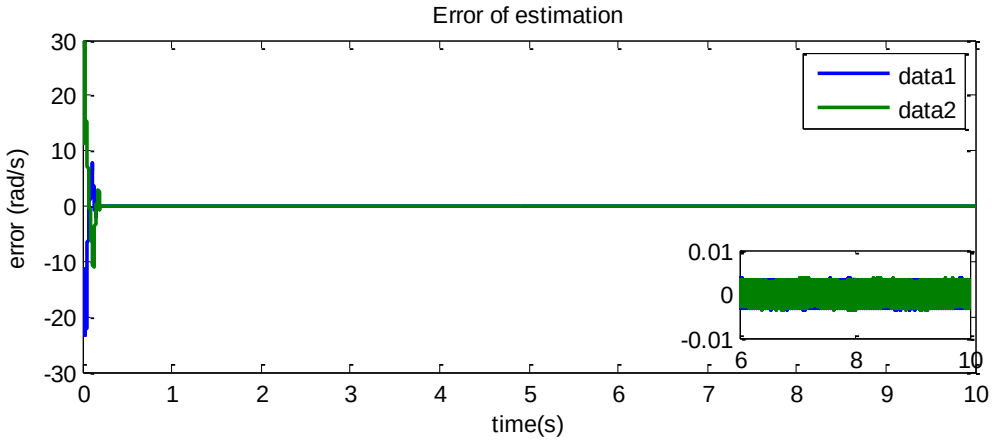

Figure 5.55: (ATSMC1) Error between the actual joint velocity and the estimated joint velocity versus time

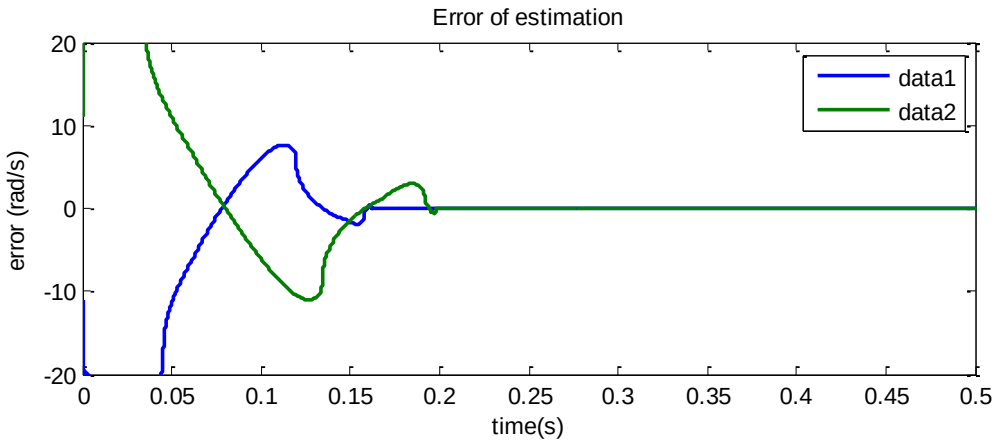

Figure 5.56: (ATSMC1) Zoom of the error between the actual joint velocity and the estimated joint velocity versus time

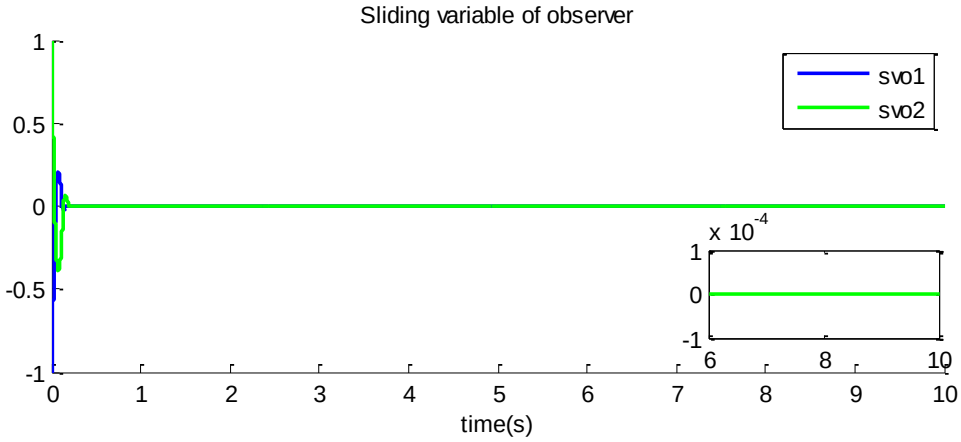

Figure 5.57: (ATSMC1) Sliding variable of observer versus time

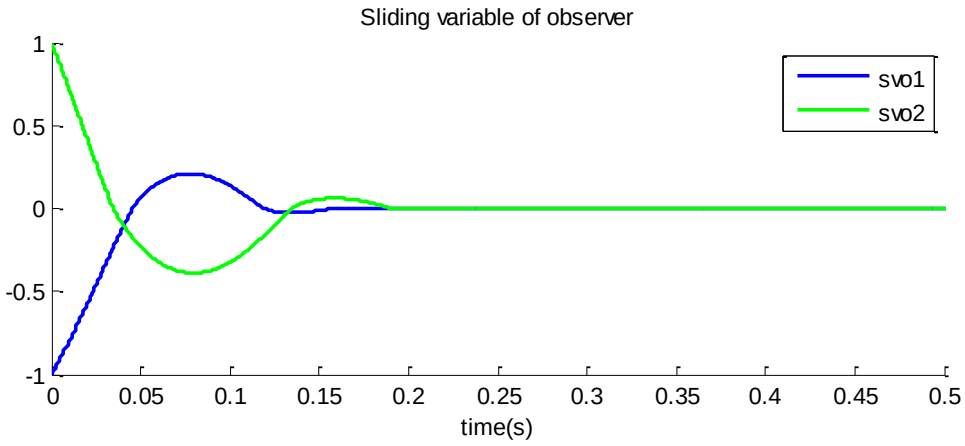

Figure 5.58: (ATSMC1) Zoom of the sliding variable of observer versus time

Figures 5.40-5.58 show the results of the traditional sliding mode control with gain adaptation. The initial value of each element of the vector of the controller gain is 30. In the corresponding row, the controller gain is increased until the sliding variable becomes a very small number; at that point, the controller gain begins to decrease again until it approaches the boundary of the disturbance (Figure 5.50). When the controller gain hits the boundary of the disturbance, the adaptive traditional sliding mode control then acts to once again increase the controller gain. These results show that the adaptive traditional sliding mode control is effective for the control of the robot manipulator without knowledge of the boundary of the disturbances/uncertainties, and without overestimation of the controller gain.

Simulation with the Second Adaptive-Gain TSMC (ATSMC1-2)

It is assumed that the boundary of the disturbance is not known. The controller gain K_i is defined by the second gain adaptation algorithm. The controller gain K_i increases much fast when the absolute value of sliding variable σ_i is larger than a certain defined value ε_i: $|\sigma_i| > \varepsilon_i$. On the other hand, the controller gain K_i decreases when the absolute value of sliding variable σ_i is smaller than a certain defined value ε_i: $|\sigma_i| < \varepsilon_i$. The controller gain K_i decreases much faster than that of the first adaptive-gain TSMC.

$$\sigma_i = \dot{e}_i + 10e_i$$

$$u_i = \ddot{q_{c_i}} - f_i(q, \dot{q}, t) + \lambda_i(\dot{e}_i) + K_i \cdot sign(\sigma_i)$$

$$\text{for } \dot{K}_i = \begin{cases} A_i + B_i sign(|\sigma_i| - \varepsilon_i) & K_i > \mu_i \\ \mu_i & K_i \leq \mu_i \end{cases}$$

$$\varepsilon_i = 0.1, \qquad \mu_i = 0.1, \qquad A_i = 20 \; for \; i = 1, 2, \qquad B_i = 30 \; for \; i = 1, 2$$

$$K_i(0) = 30 \; for \; i = 1, 2$$

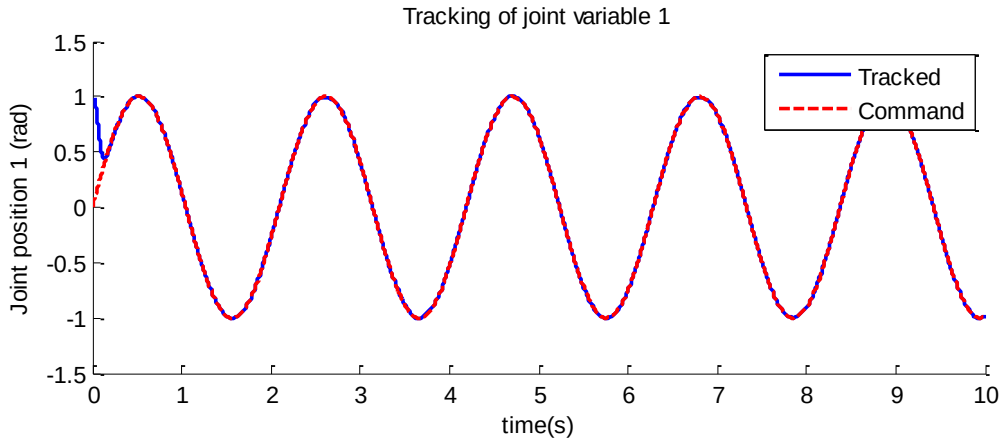

Figure 5.59: (ATSMC1-2) The actual joint variable and the command joint variable versus time 1

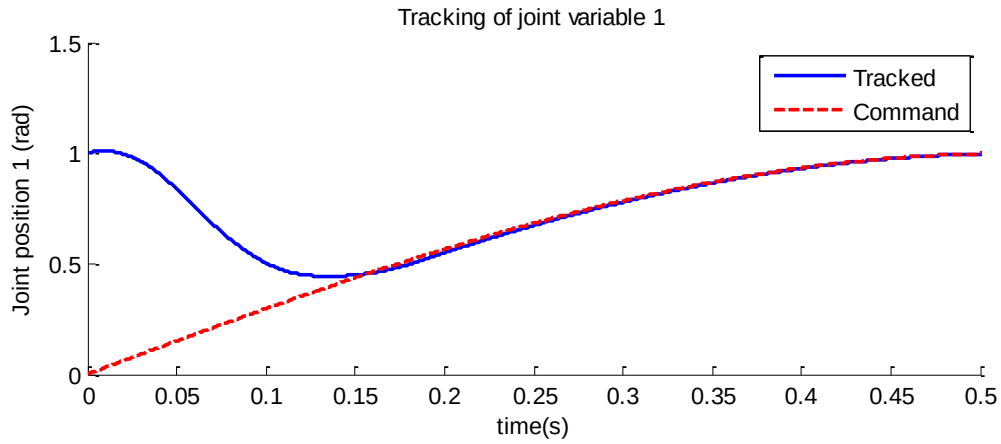

Figure 5.60: (ATSMC1-2) Zoom of the actual joint variable and the command joint variable versus time 1

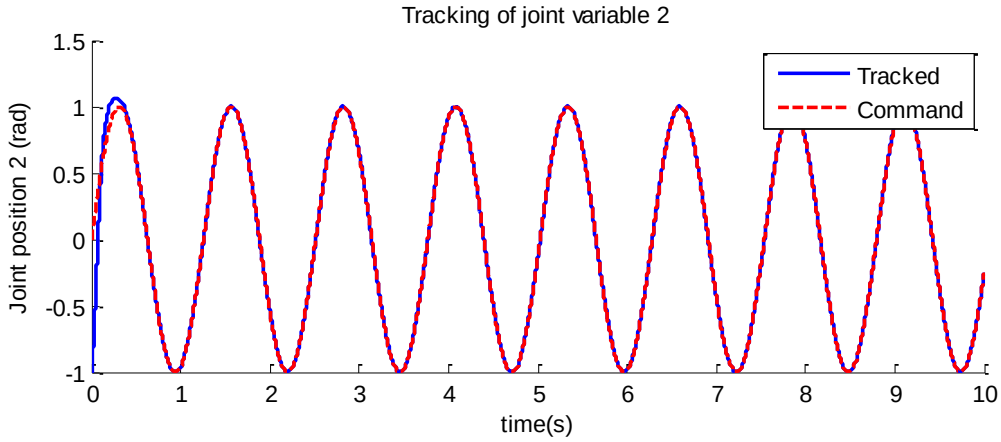

Figure 5.61: (ATSMC1-2) The actual joint variable and the command joint variable versus time 2

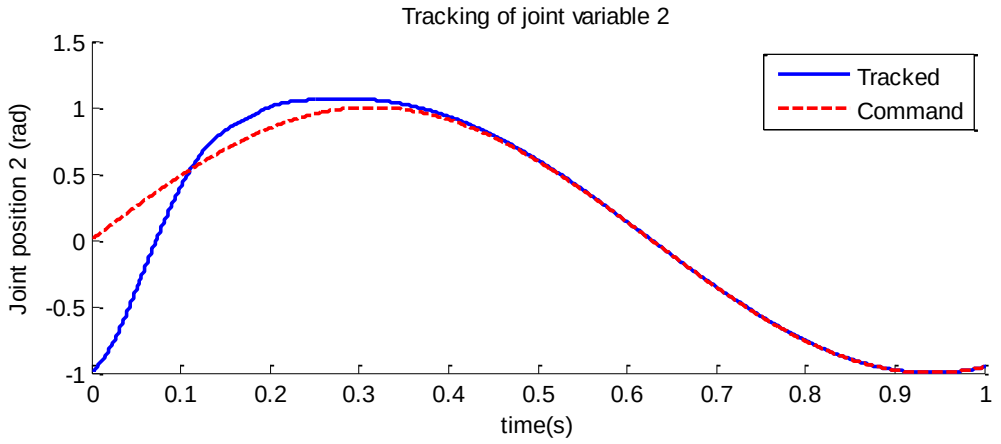

Figure 5.62: (ATSMC1-2) Zoom of the actual joint variable and the command joint variable versus time 2

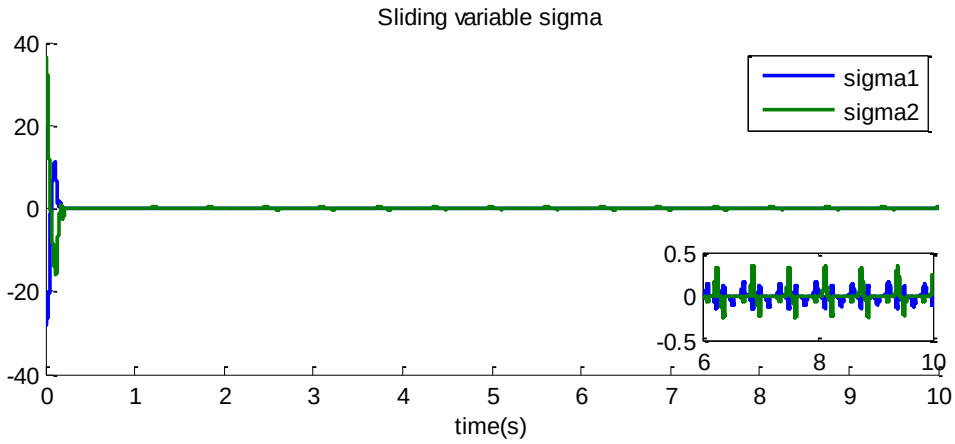

Figure 5.63: (ATSMC1-2) Sliding variable sigma versus time

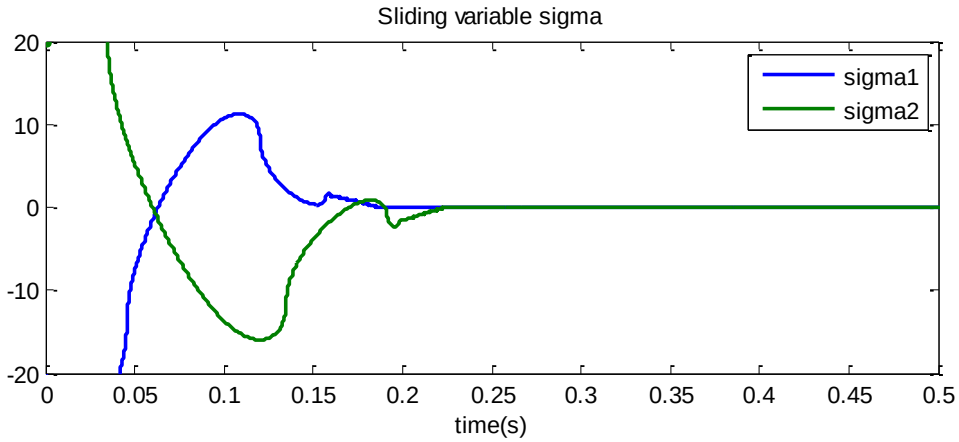

Figure 5.64: (ATSMC1-2) Zoom of the sliding variable sigma versus time

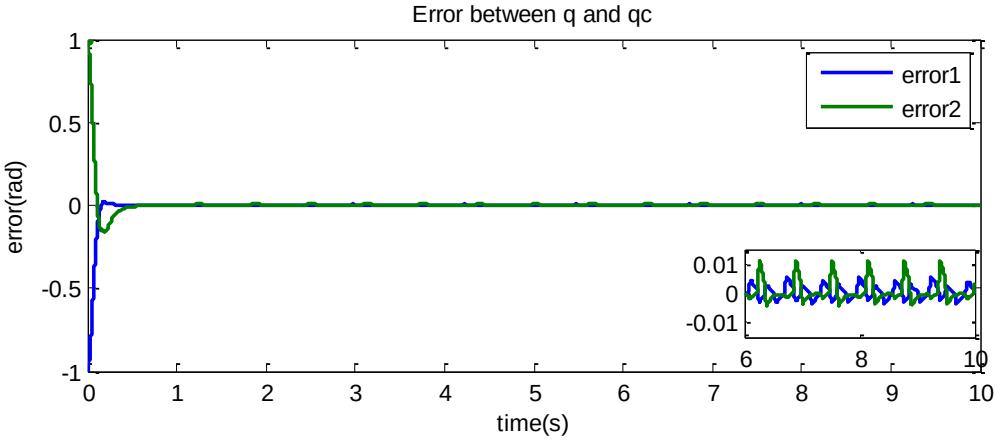

Figure 5.65: (ATSMC1-2) Error between the command joint variables and the actual joint variables versus time

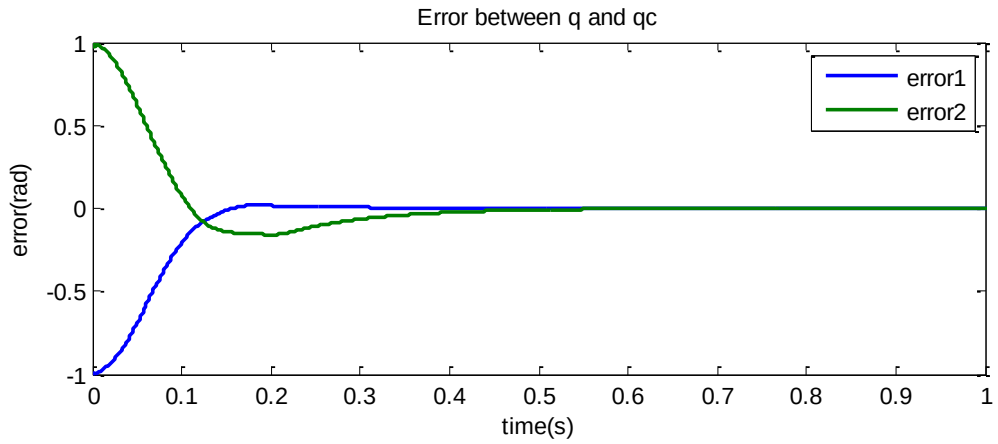

Figure 5.66: (ATSMC1-2) Zoom of the error between the command joint variables and the actual joint variables versus time

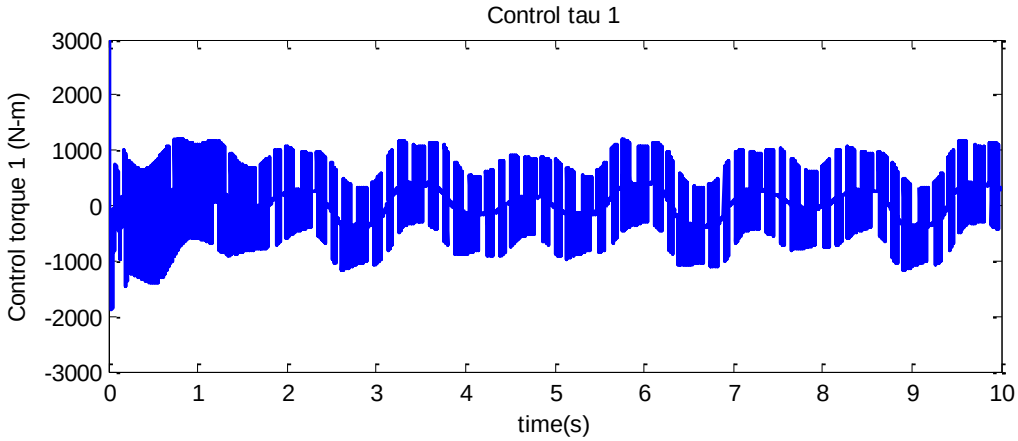

Figure 5.67: (ATSMC1-2) The control τ versus time1

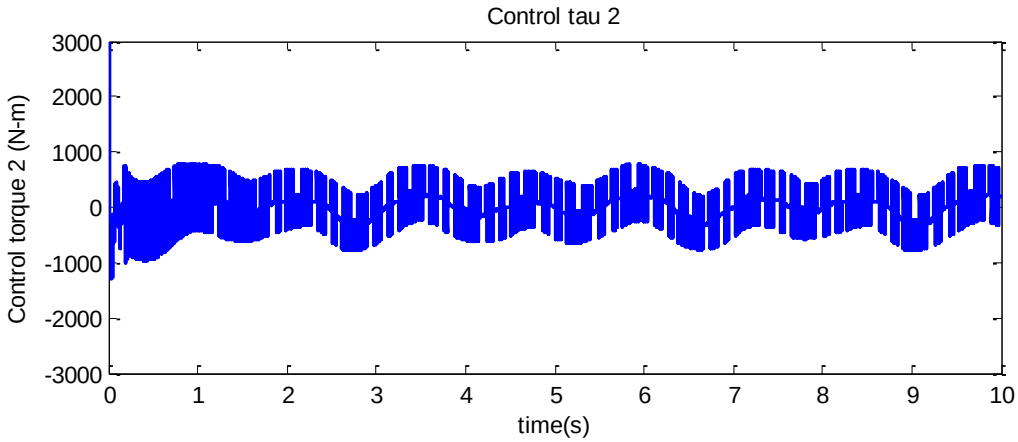

Figure 5.68: (ATSMC1-2) The control τ versus time 2

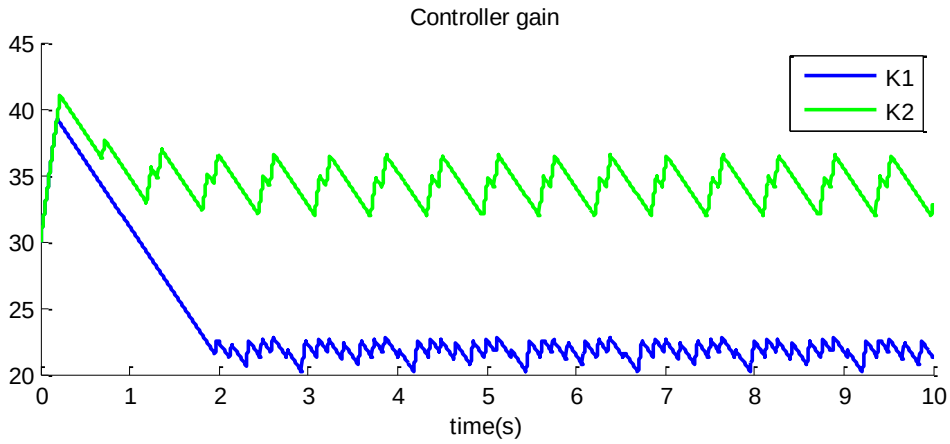

Figure 5.69: (ATSMC1-2) The controller gains versus time

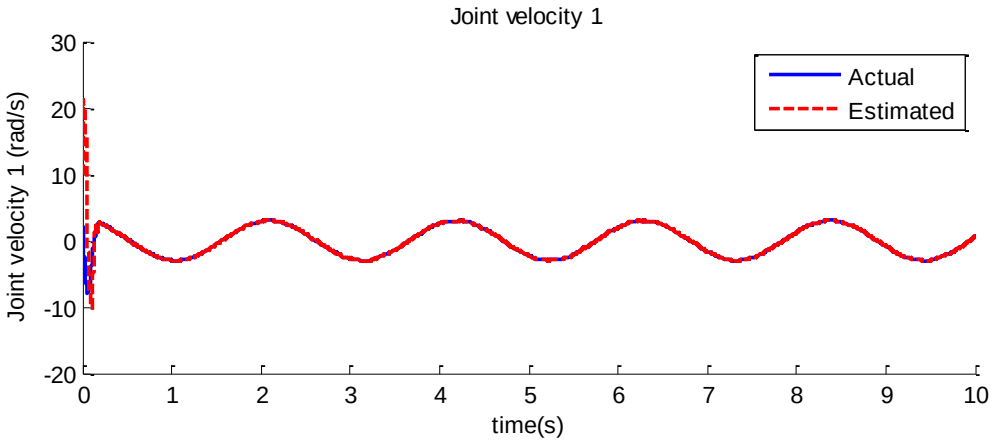

Figure 5.70: (ATSMC1-2) The actual joint velocity and the estimated joint velocity versus time 1

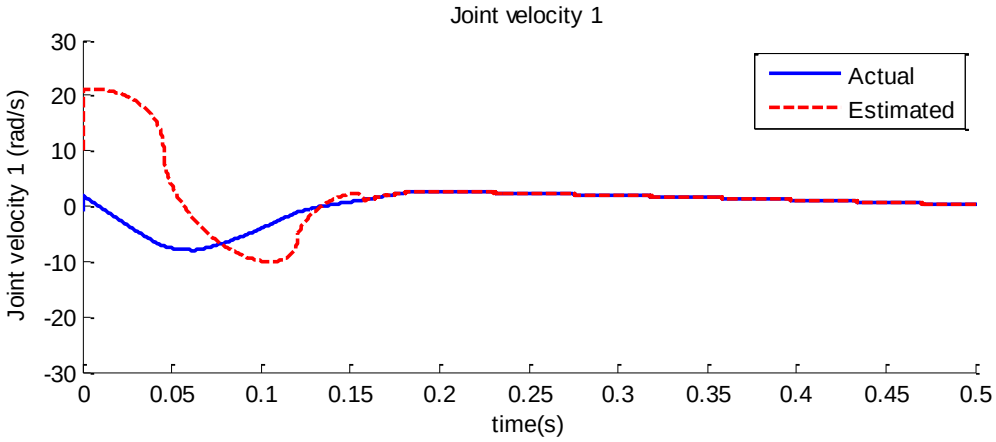

Figure 5.71: (ATSMC1-2) Zoom of the actual joint velocity and the estimated joint velocity versus time 1

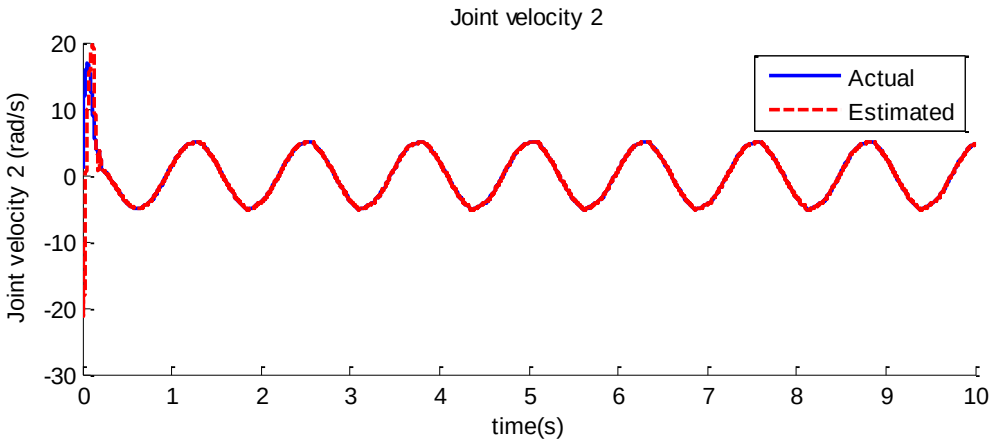

Figure 5.72: (ATSMC1-2) The actual joint velocity and the estimated joint velocity versus time 2

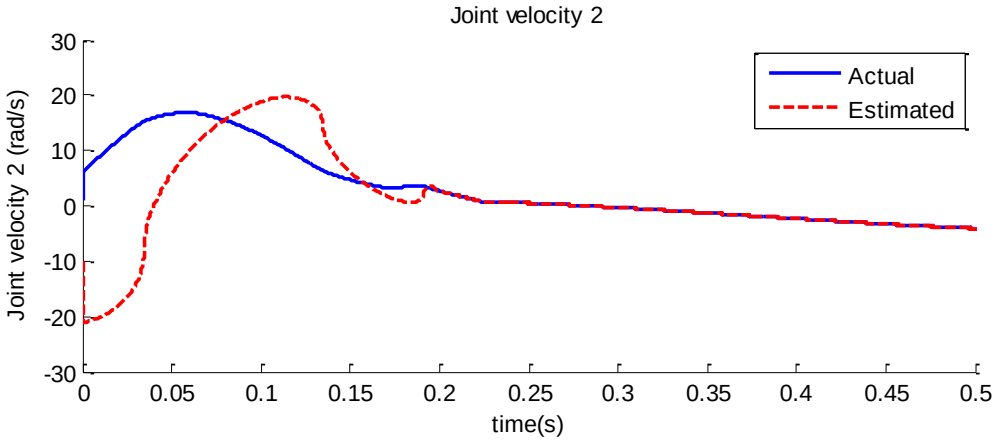

Figure 5.73: (ATSMC1-2) Zoom of the actual joint velocity and the estimated joint velocity versus time 2

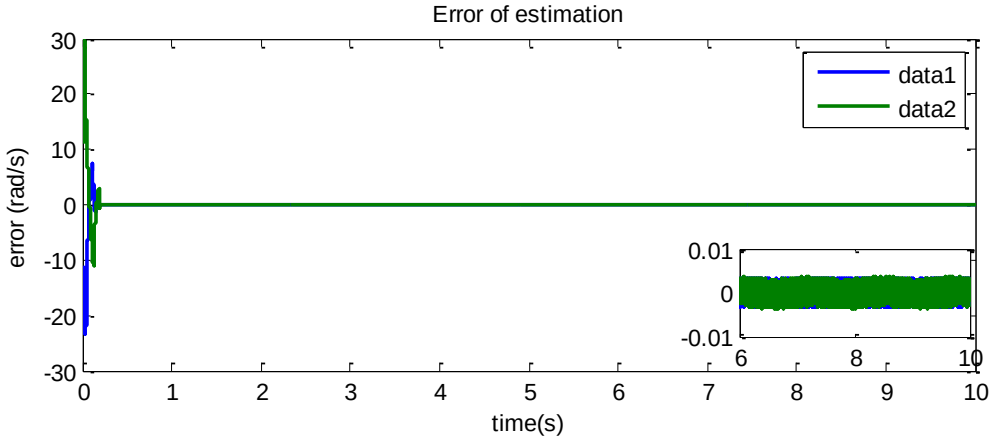

Figure 5.74: (ATSMC1-2) Error between the actual joint velocity and the estimated joint velocity versus time

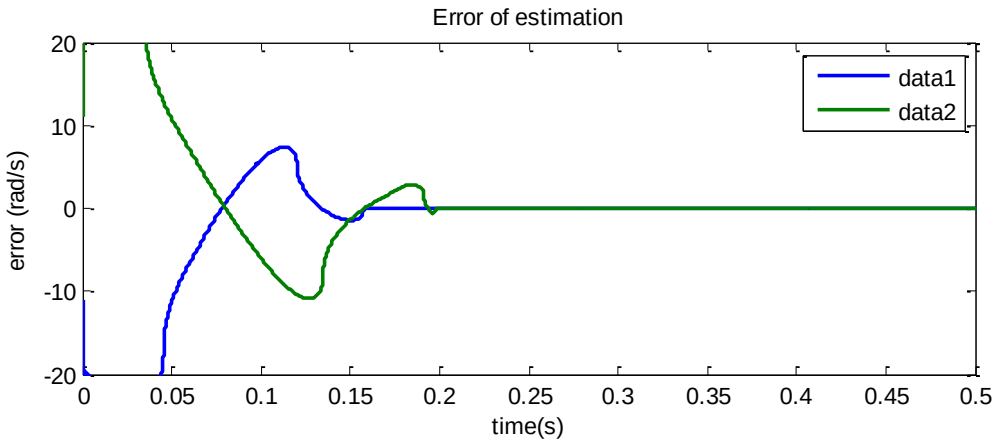

Figure 5.75: (ATSMC1-2) Zoom of the error between the actual joint velocity and the estimated joint velocity versus time

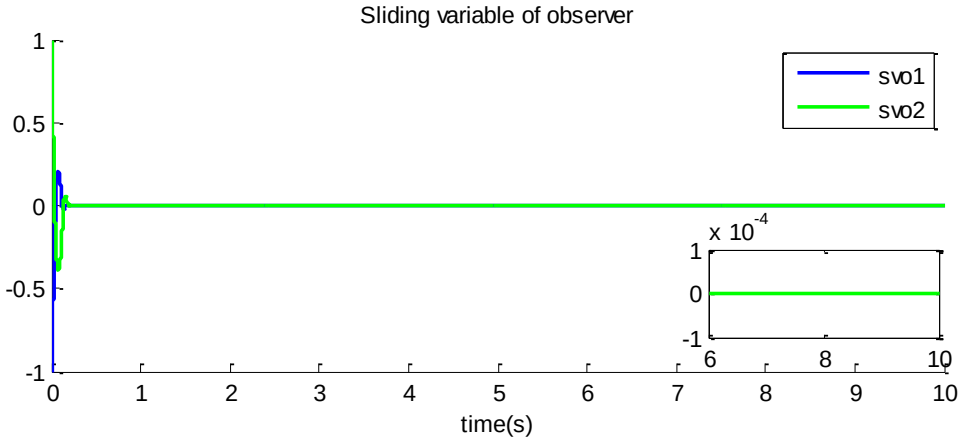

Figure 5.76: (ATSMC1-2) Sliding variable of observer versus time

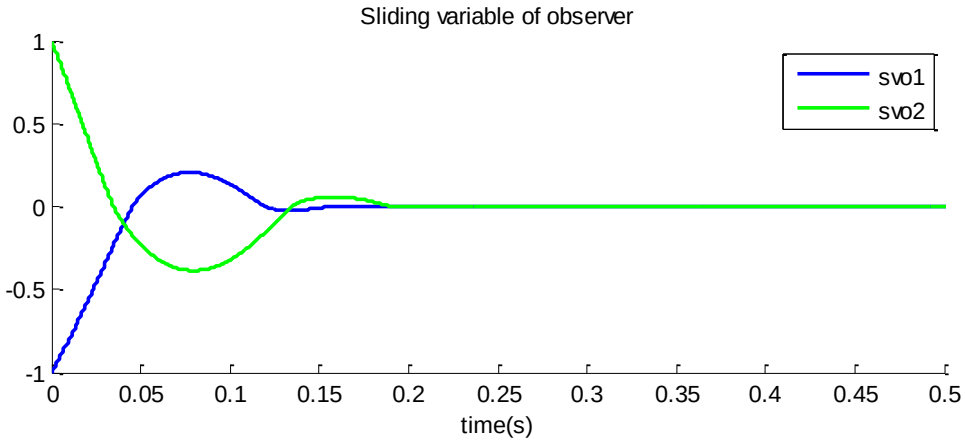

Figure 5.77: (ATSMC1-2) Zoom of the sliding variable of observer versus time

Figures 5.59-5.77 show the results of the simulation of the second adaptive sliding mode control with 2-link robot manipulator. The controller gain decreases much faster than the controller gain which is obtained in (ATSMC1) (Figure 5.50 and Figure 5.69). In the corresponding row, the controller gain increases much faster than the speed of decrease, when the controller gain becomes smaller than the boundary of the disturbance.

5.2.3. Parameters of Simulation for Auxiliary Sliding Variable $s = \dot{\sigma} + 10\sigma$

1) Traditional sliding mode control design (TSMC2), (TSMC2-2)

   The controller gain K_i is constant in this controller design; without gain adaptation. The controller gain K_i is to be estimated by using the information which is given in the simulation parameters.

$$\sigma_i = \dot{e}_i + 10e_i$$

$$s_i = \dot{\sigma}_i + 10\sigma_i$$

$$\dot{u}_i = \ddot{q}_{c_i} - \dot{f}_i(q, \dot{q}, t) + 20\{\ddot{q}_{c_i} - u_i - f_i(q, \dot{q}, t)\} + 100\dot{e}_i + K_i \cdot sign(s_i)$$

2) The first adaptive-gain traditional sliding mode control design (ATSMC2)

   The controller gain K_i is to be defined by the first gain adaptation algorithm in this controller design. This adaptive-gain traditional sliding mode control does not overestimate the boundary of the disturbances/uncertainties. The gain adaptation mitigates chattering by means of the decrease of the controller gain. The speed of decrease is very slow.

$$\sigma_i = \dot{e}_i + 10e_i$$

$$s_i = \dot{\sigma}_i + 10\sigma_i$$

$$\dot{u}_i = \ddot{q}_{c_i} - \dot{f}_i(q, \dot{q}, t) + 20\{\ddot{q}_{c_i} - u_i - f_i(q, \dot{q}, t)\} + 100\dot{e}_i + K_i \cdot sign(s_i)$$

$$\text{for } \dot{K}_i = \begin{cases} \overline{K}_i |s_i| sign(|s_i| - \varepsilon_i) & K_i > \mu_i \\ \mu_i & K_i \leq \mu_i \end{cases}$$

$$\varepsilon_i = 1, \qquad \mu_i = 0.1, \qquad \overline{K}_i = 20 \; for \; i = 1, 2$$

$$K_i(0) = 1300 \; for \; i = 1, 2$$

3) The second adaptive-gain traditional sliding mode control design (ATSMC2-2)

The controller gain K_i is to be defined by the second gain adaptation algorithm in this controller design. This adaptive-gain traditional sliding mode control decreases the controller gain much faster than the first adaptive-gain traditional sliding mode control does.

$$\sigma_i = \dot{e}_i + 10e_i$$

$$s_i = \dot{\sigma}_i + 10\sigma_i$$

$$\dot{u}_i = \ddot{q}_{c_i} - \dot{f}_i(q, \dot{q}, t) + 20\{\ddot{q}_{c_i} - u_i - f_i(q, \dot{q}, t)\} + 100\dot{e}_i + K_i \cdot sign(s_i)$$

$$\text{for } \dot{K}_i = \begin{cases} A_i + B_i sign(|s_i| - \varepsilon_i) & K_i > \mu_i \\ \mu_i & K_i \le \mu_i \end{cases}$$

$$\varepsilon_i = 1, \qquad \mu_i = 0.1, \qquad A_i = 40 \; for \; i = 1, 2, \qquad B_i = 60 \; for \; i = 1, 2$$

$$K_i(0) = 1300 \; for \; i = 1, 2$$

5.2.4. Simulations for Auxiliary Sliding Variable $s = \dot{\sigma} + 10\sigma$, (TSMC2), (TSMC2-2), (ATSMC2), (ATSMC2-2)

The goal of this simulation is to show that the adaptive traditional sliding mode control decreases the controller gain without violating the stability.

Simulation without gain adaptation (TSMC2)

It assumed that the boundary of the disturbance is known, and the controller gain K_i is estimated from the given parameters in this simulation. The controller gain K_i is estimated as follows by using Inequality (4.16):

$$\left|\dot{d}_i(q,\dot{q},t) + (\lambda_i + \omega_i)d_i(q,\dot{q},t)\right| < K_i, \qquad \lambda_i = \omega_i = 10 \; for \; i = 1{,}2$$

where $d_i = M^{-1}\tau_{d_i}$, and the disturbance τ_d is given in simulation parameters as:

$$\tau_d = \begin{bmatrix}\tau_{1d}\\ \tau_{2d}\end{bmatrix} = \begin{bmatrix}20 \cdot \sin(10t)\\ 30 \cdot \sin(20t)\end{bmatrix}$$

It is impossible to estimate the boundary of Inequality (4.16) exactly, but it is thinkable that the boundary of Inequality (4.16) is less than 2000. The controller gain K_i is set to 1500 for i=1,2.

$$\sigma_i = \dot{e}_i + 10e_i, \qquad s_i = \dot{\sigma}_i + 10\sigma_i$$

$$\dot{u}_i = \ddot{q}_{c_i} - \dot{f}_i(q,\dot{q},t) + 20\left\{\ddot{q}_{c_i} - u_i - f_i(q,\dot{q},t)\right\} + 100\dot{e}_i + K_i \cdot sign(s_i)$$

$$K_i = 1500 \; for \; i = 1,2$$

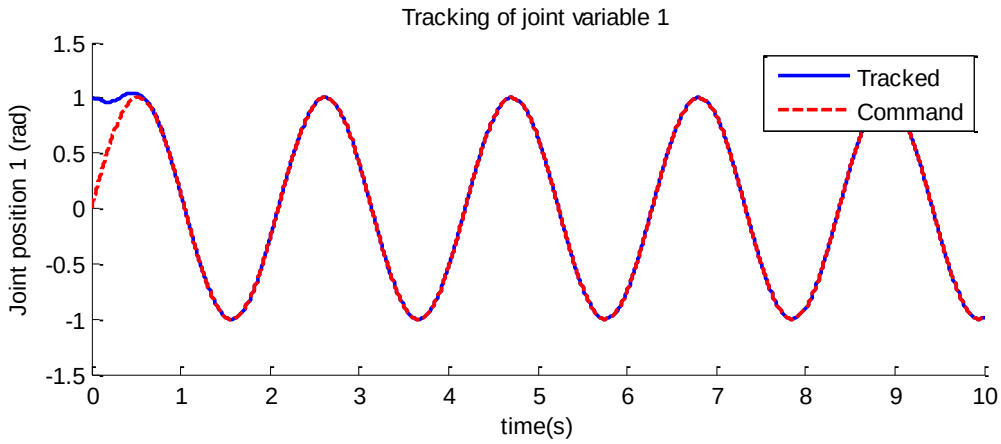

Figure 5.78: (TSMC2) The actual joint variable and the command of joint variable versus time 1

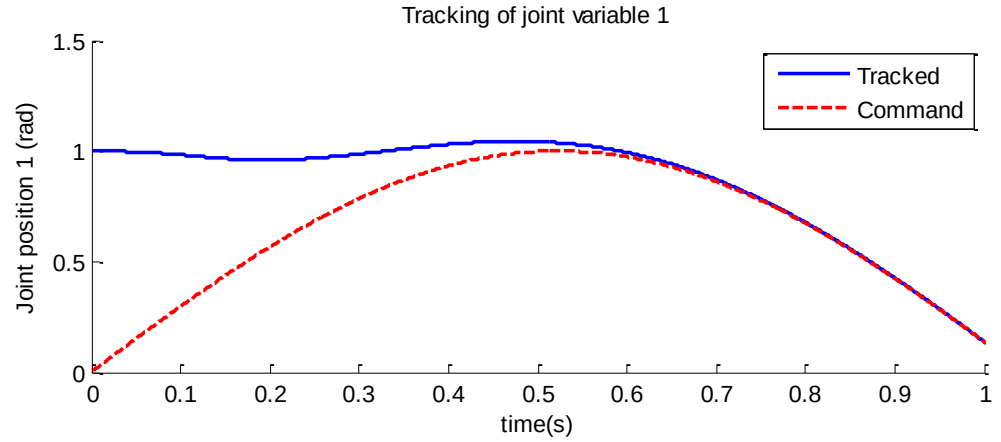

Figure 5.79: (TSMC2) Zoom of the actual joint variable and the command of joint variable versus time 1

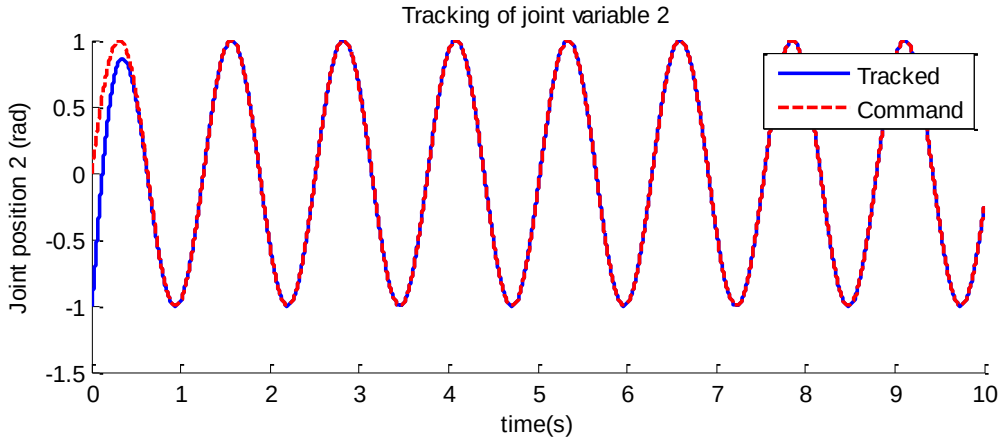

Figure 5.80: (TSMC2) The actual joint variable and the command of joint variable versus time 2

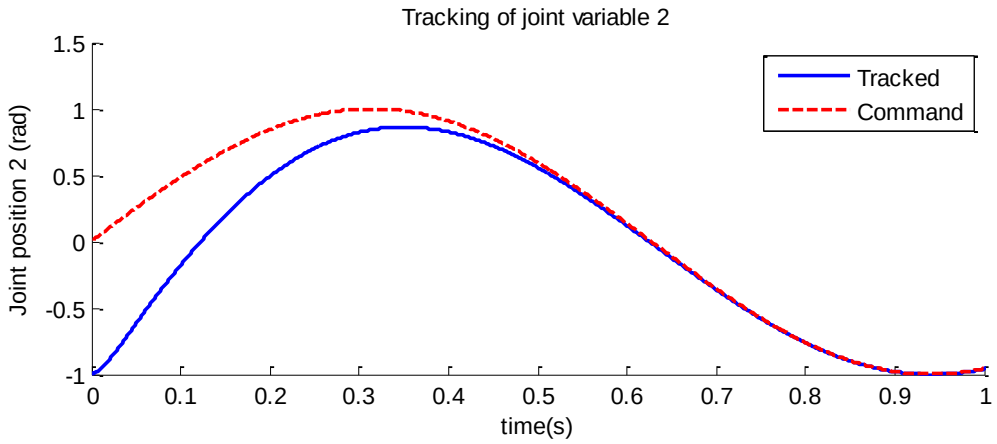

Figure 5.81: (TSMC2) Zoom of the actual joint variable and the command of joint variable versus time 2

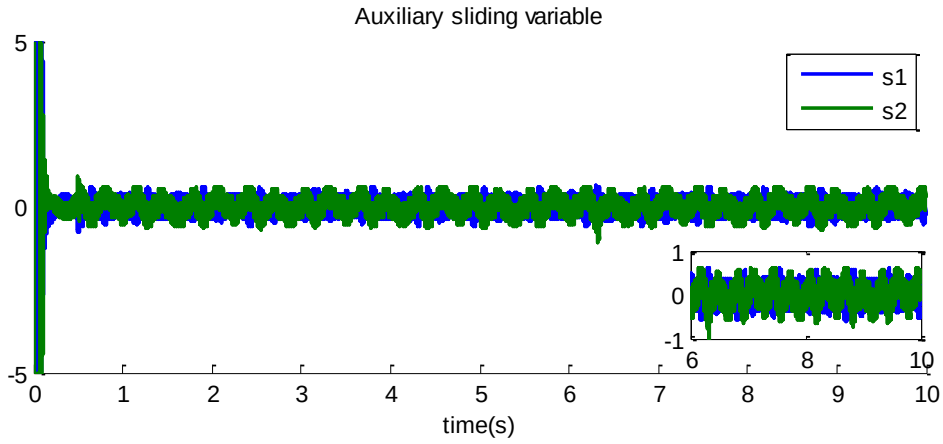

Figure 5.82: (TSMC2) Auxiliary sliding variables versus time

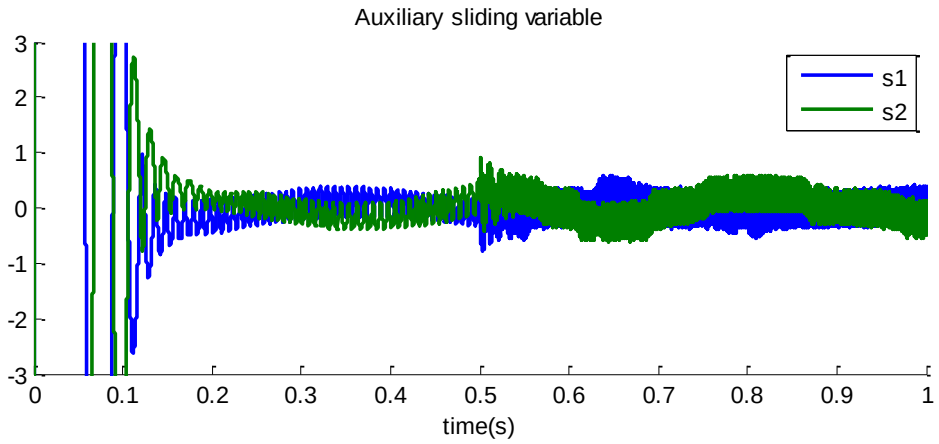

Figure 5.83: (TSMC2) Zoom of the auxiliary sliding variables versus time

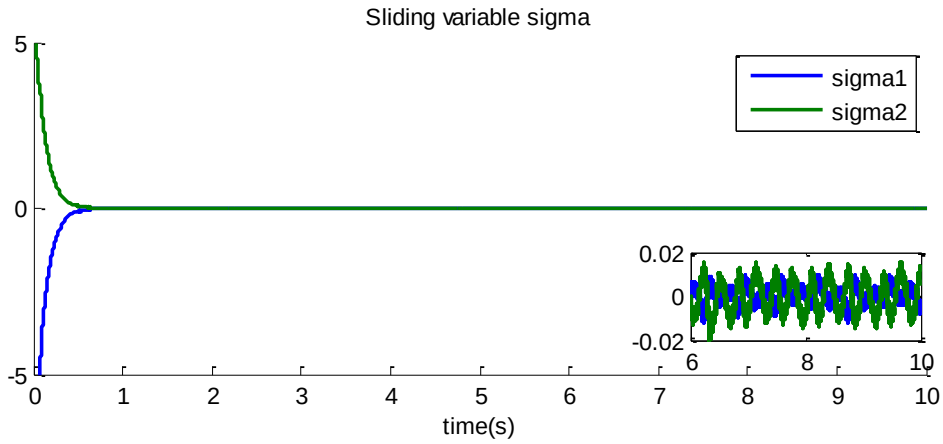

Figure 5.84: (TSMC2) Sliding variables σ versus time

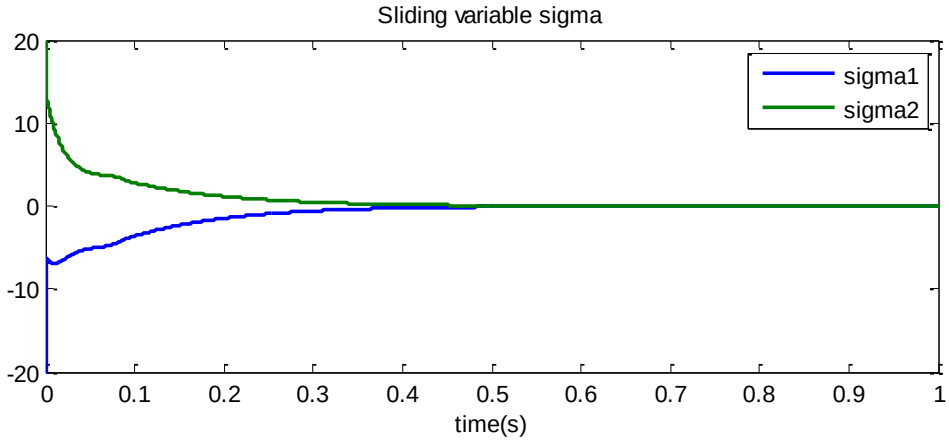

Figure 5.85: (TSMC2) Zoom of the sliding variables σ versus time

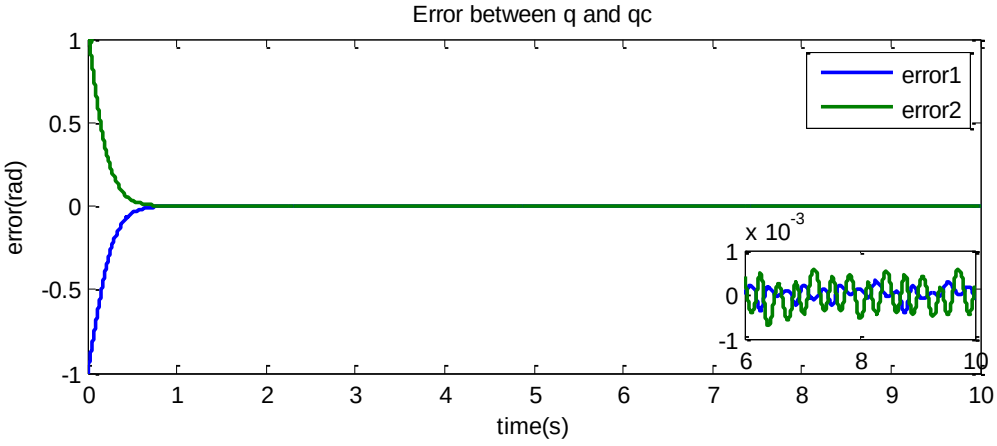

Figure 5.86: (TSMC2) Error between the command joint variables and the actual joint variables versus time

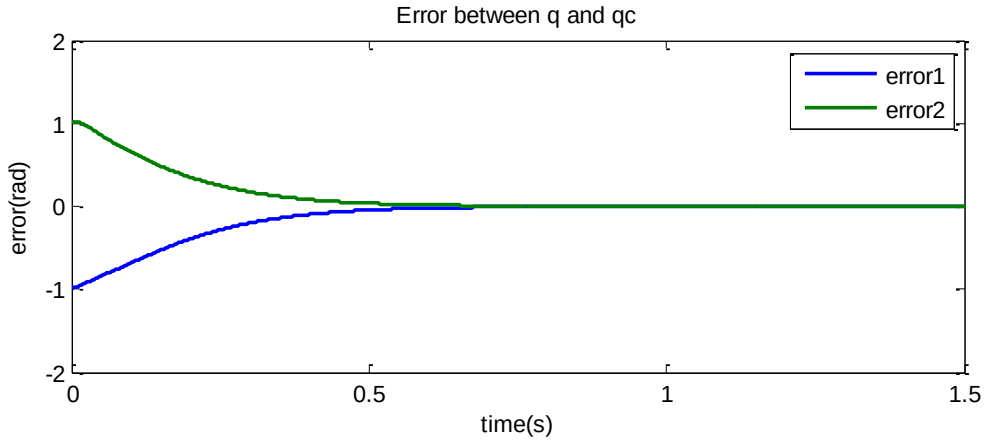

Figure 5.87: (TSMC2) Zoom of the error between the command joint variables and the actual joint variables versus time

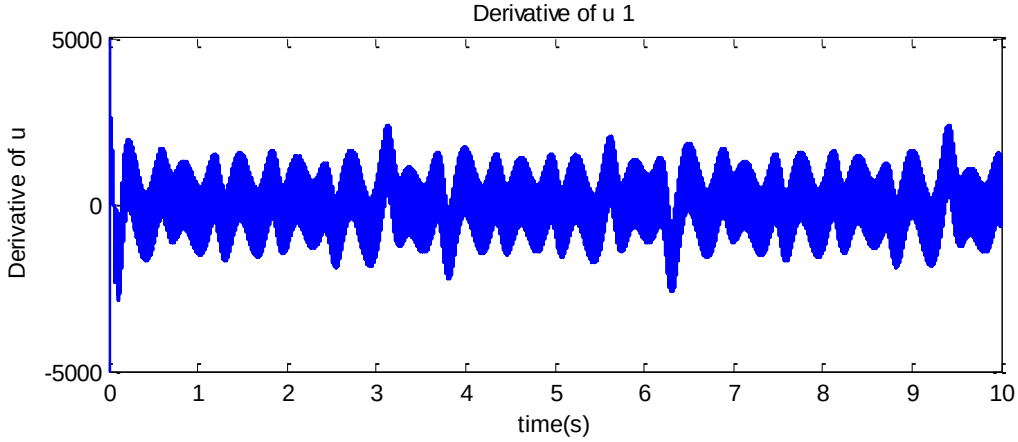

Figure 5.88: (TSMC2) The derivative of control *u* 1

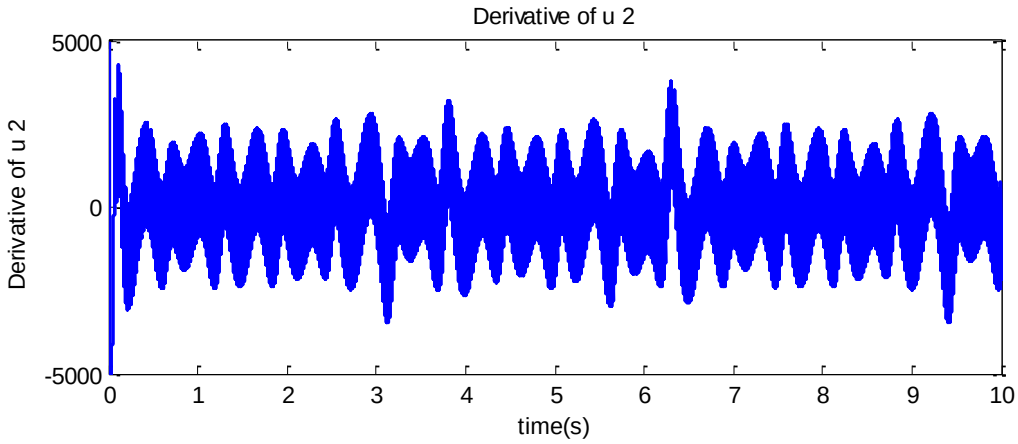

Figure 5.89: (TSMC2) The derivative of control *u* 2

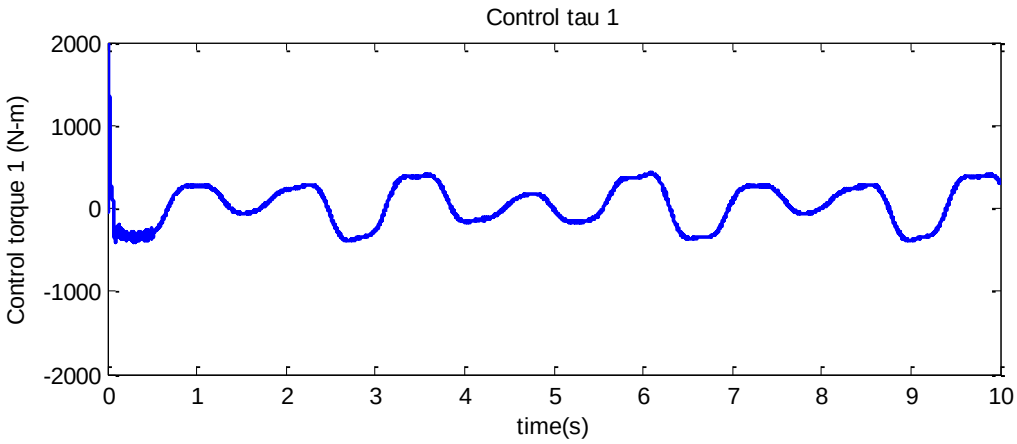

Figure 5.90: (TSMC2) The control τ versus time 1

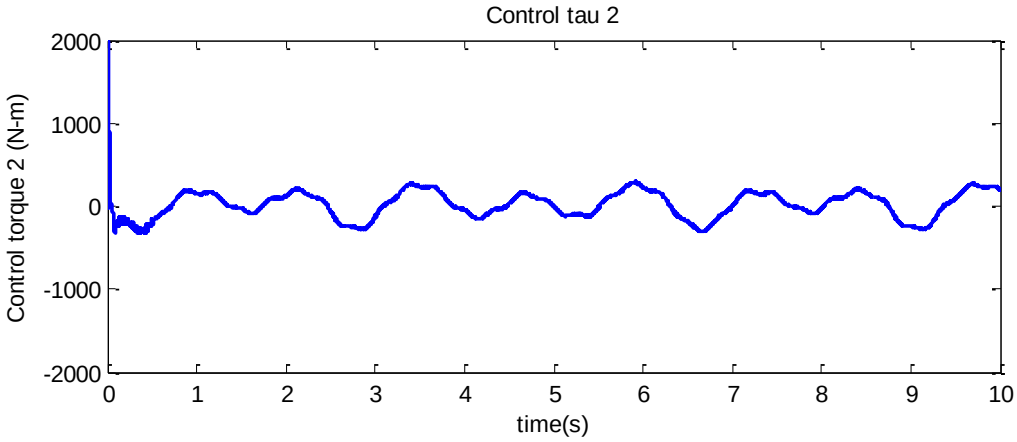

Figure 5.91: (TSMC2) The control τ versus time 2

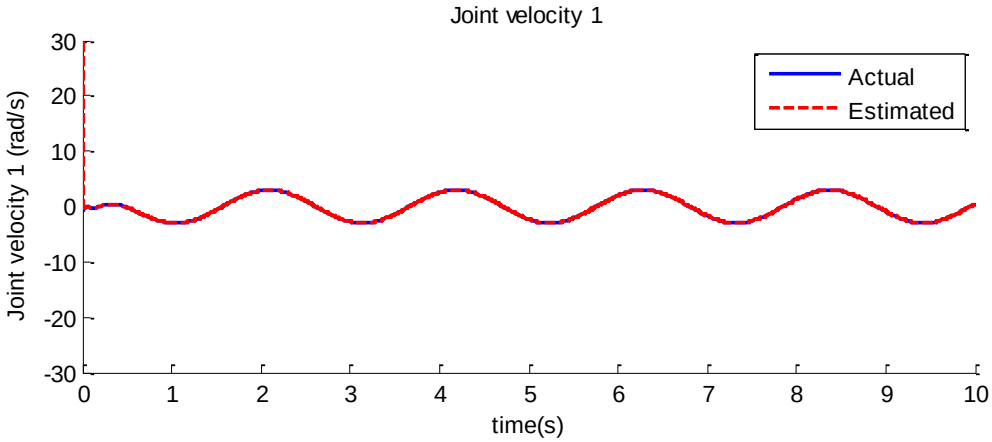

Figure 5.92: (TSMC2) The actual joint velocity and the estimated joint velocity versus time 1

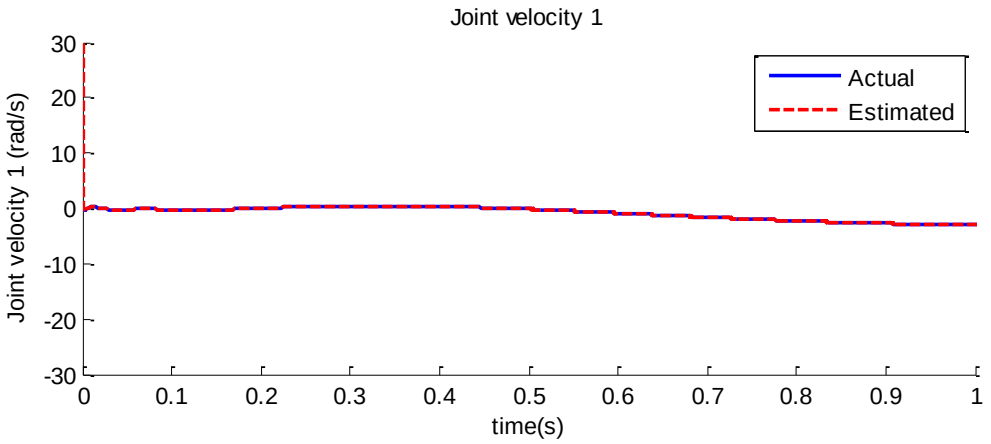

Figure 5.93: (TSMC2) Zoom of the actual joint velocity and the estimated joint velocity versus time 1

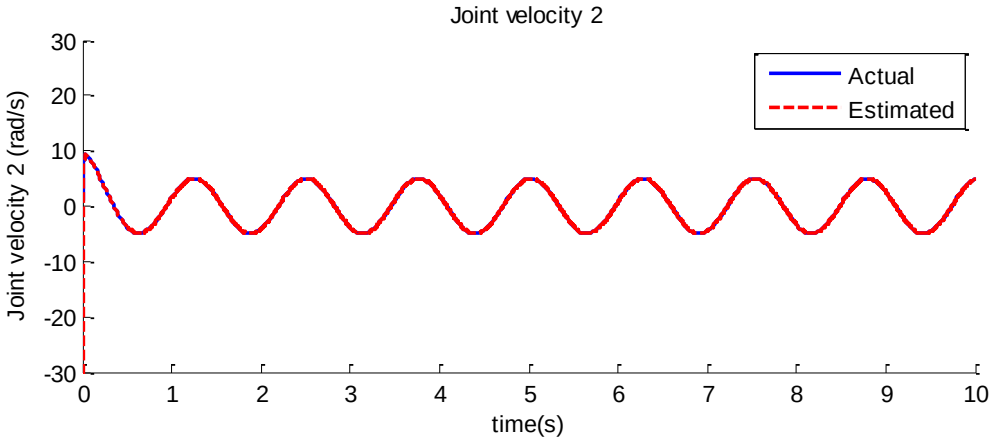

Figure 5.94: (TSMC2) The actual joint velocity and the estimated joint velocity versus time 2

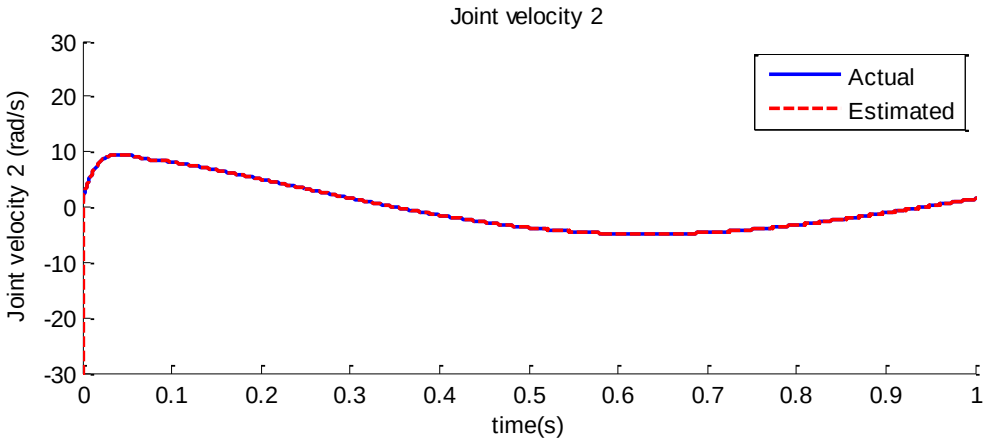

Figure 5.95: (TSMC2) Zoom of the actual joint velocity and the estimated joint velocity versus time 2

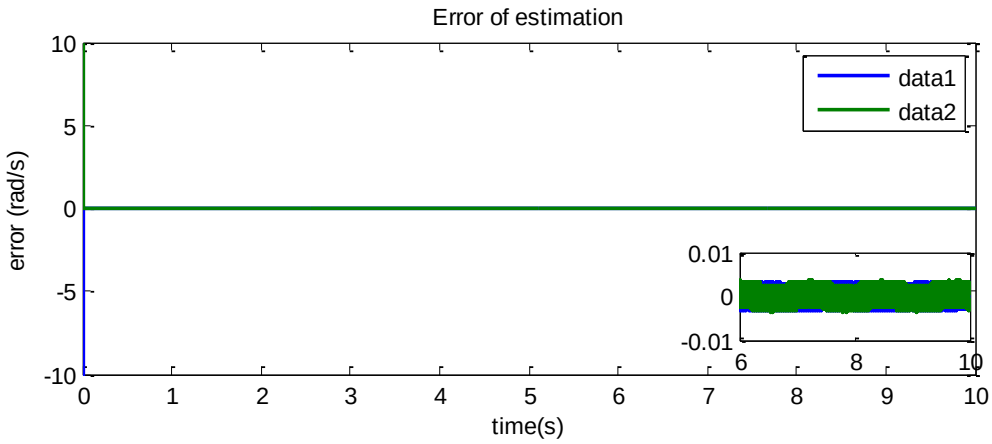

Figure 5.96: (TSMC2) Error between the actual joint velocity and the estimated joint velocity versus time

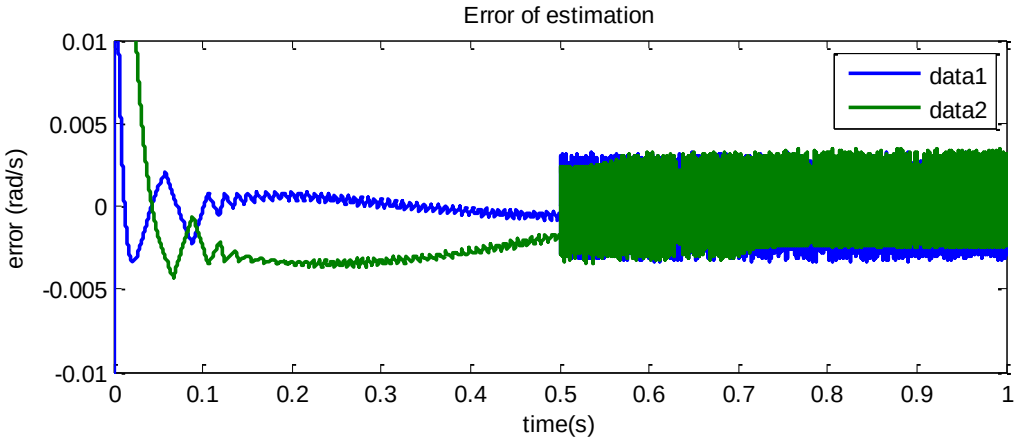

Figure 5.97: (TSMC2) Error between the actual joint velocity and the estimated joint velocity versus time

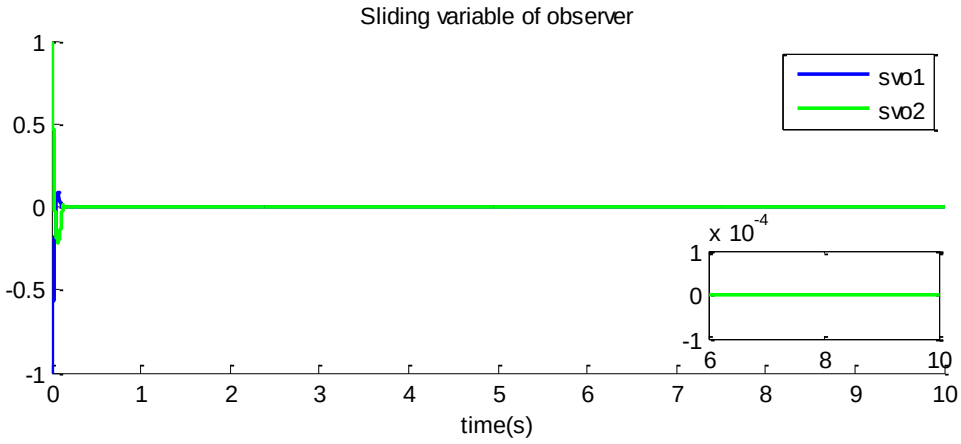

Figure 5.98: (TSMC2) Sliding variables of observer versus time

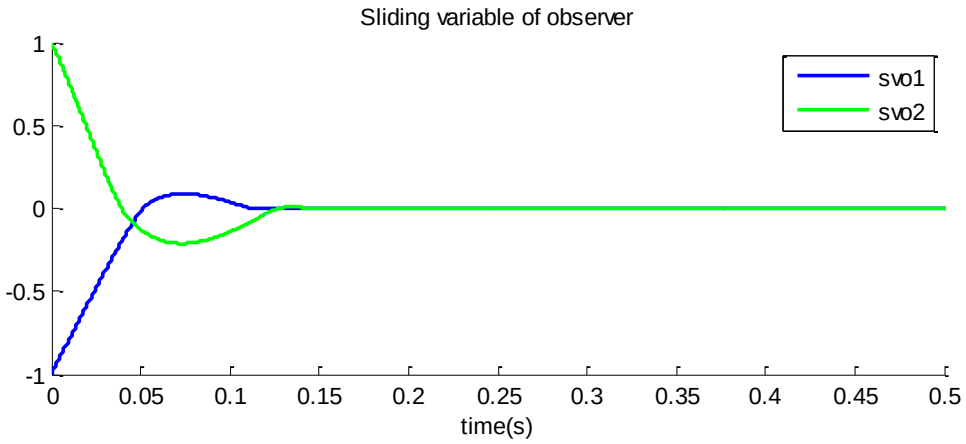

Figure 5.99: (TSMC2) Zoom of the sliding variables of observer versus time

Figures 5.78-5.99 show the results of the simulation without gain adaptation. The controller gain is estimated from parameters. In the corresponding row, the actual joint variable tracks the command joint variable (Figures 5.78 - 5.81). The sliding variables and the errors between the actual and the command joint variables converge to 0 in finite time (Figures 5.82- 5.87).

Simulation with the large controller **gain (TSMC2-2)**

This simulation shows the results when the controller gain is overestimated. Chattering, loss of accuracy, and discontinuous control function can be expected when the controller gain is overestimated.

$$\sigma_i = \dot{e}_i + 10e_i, \qquad s_i = \dot{\sigma}_i + 10\sigma_i$$

$$u_i = \ddot{q}_{c_i} - \dot{f}_i(q, \dot{q}, t) + (\lambda_i + \omega_i)\{\dot{q}_{c_i} - u_i - f_i(q, \dot{q}, t)\} + \omega_i \lambda_i \dot{e}_i + \int K_i \cdot sign(s_i)\, dt$$

$$K_i = 10000 \; for \; i = 1, 2$$

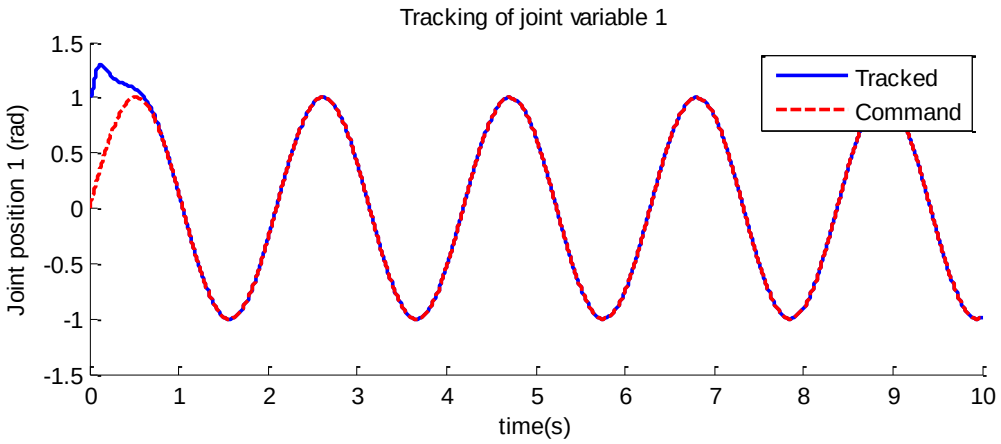

Figure 5.100: (TSMC2-2) The actual joint variable and the command joint variable versus time 1

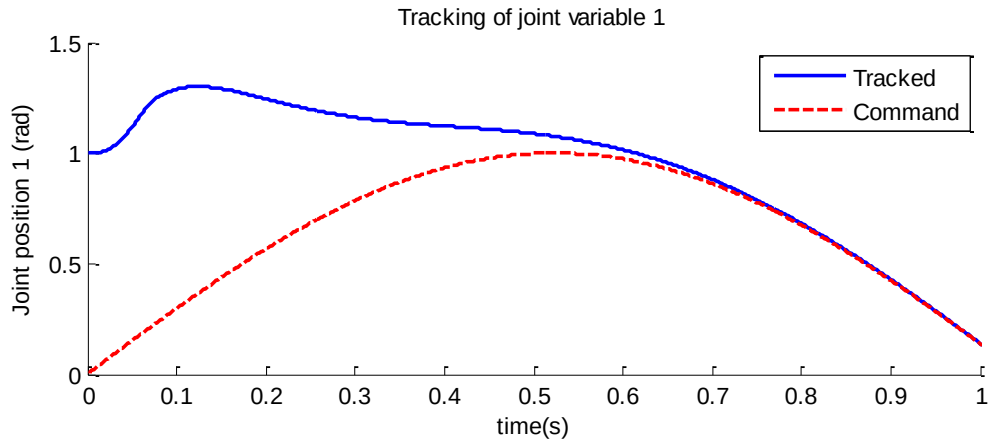

Figure 5.101: (TSMC2-2) Zoom of the actual joint variable and the command joint variable versus time 1

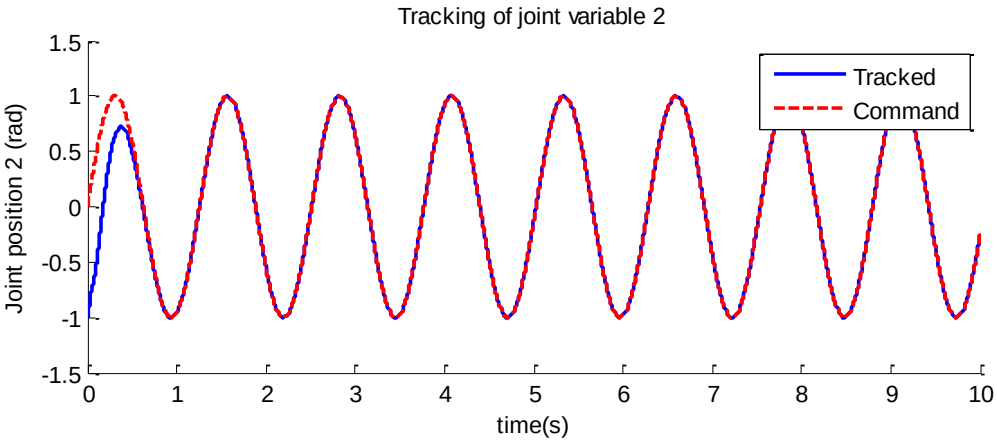

Figure 5.102: (TSMC2-2) The actual joint variable and the command joint variable versus time 2

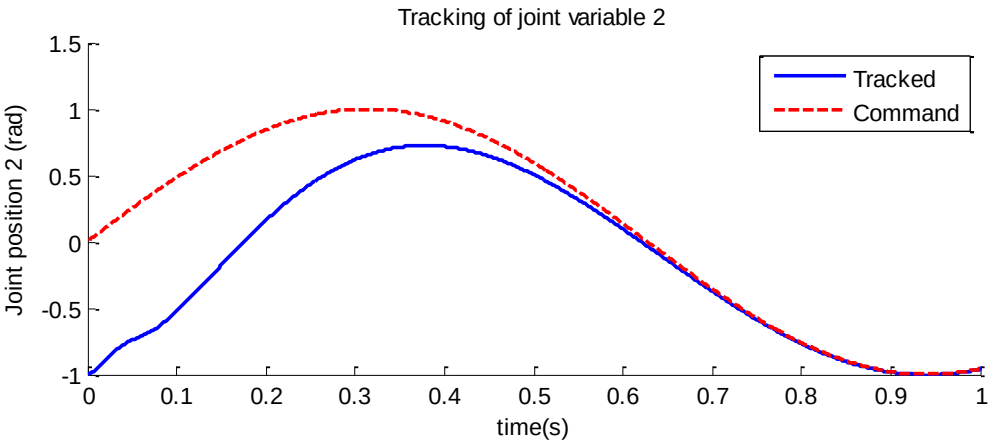

Figure 5.103: (TSMC2-2) Zoom of the actual joint variable and the command joint variable versus time 2

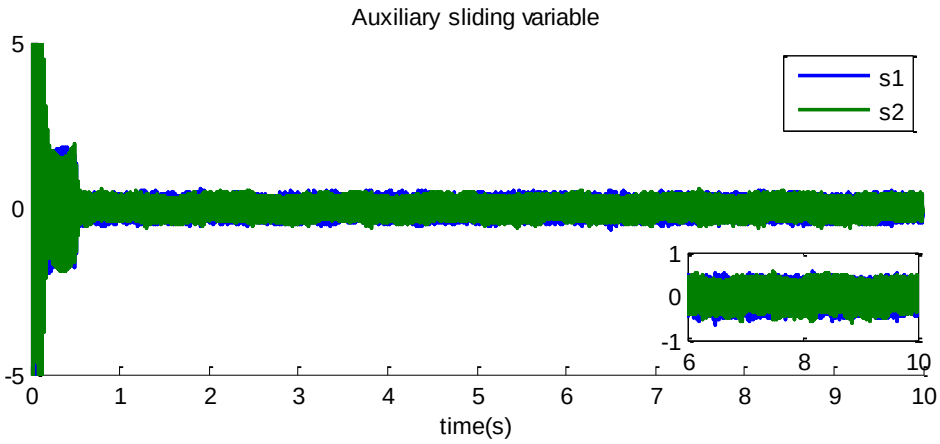

Figure 5.104: (TSMC2-2) Auxiliary sliding variables versus time

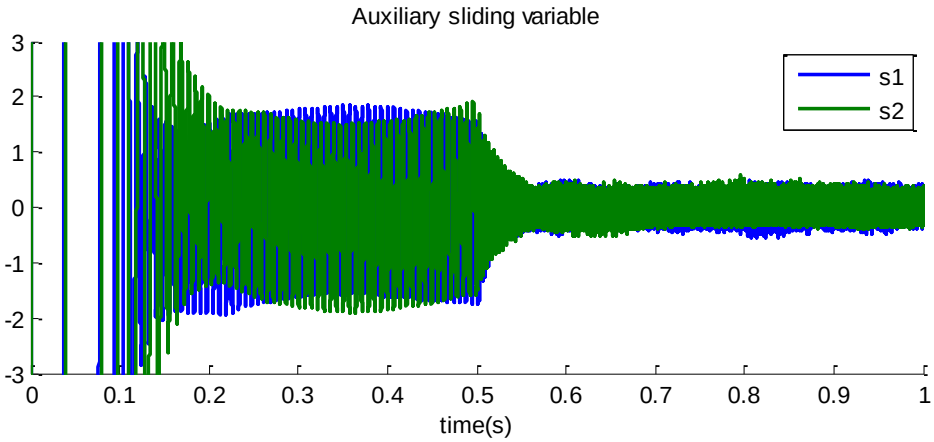

Figure 5.105: (TSMC2-2) Zoom of the auxiliary sliding variables versus time

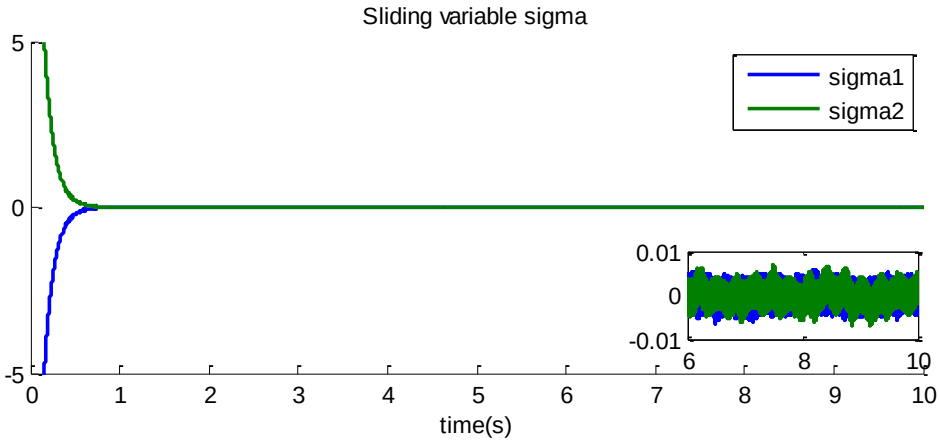

Figure 5.106: (TSMC2-2) Sliding variables versus time

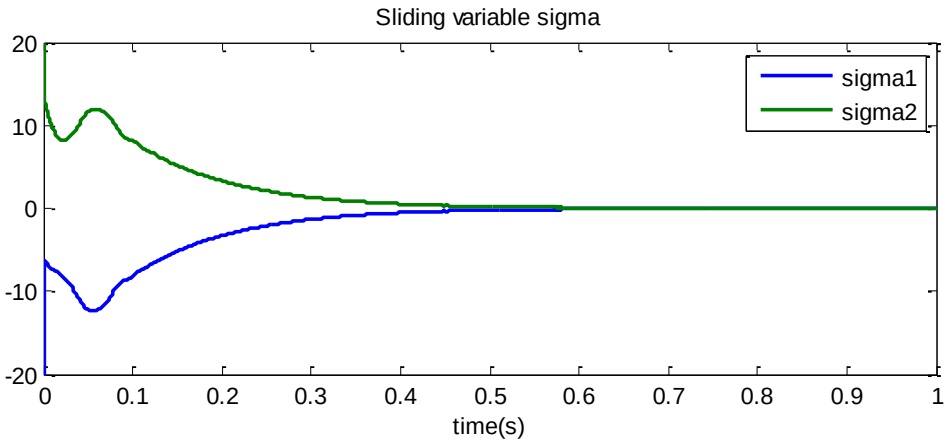

Figure 5.107: (TSMC2-2) Zoom of the sliding variables versus time

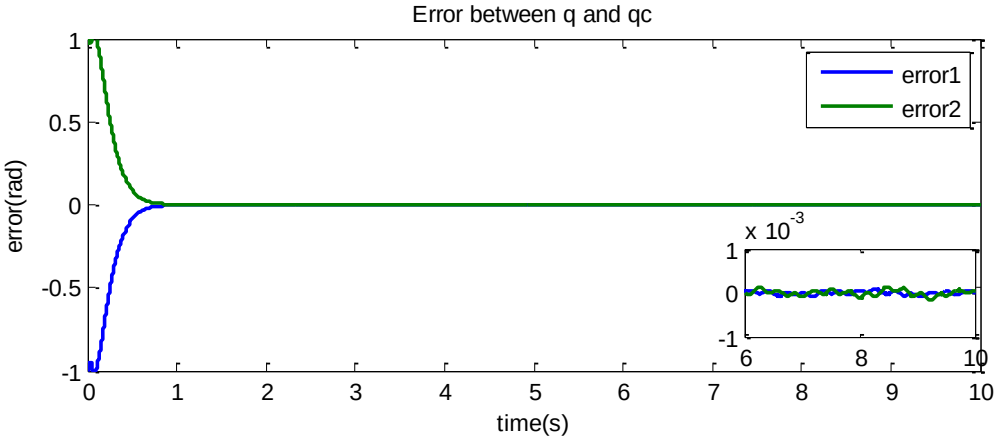

Figure 5.108: (TSMC2-2) Error between the actual joint variables and the command joint variables versus time

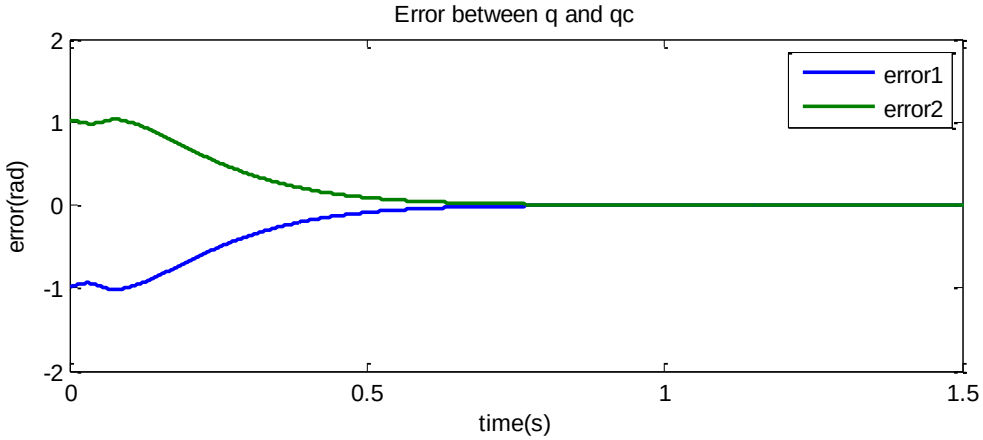

Figure 5.109: (TSMC2-2) Error between the actual joint variables and the command joint variables versus time

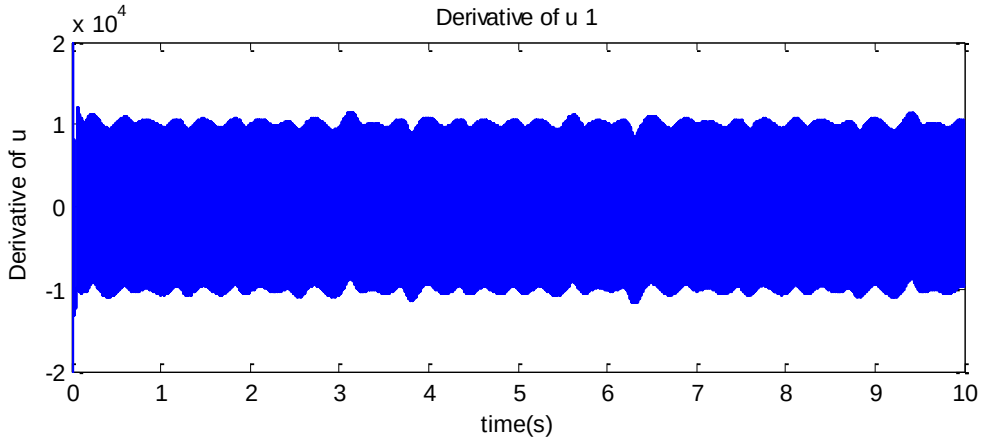

Figure 5.110: (TSMC2-2) The derivative of control *u* 1

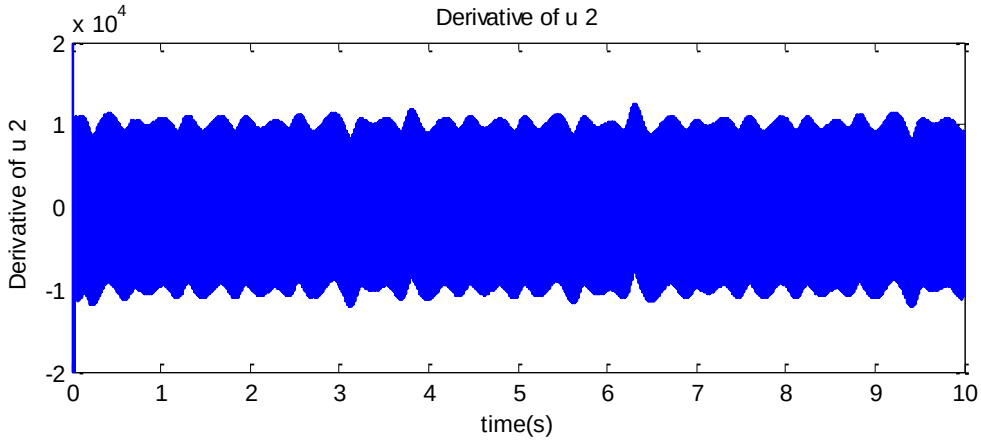

Figure 5.111: (TSMC2-2) The derivative of control *u* 2

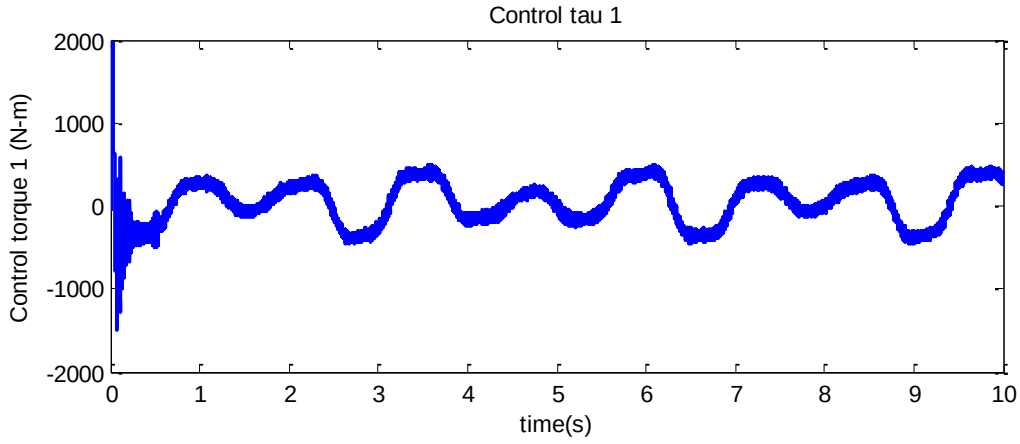

Figure 5.112: (TSMC2-2) The control τ versus time 1

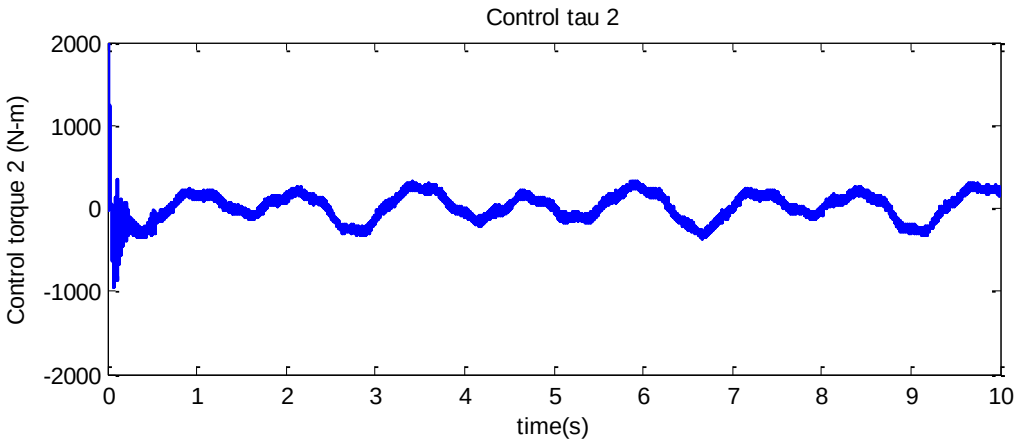

Figure 5.113: (TSMC2-2) The control τ versus time 2

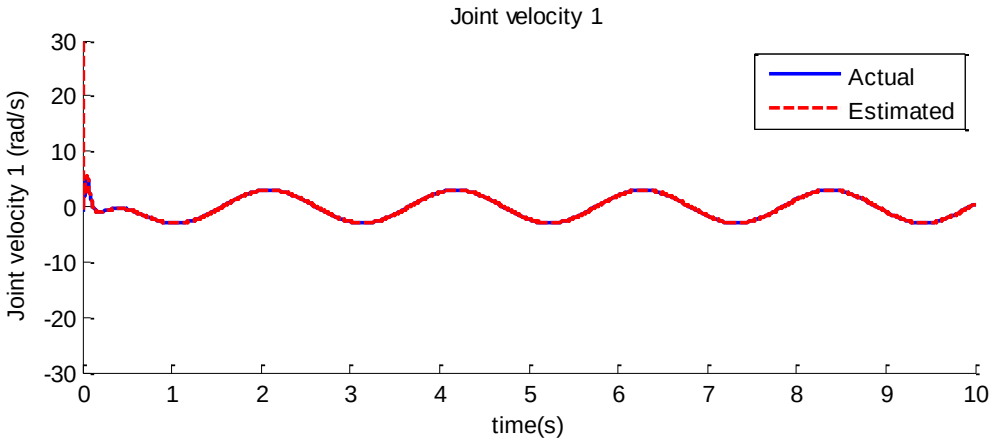

Figure 5.114: (TSMC2-2) The actual joint velocity and the command joint velocity versus time 1

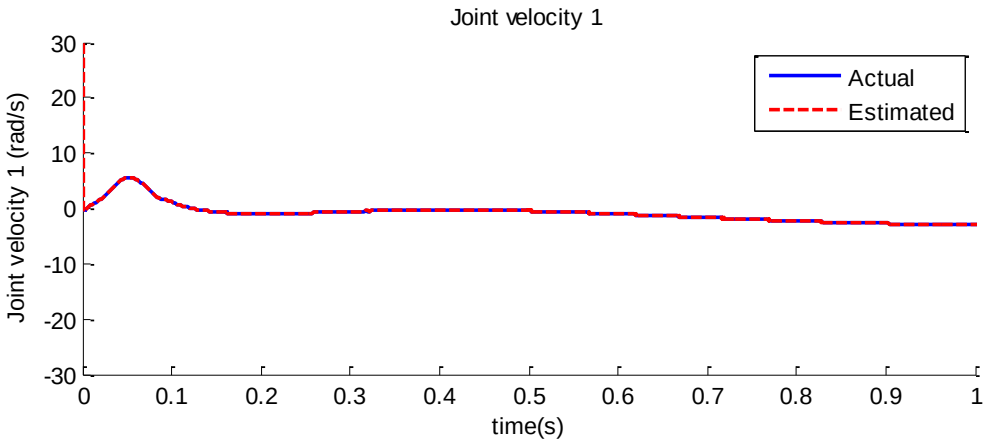

Figure 5.115: (TSMC2-2) Zoom of the actual joint velocity and the command joint velocity versus time 1

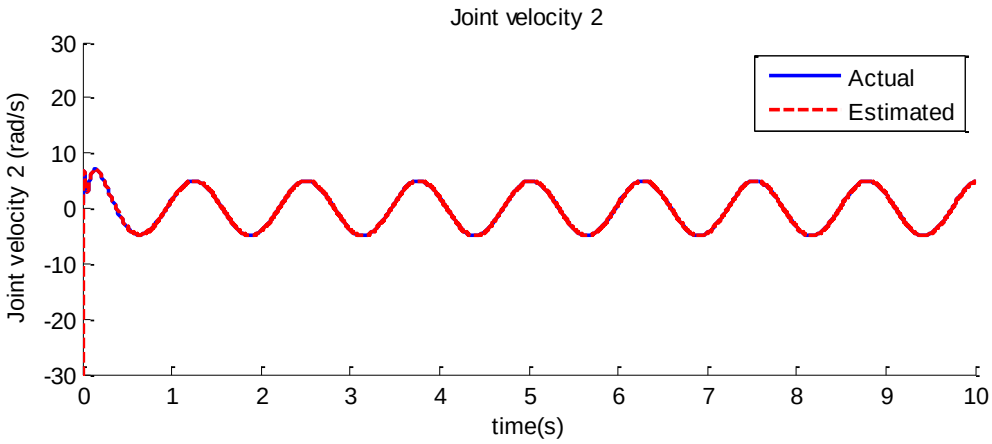

Figure 5.116: (TSMC2-2) The actual joint velocity and the command joint velocity versus time 2

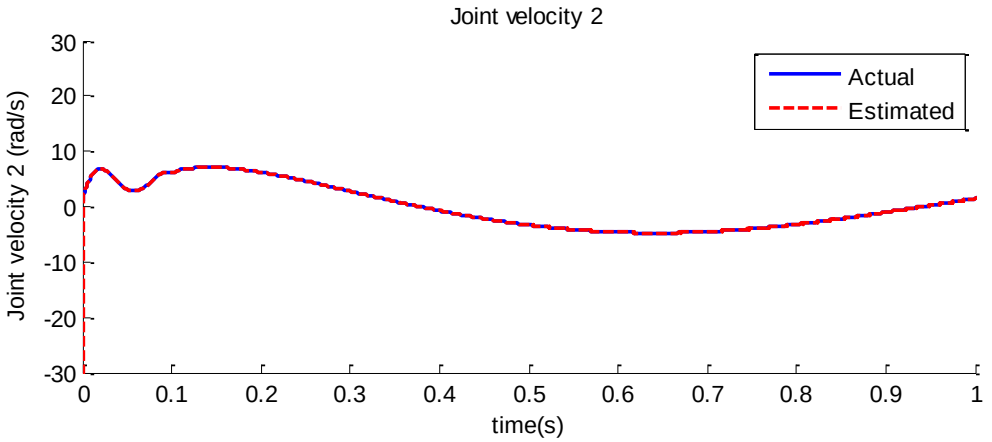

Figure 5.117: (TSMC2-2) Zoom of the actual joint velocity and the command joint velocity versus time 2

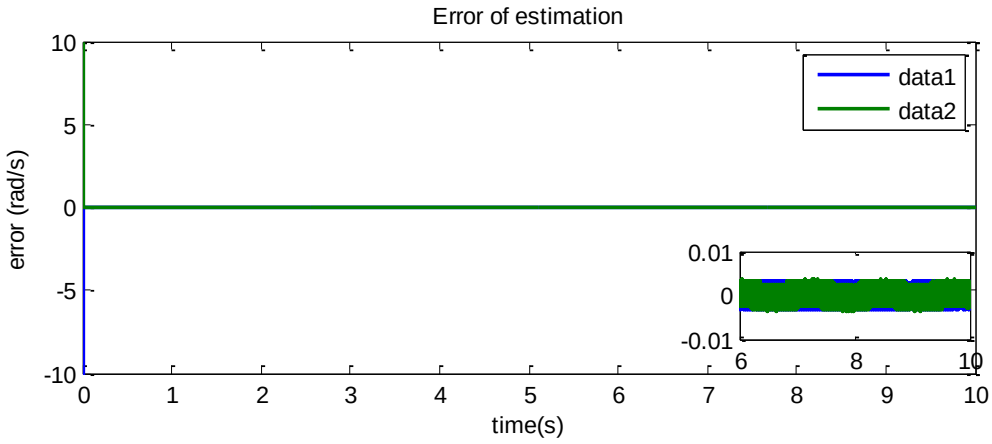

Figure 5.118: (TSMC2-2) Error between the estimated joint velocity and the command joint velocity versus time

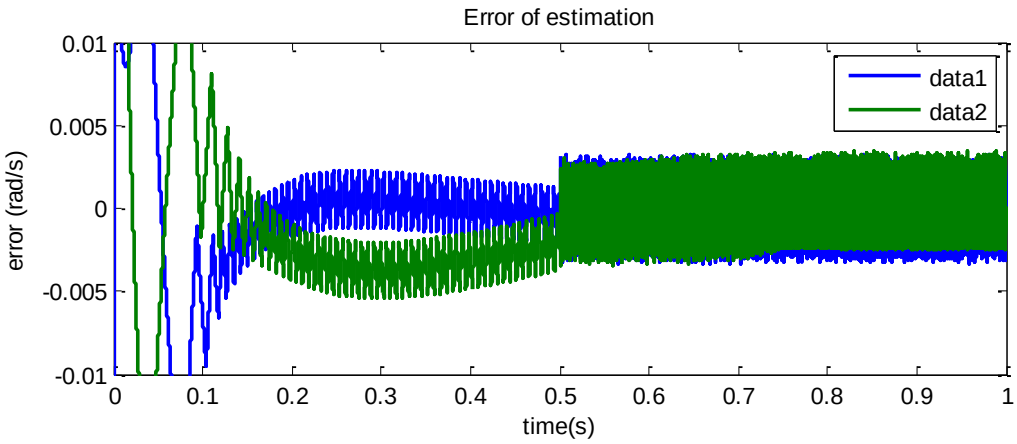

Figure 5.119: (TSMC2-2) Zoom of the error between the estimated joint velocity and the command joint velocity versus time

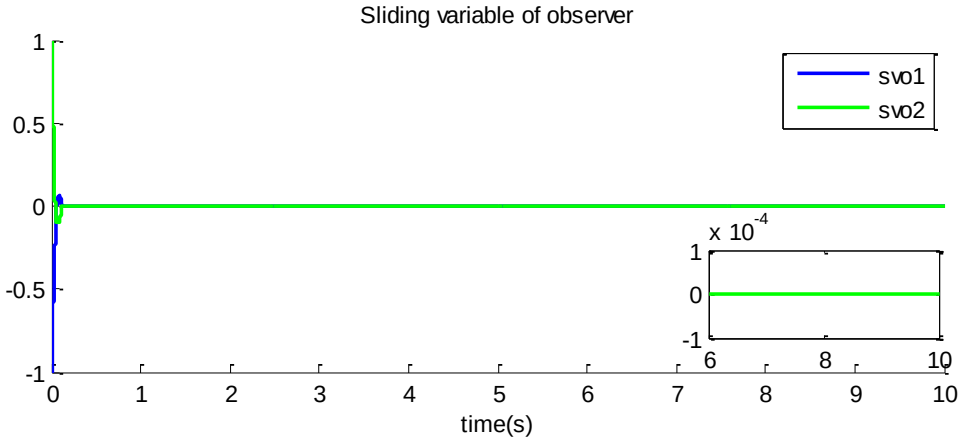

Figure 5.120: (TSMC2-2) Sliding variables of observer versus time

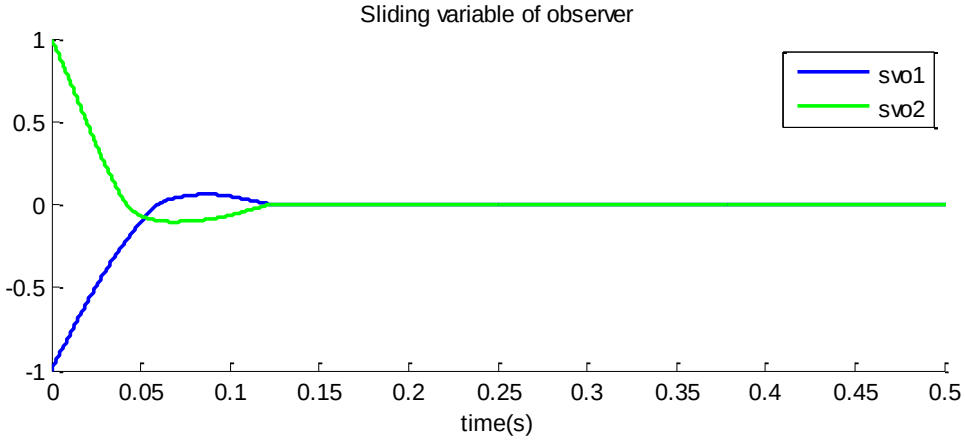

Figure 5.121: (TSMC2-2) Zoom of the sliding variables of observer versus time

Figures 5.100-5.121 show the results of the simulation of the traditional sliding mode control with the auxiliary sliding variable. The controller gain is overestimated. Comparing the results of TSMC2-2 with the results of (TSMC2), the amplitude of the switching term of the control becomes large (Figures 5.112-5.113). The chattering of the auxiliary sliding variables also becomes larger than that of TSMC2. In this case, the overestimated controller gain causes chattering on the control function. The following figure is the zoom of the control forces of TSMC2 and TSMC2-2. It is obvious that the amplitude of the control function in TSMC2-2 is much larger than that of TSMC2.

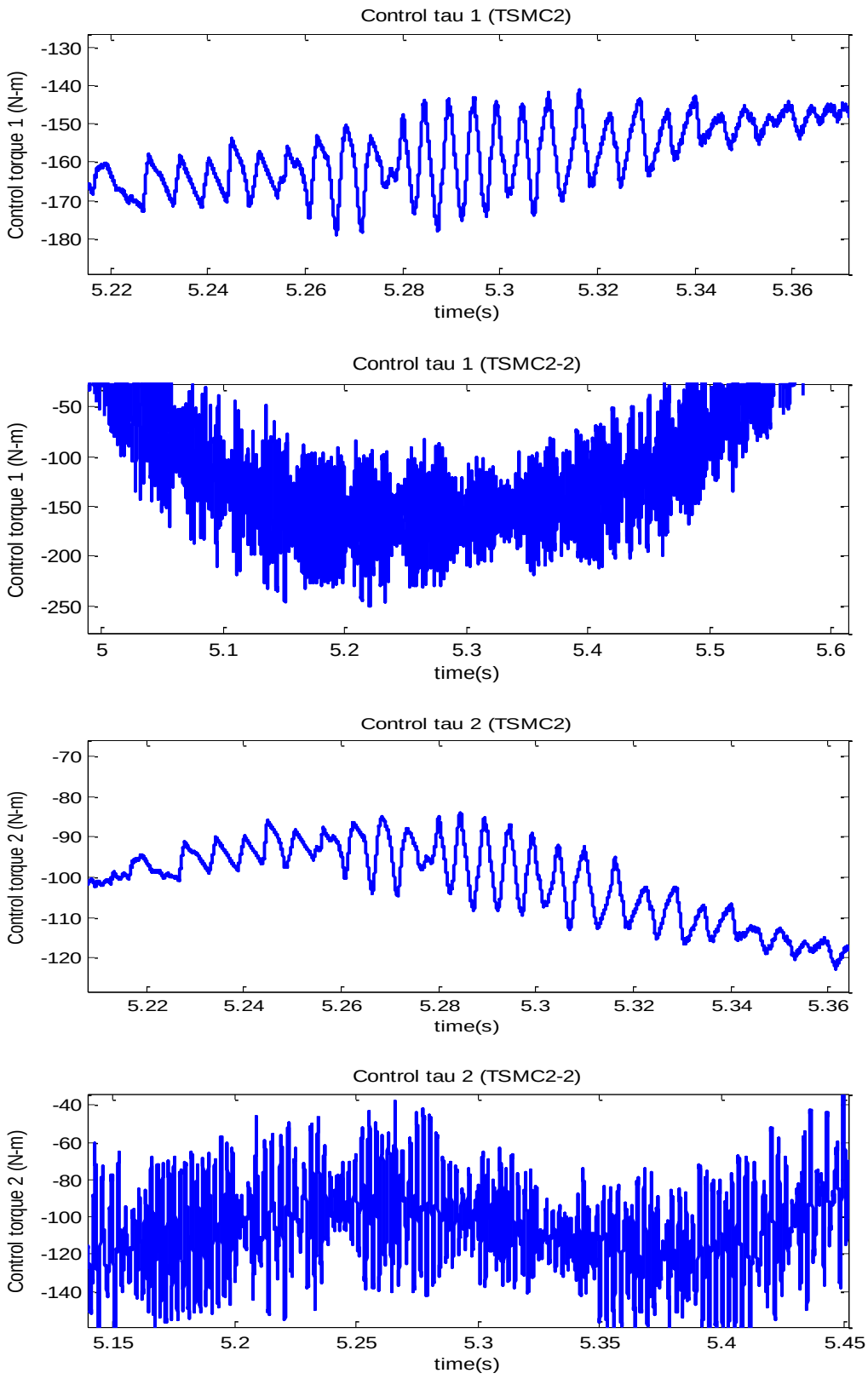

Figure 5.122: Comparing the control force of TSMC2 and TSMC2-2

Simulation with gain adaptation (ATSMC2)

It is assumed that the boundary of the disturbance is not known. The controller gain K_i is defined by the first gain adaptation algorithm. The controller gain K_i increases much fast when the absolute value of sliding variable σ_i is larger than a certain defined value ε_i: $|s_i| > \varepsilon_i$. On the other hand, the controller gain K_i decreases much slow when the absolute value of sliding variable σ_i is smaller than a certain defined value ε_i: $|s_i| < \varepsilon_i$.

$$\sigma_i = \dot{e}_i + 10e_i$$

$$s_i = \dot{\sigma}_i + 10\sigma_i$$

$$u_i = \ddot{q}_{c_i} - \dot{f}_i(q, \dot{q}, t) + (\lambda_i + \omega_i)\{\dot{q}_{c_i} - u_i - f_i(q, \dot{q}, t)\} + \omega_i\lambda_i\dot{e}_i + \int K_i \cdot sign(s_i)\, dt$$

$$\text{for } \dot{K}_i = \begin{cases} \overline{K}_i |s_i| sign(|s_i| - \varepsilon_i) & K_i > \mu_i \\ \mu_i & K_i \leq \mu_i \end{cases}$$

$$\varepsilon_i = 1, \qquad \mu_i = 0.1, \qquad \overline{K}_i = 20 \quad for\ i = 1, 2$$

$$K_i(0) = 1300\ for\ i = 1, 2$$

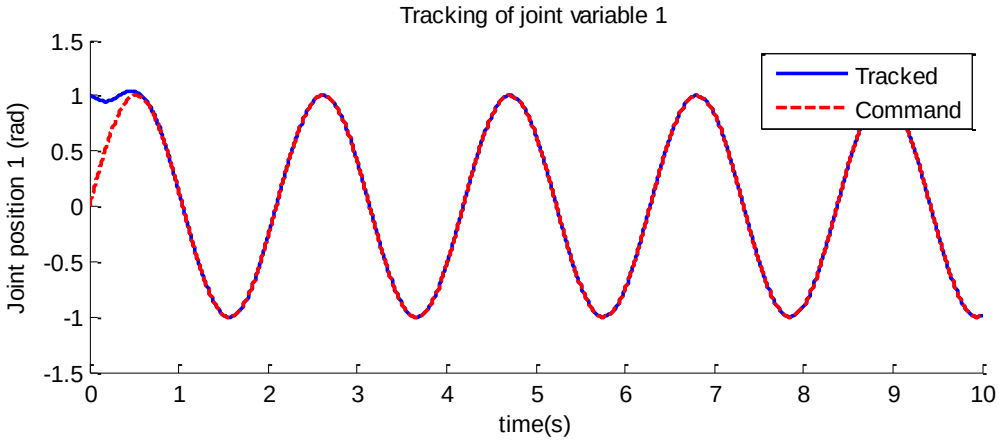

Figure 5.123: (ATSMC2) The actual joint variable and the command joint variable versus time 1

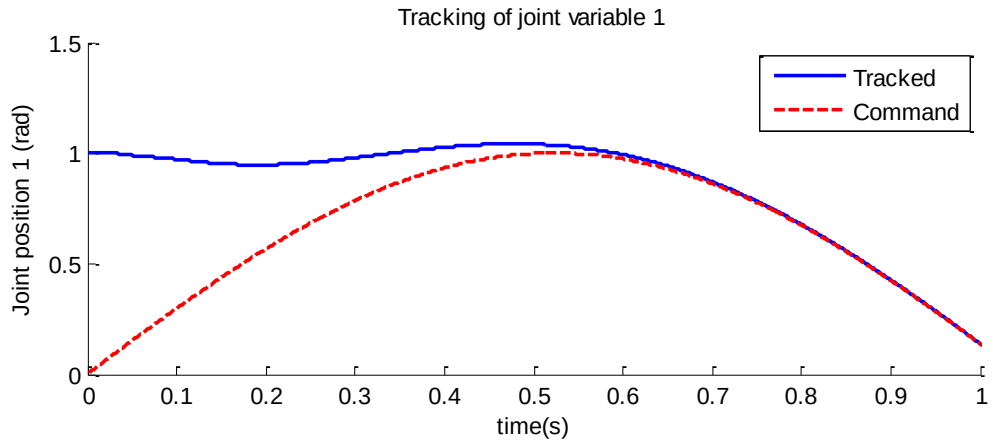

Figure 5.124: (ATSMC2) Zoom of the actual joint variable and the command joint variable versus time 1

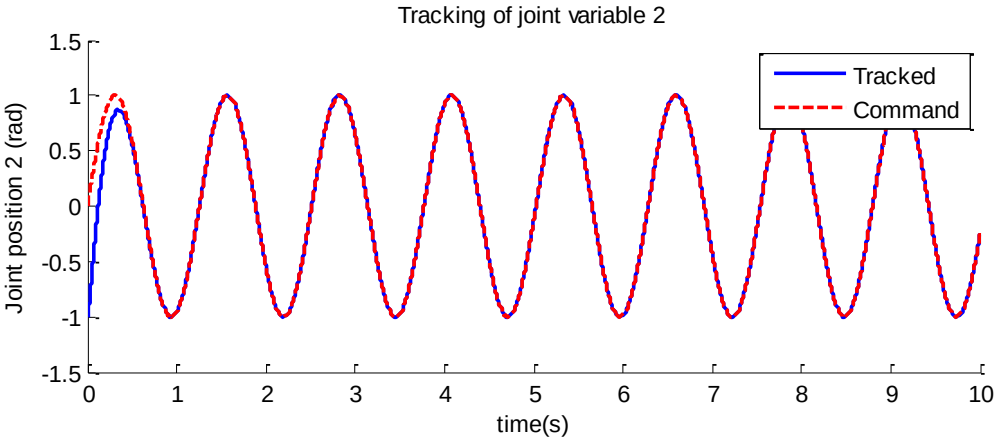

Figure 5.125: (ATSMC2) The actual joint variable and command joint variable versus time 2

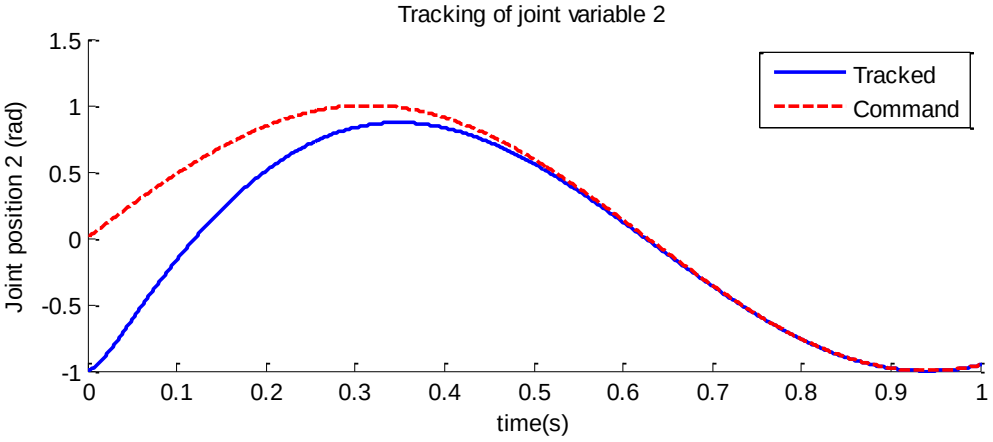

Figure 5.126: (ATSMC2) Zoom of the actual joint variable and command joint variable versus time 2

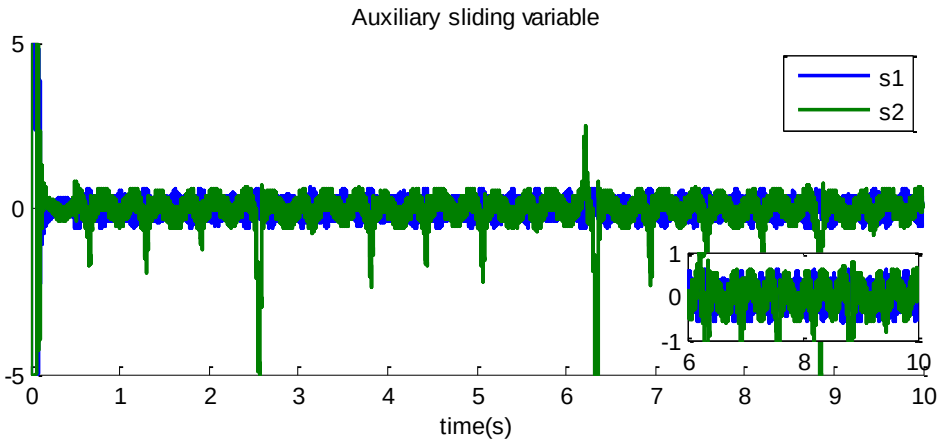

Figure 5.127: (ATSMC2) Auxiliary sliding variables versus time

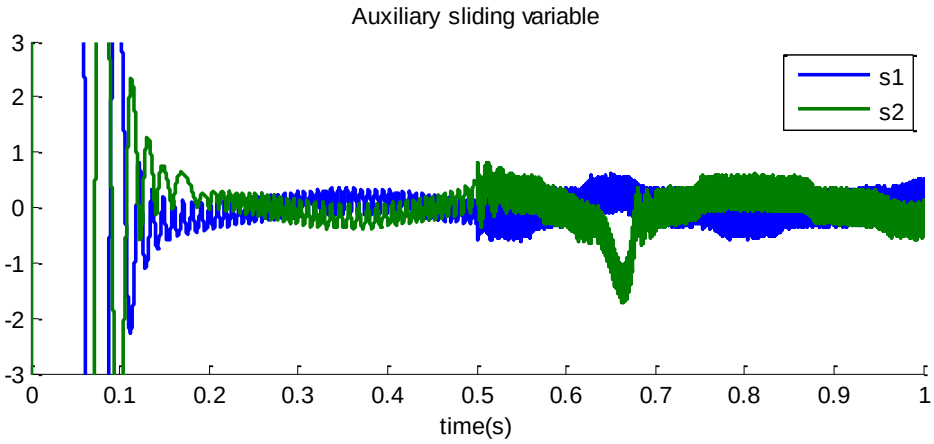

Figure 5.128: (ATSMC2) Zoom of the auxiliary sliding variables versus time

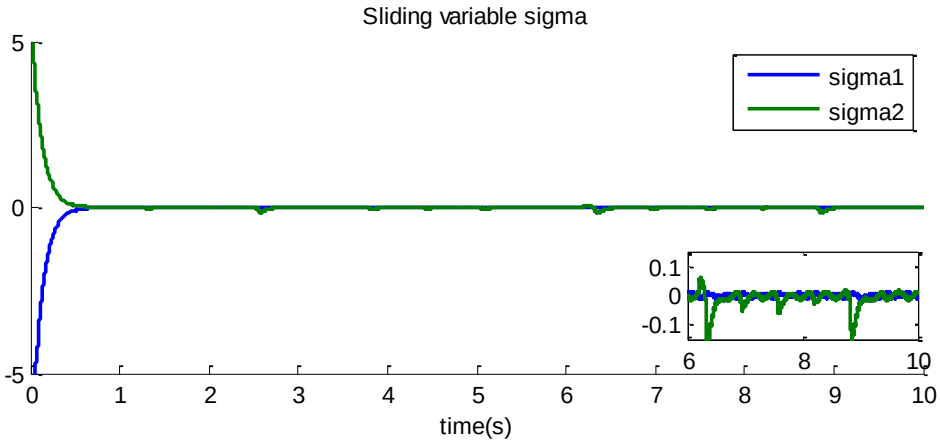

Figure 5.129: (ATSMC2) Sliding variables σ versus time

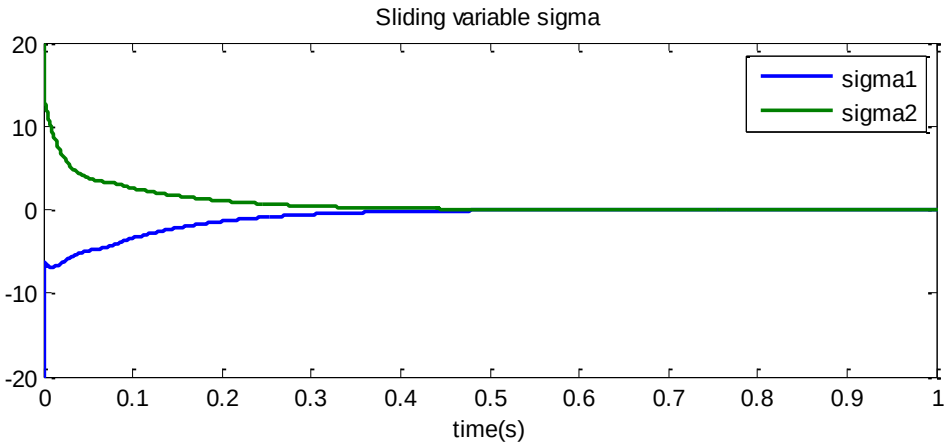

Figure 5.130: (ATSMC2) Zoom of the sliding variables σ versus time

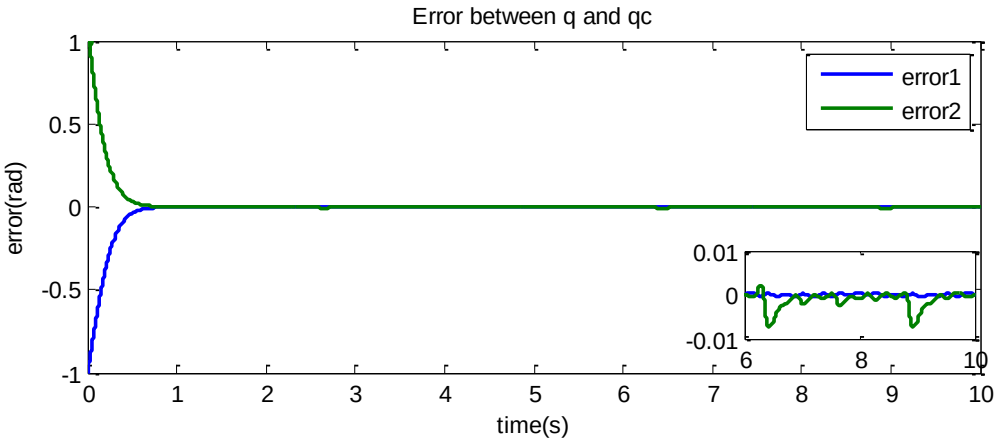

Figure 5.131: (ATSMC2) Error between the actual joint variables and the command of joint variables versus time

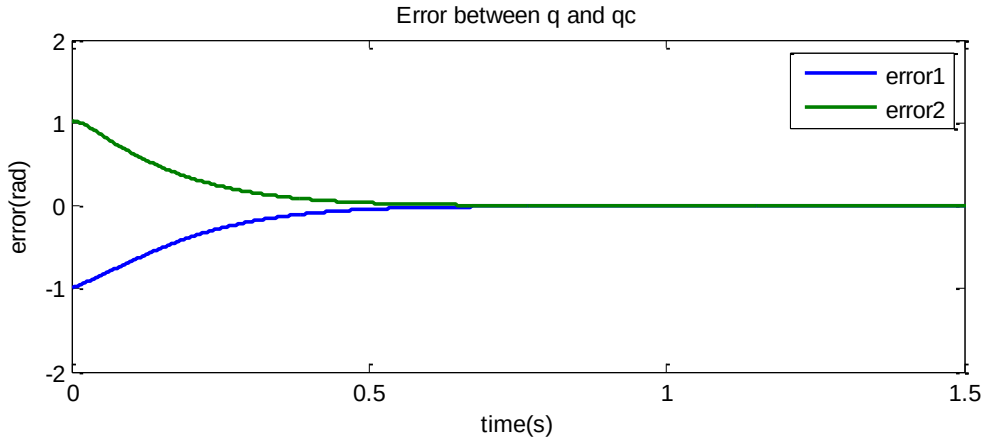

Figure 5.132: (ATSMC2) Zoom of the error between the actual joint variables and the command of joint variables versus time

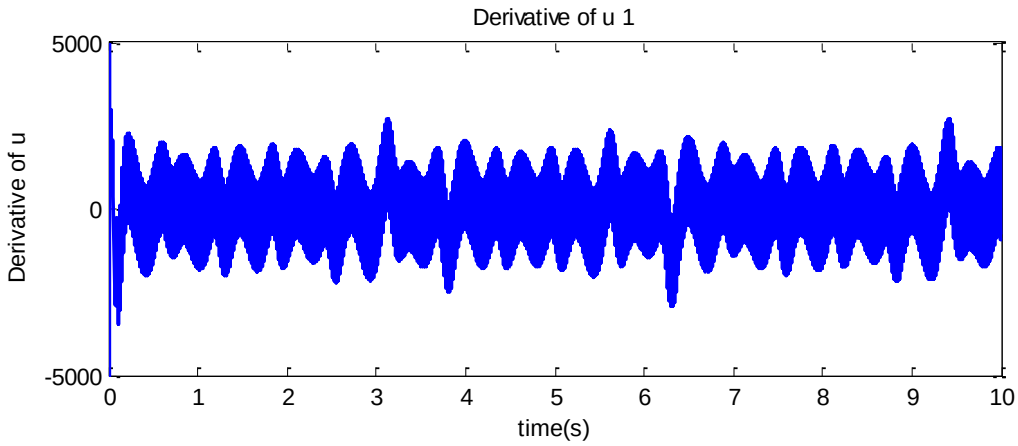

Figure 5.133: (ATSMC2) The derivative of control *u* 1

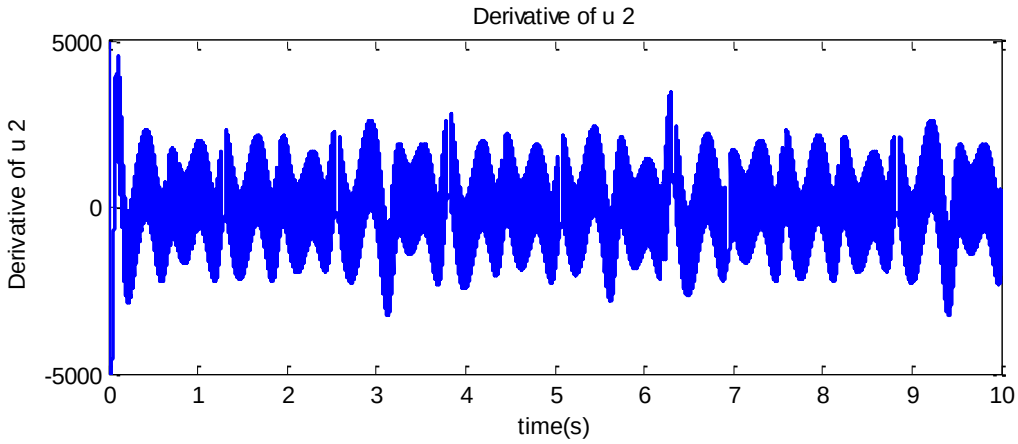

Figure 5.134: (ATSMC2) The derivative of control *u* 2

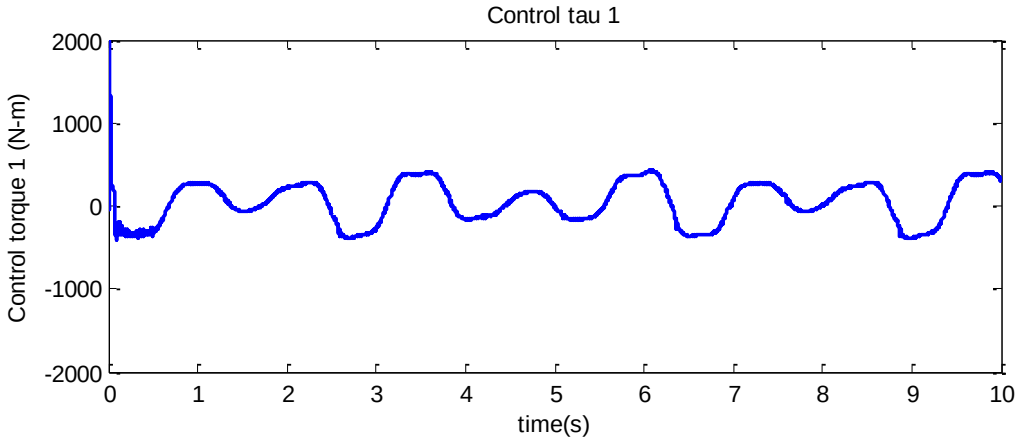

Figure 5.135: (ATSMC2) The control τ versus time 1

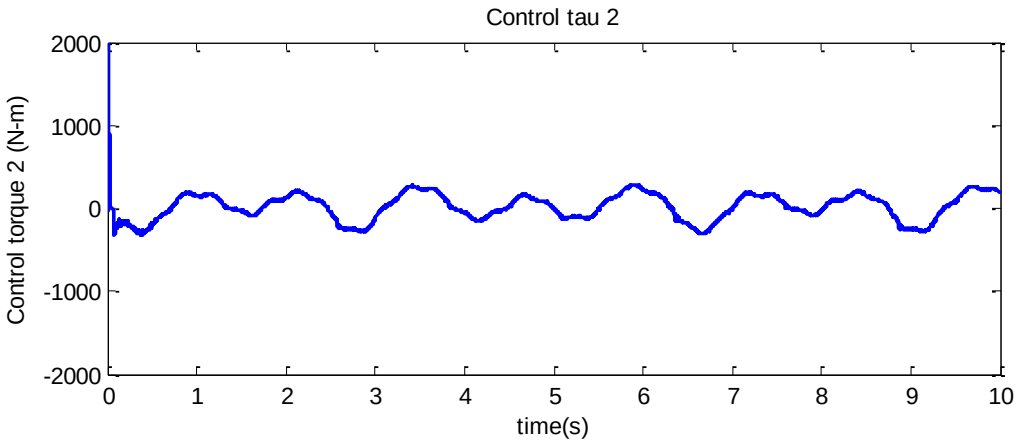

Figure 5.136: (ATSMC2) The control τ versus time 2

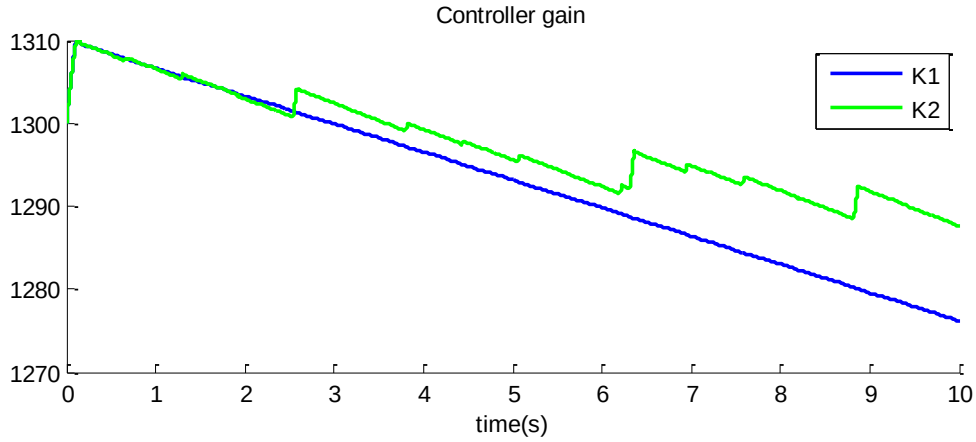

Figure 5.137: (ATSMC2) Gain of control τ versus time

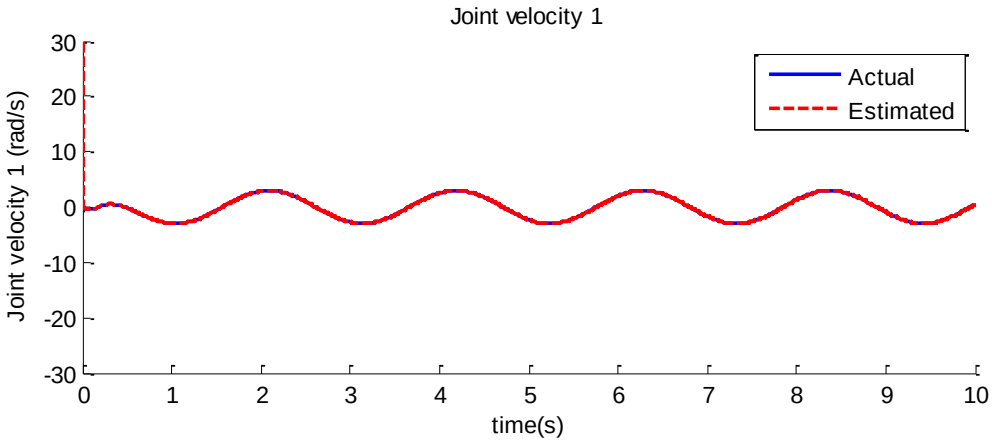

Figure 5.138: (ATSMC2) The actual joint velocity and the estimated joint velocity versus time 1

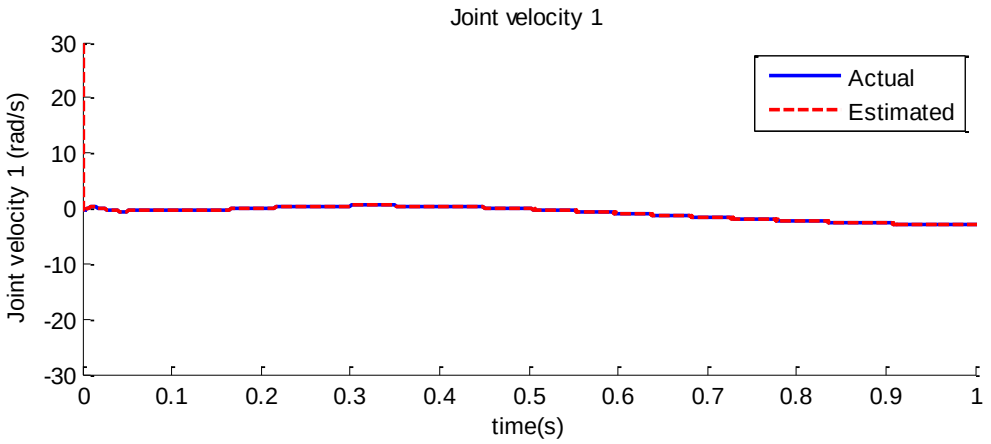

Figure 5.139: (ATSMC2) Zoom of the actual joint velocity and the estimated joint velocity versus time 1

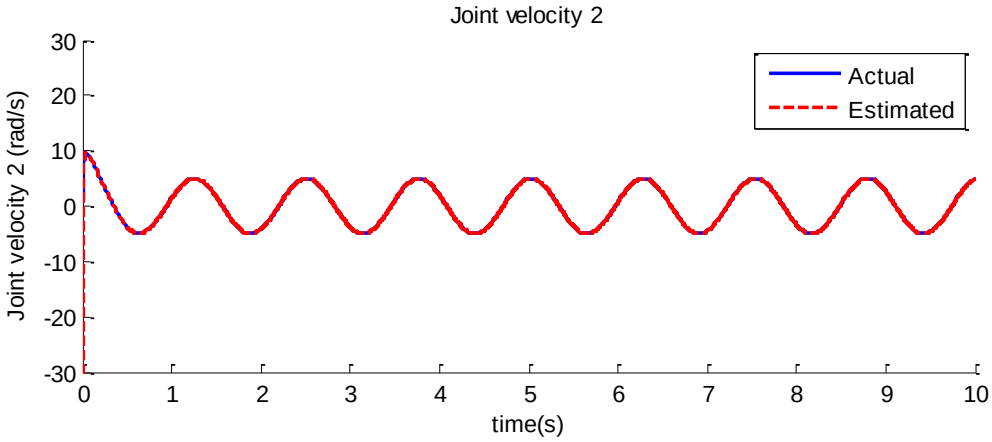

Figure 5.140: (ATSMC2) The actual joint velocity and the estimated joint velocity versus time 2

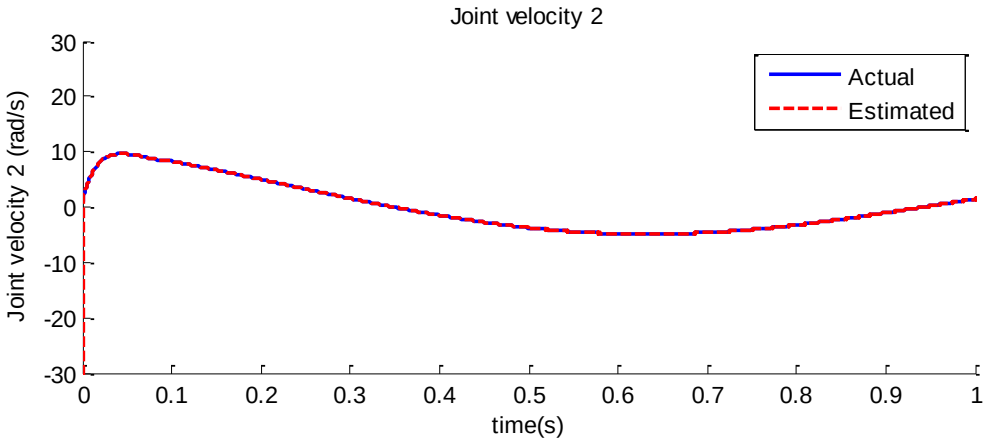

Figure 5.141: (ATSMC2) The actual joint velocity and the estimated joint velocity versus time 2

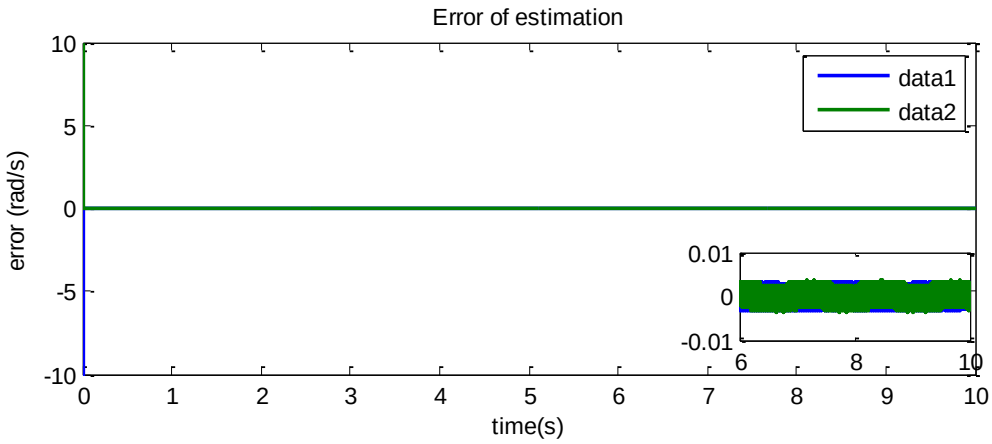

Figure 5.142: (ATSMC2) Error between the actual joint velocity and the estimated joint velocity versus time

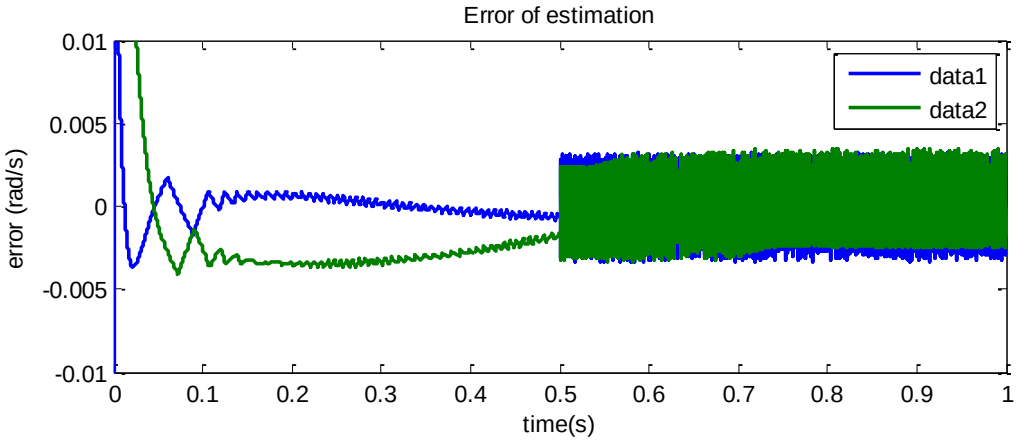

Figure 5.143: (ATSMC2) Zoom of the error between the actual joint velocity and the estimated joint velocity versus time

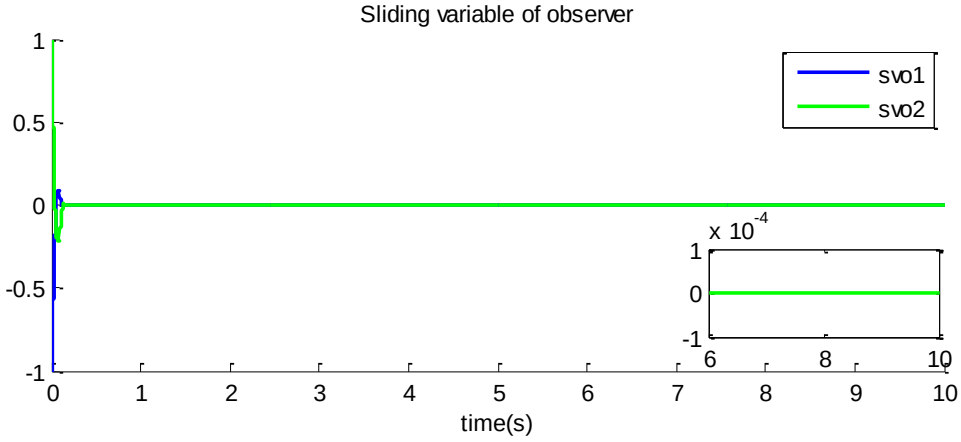

Figure 5.144: (ATSMC2) Sliding variables of observer versus time

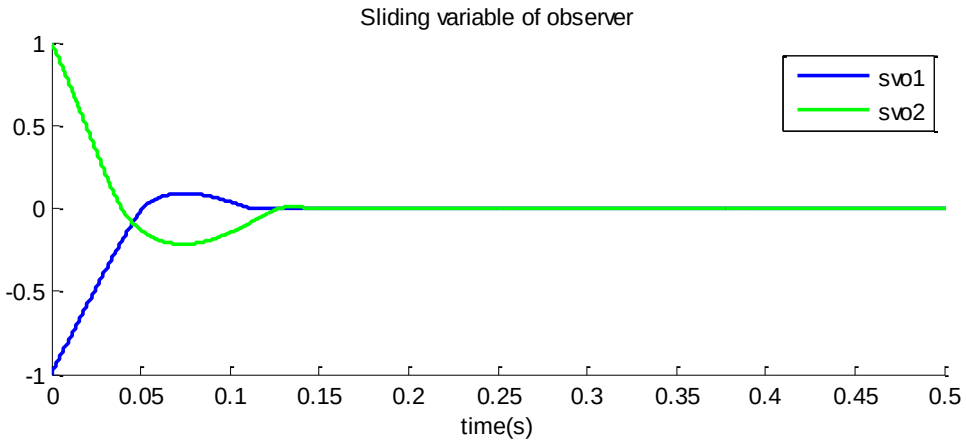

Figure 5.145: (ATSMC2) Sliding variables of observer versus time

Figures 5.123-5.145 show the results of the simulation with gain adaptation. The amplitude of the high frequency term of the control function is mitigated (Figures 5.135 and 5.136). The controller gain K_2 increases when the absolute value of the auxiliary sliding variable s_2 becomes larger than 1 (Figures 5.136 and 5.137).

Simulation with the Second Adaptive TSMC (ATSMC2-2)

It is assumed that the boundary of the disturbance is not known. The controller gain K_i is defined by the second gain adaptation algorithm. The controller gain K_i increases much fast when the absolute value of sliding variable σ_i is larger than a certain defined value ε_i: $|s_i| > \varepsilon_i$. On the other hand, the controller gain K_i decreases when the absolute value of sliding variable σ_i is smaller than a certain defined value ε_i: $|s_i| < \varepsilon_i$. The controller gain K_i decreases much faster than that of the first adaptive-gain TSMC.

$$\sigma_i = \dot{e}_i + 10e_i$$

$$s_i = \dot{\sigma}_i + 10\sigma_i$$

$$u_i = \ddot{q}_{c_i} - \dot{f}_i(q, \dot{q}, t) + (\lambda_i + \omega_i)\{\dot{q}_{c_i} - u_i - f_i(q, \dot{q}, t)\} + \omega_i\lambda_i\dot{e}_i + \int K_i \cdot sign(s_i)\, dt$$

$$\text{for } \dot{K}_i = \begin{cases} A_i + B_i sign(|s_i| - \varepsilon_i) & K_i > \mu_i \\ \mu_i & K_i \le \mu_i \end{cases}$$

$$\varepsilon_i = 1, \qquad \mu_i = 0.1, \qquad A_i = 40\ for\ i = 1,2, \qquad B_i = 60\ for\ i = 1,2$$

$$K_i(0) = 1300\ for\ i = 1,2$$

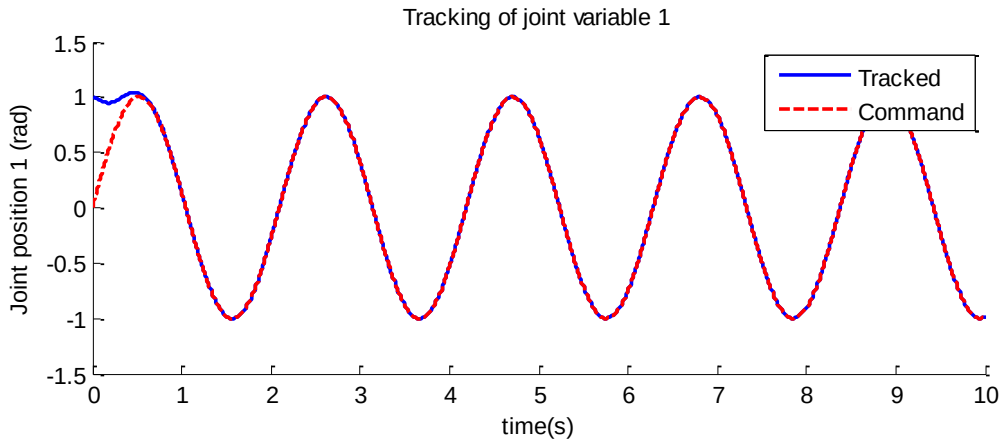

Figure 5.146: (ATSMC2-2) The actual joint variable and the command joint variable versus time 1

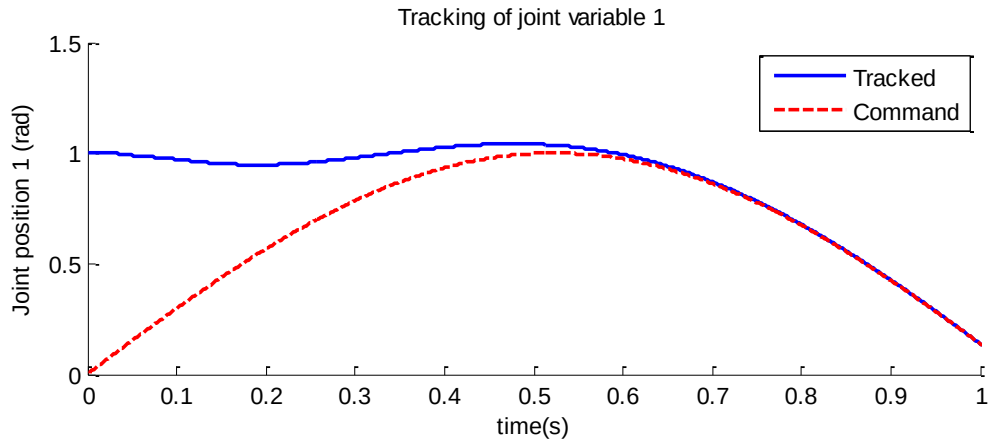

Figure 5.147: (ATSMC2-2) Zoom of the actual joint variable and the command joint variable versus time 1

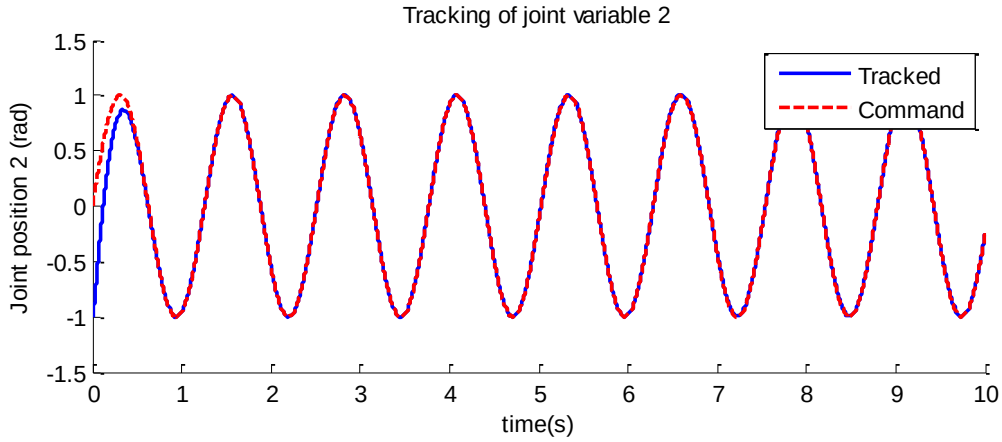

Figure 5.148: (ATSMC2-2) The actual joint variable and the command joint variable versus time 2

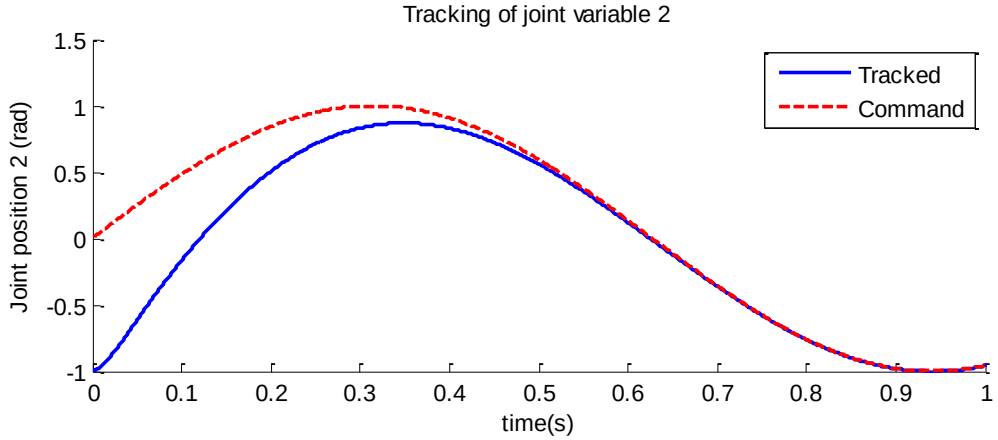

Figure 5.149: (ATSMC2-2) Zoom of the actual joint variable and the command joint variable versus time 2

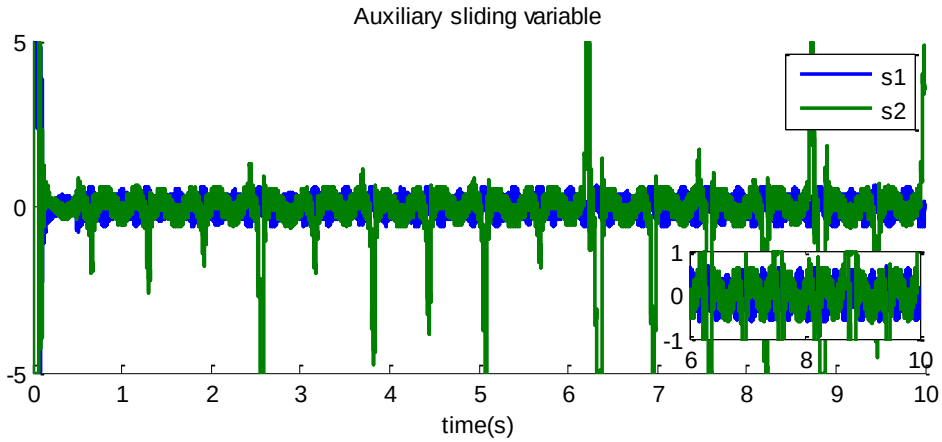

Figure 5.150: (ATSMC2-2) Auxiliary sliding variables versus time

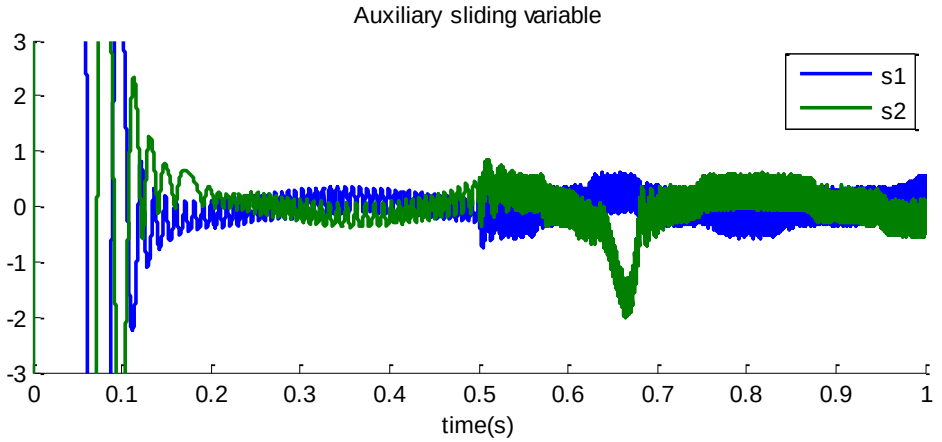

Figure 5.151: (ATSMC2-2) Zoom of the auxiliary sliding variables versus time

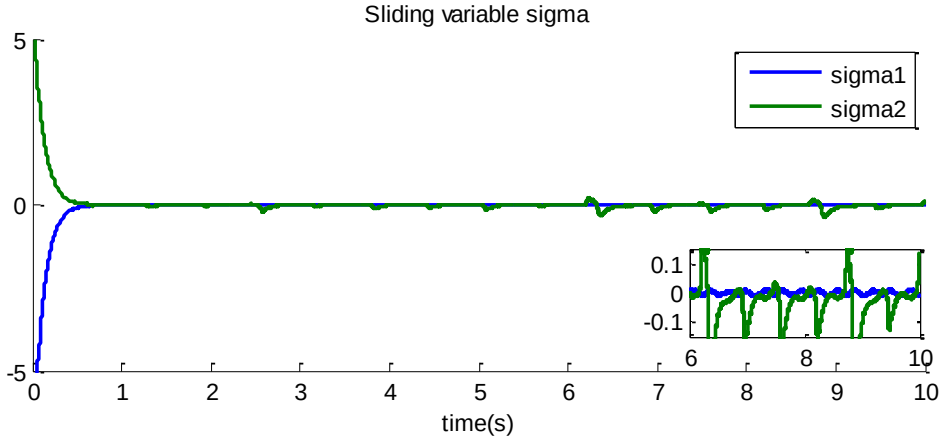

Figure 5.152: (ATSMC2-2) Sliding variables σ versus time

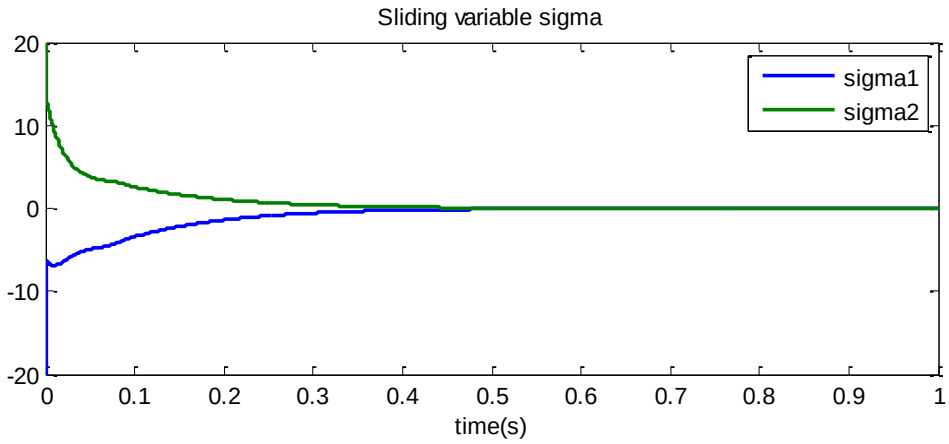

Figure 5.153: (ATSMC2-2) Zoom of the sliding variables σ versus time

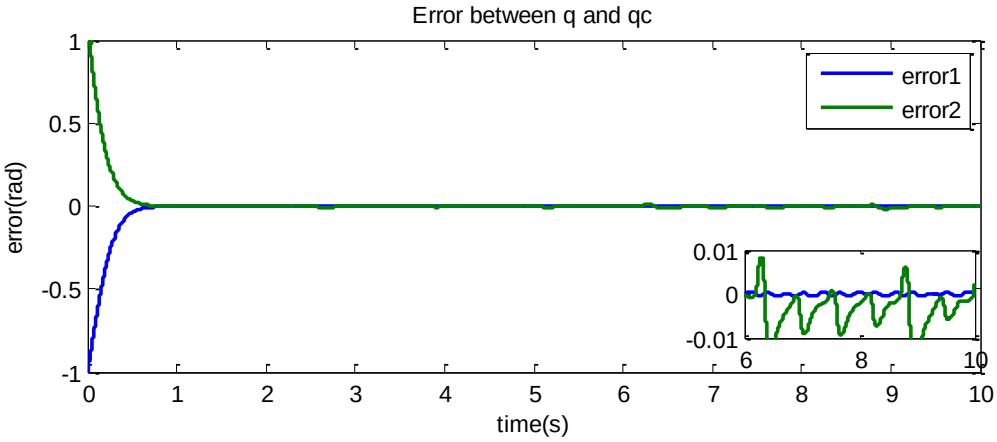

Figure 5.154: (ATSMC2-2) Error between the actual joint variables and the command of joint variables versus time

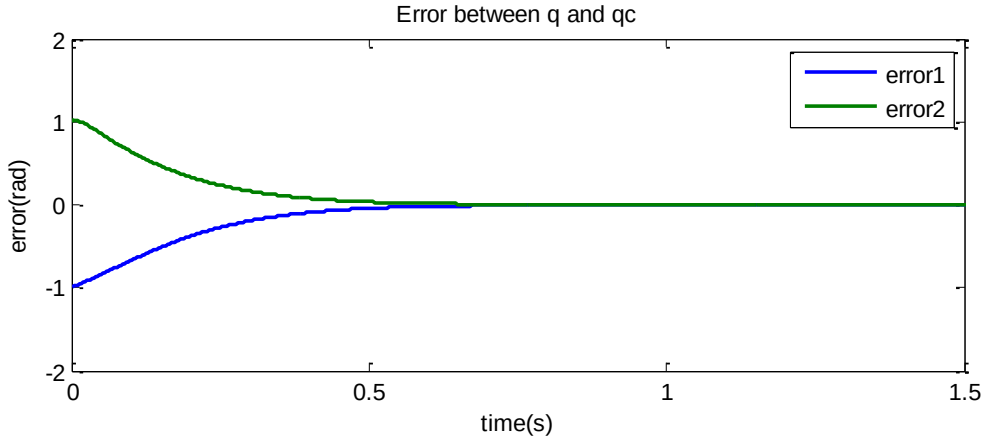

Figure 5.155: (ATSMC2-2) Error between the actual joint variables and the command of joint variables versus time

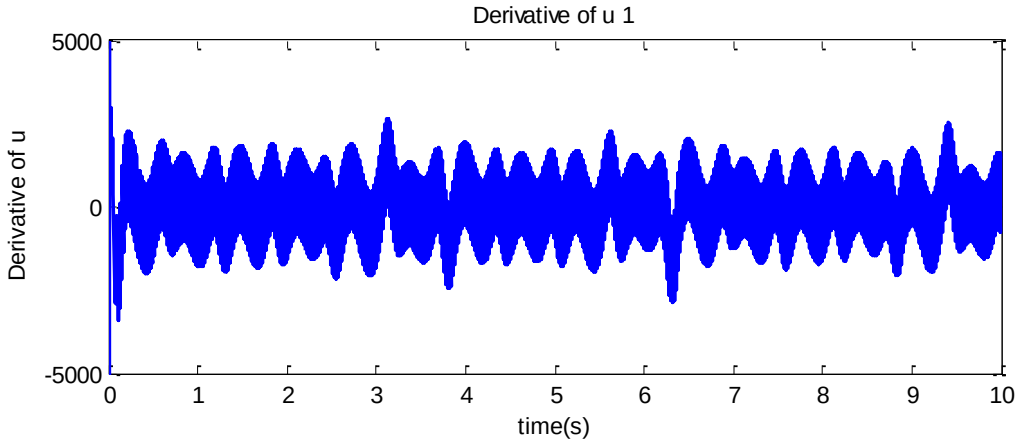

Figure 5.156: (ATSMC2-2) The derivative of control *u* 1

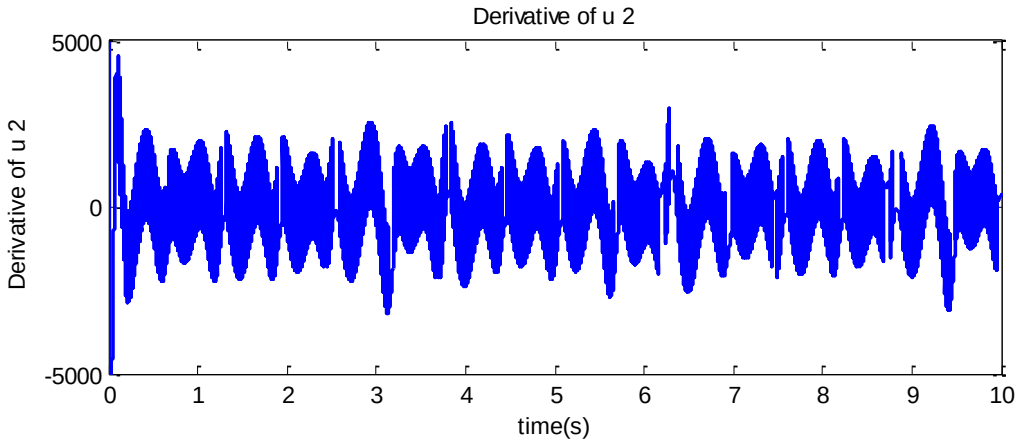

Figure 5.157: (ATSMC2-2) The derivative of control *u* 2

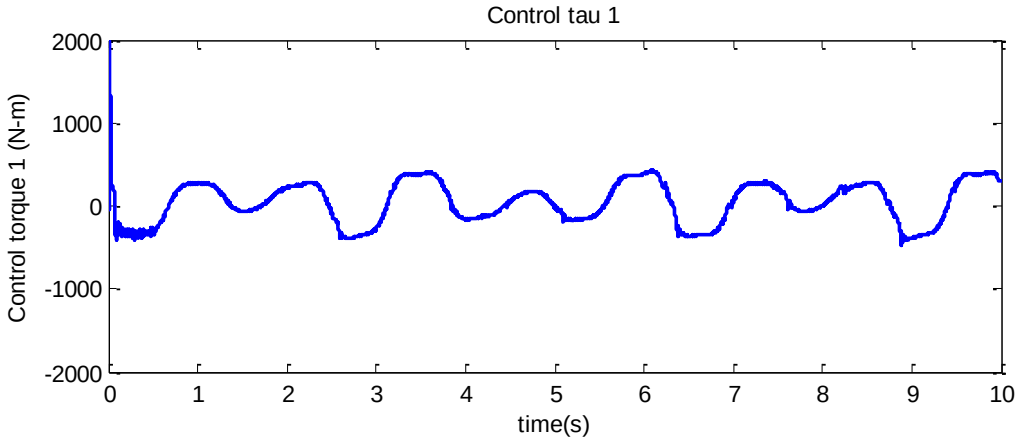

Figure 5.158: (ATSMC2-2) The control τ versus time 1

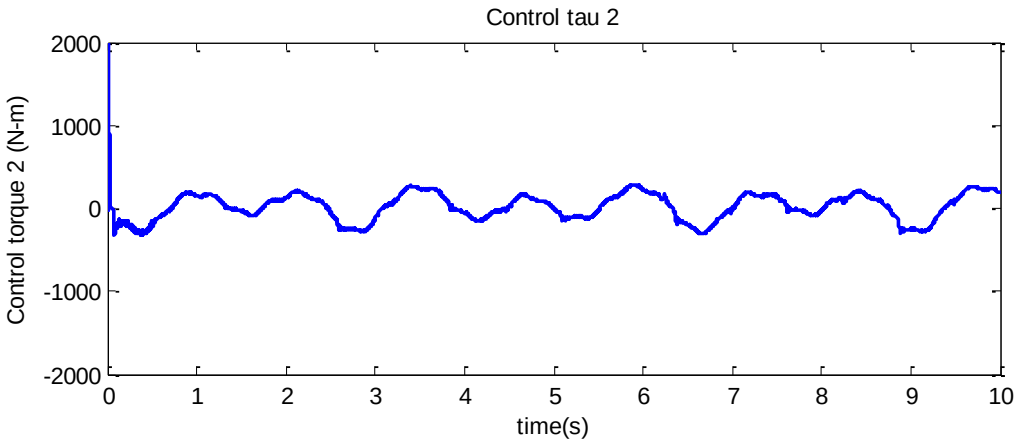

Figure 5.159: (ATSMC2-2) The control τ versus time 2

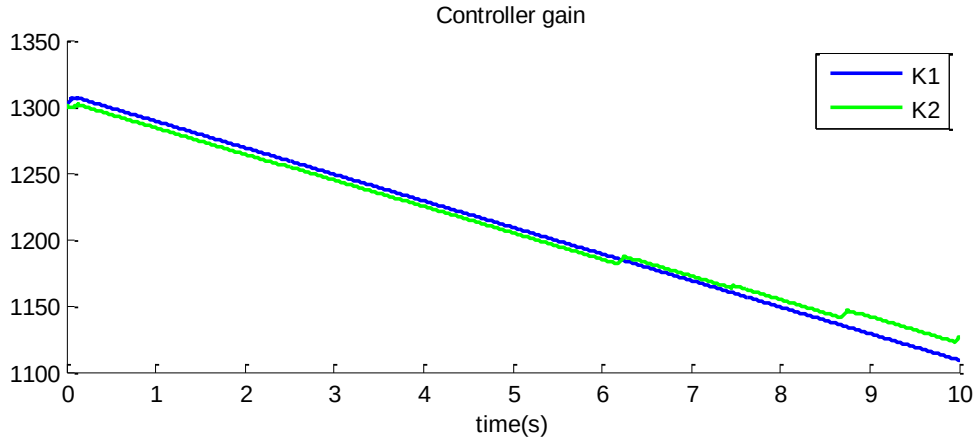

Figure 5.160: (ATSMC2-2) The controller gain versus time

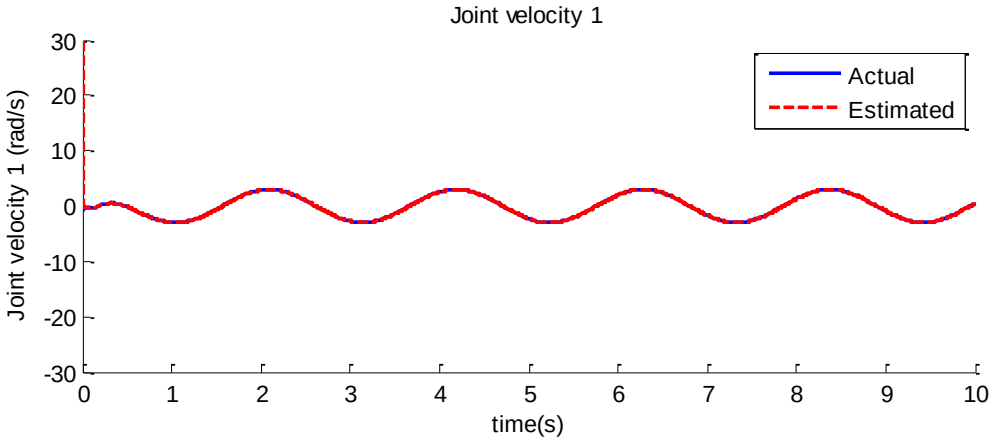

Figure 5.161: (ATSMC2-2) The actual joint velocity and the estimated joint velocity versus time 1

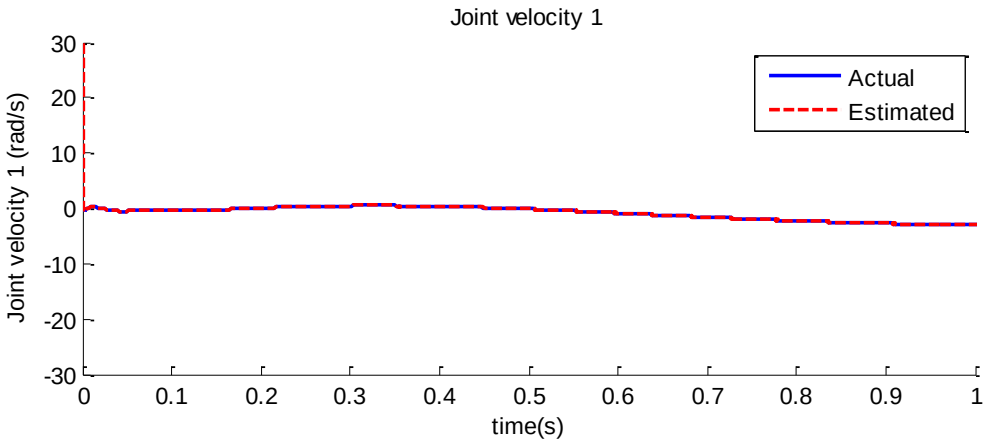

Figure 5.162: (ATSMC2-2) The actual joint velocity and the estimated joint velocity versus time 1

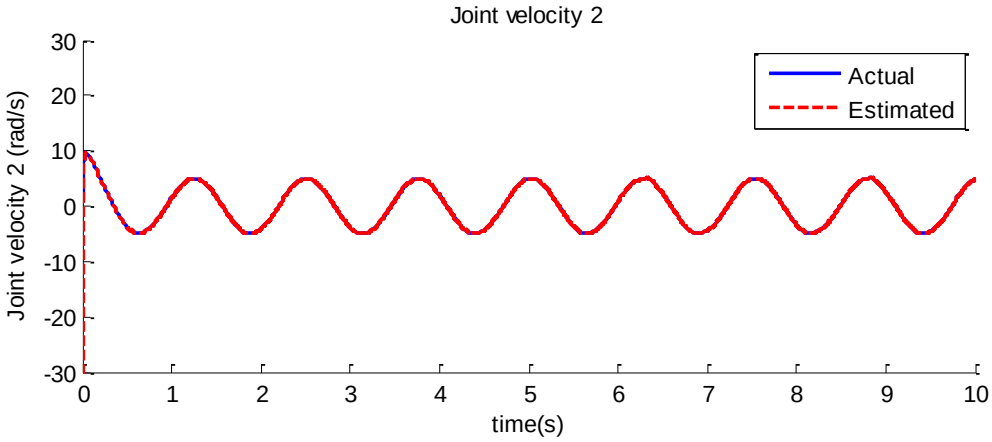

Figure 5.163: (ATSMC2-2) The actual joint velocity and the estimated joint velocity versus time 2

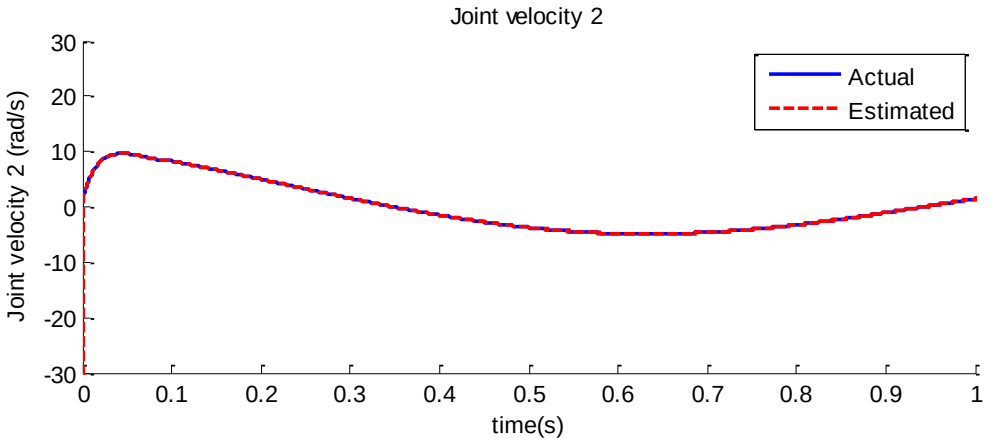

Figure 5.164: (ATSMC2-2) Zoom of the actual joint velocity and the estimated joint velocity versus time 2

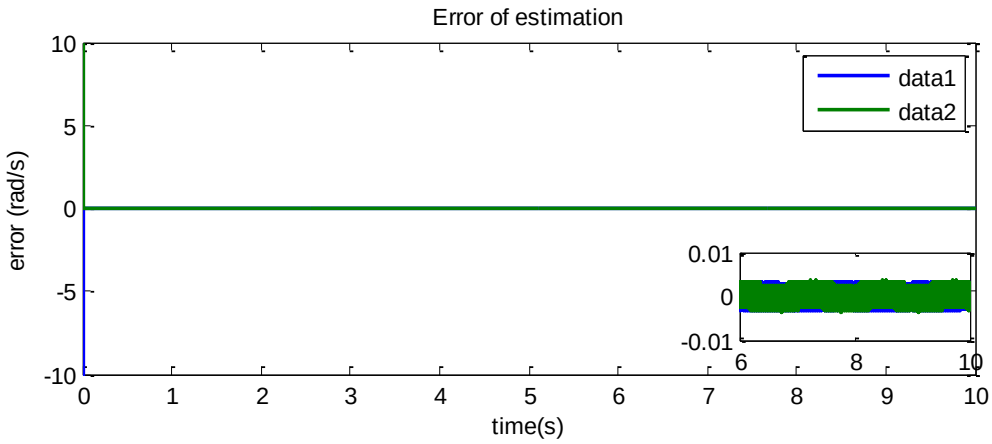

Figure 5.165: (ATSMC2-2) Error between the actual joint velocity and the estimated joint velocity versus time

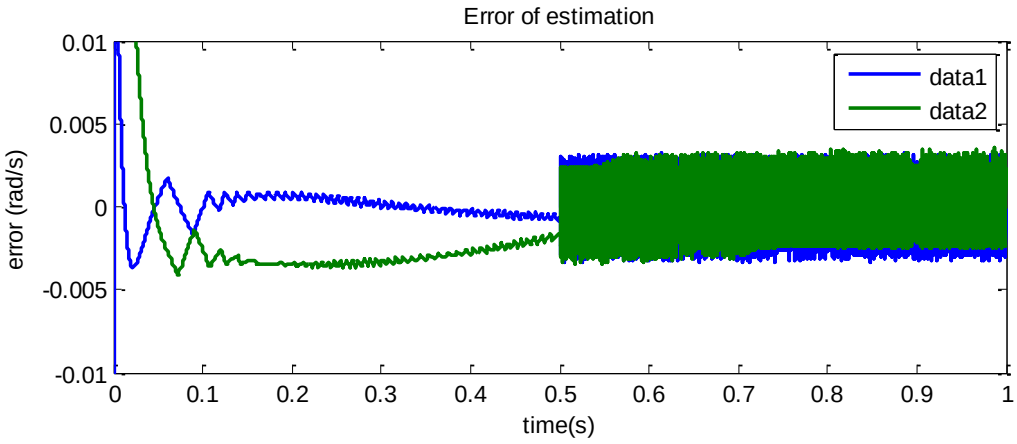

Figure 5.166: (ATSMC2-2) Error between the actual joint velocity and the estimated joint velocity versus time

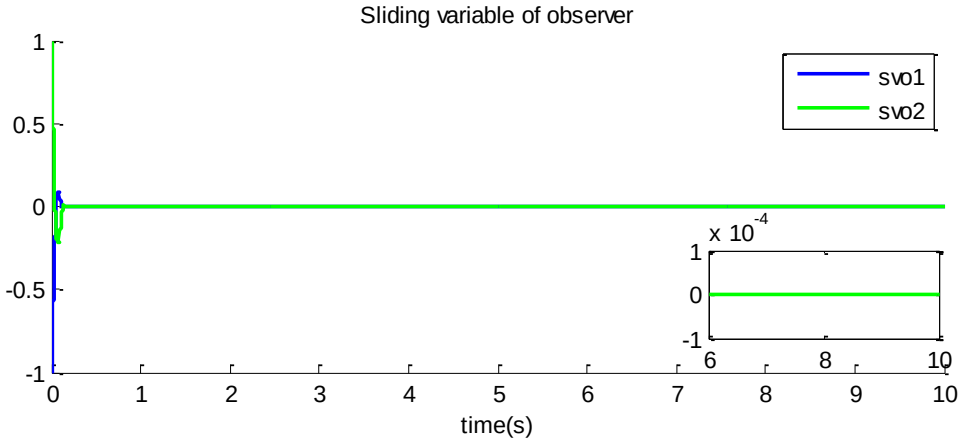

Figure 5.167: (ATSMC2-2) Sliding variables of observer versus time

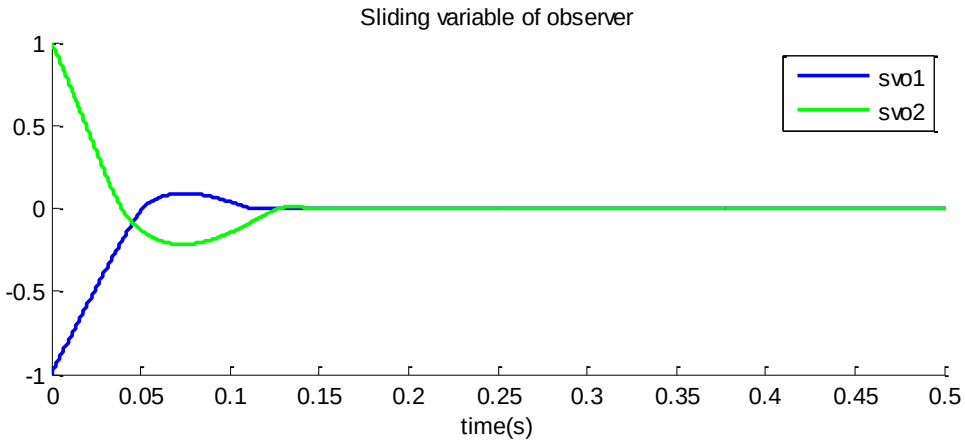

Figure 5.168: (ATSMC2-2) Sliding variables of observer versus time

Figures 5.146-5.168 show the results of the simulation of the second adaptive sliding mode control with 2-link robot manipulator. The controller gain decreases much faster than the controller gain which is obtained in (ATSMC2) (Figure 5.137 and Figure 5.160). When the controller gain becomes smaller than the boundary of the disturbance, the controller gain increases much faster than the speed of the decrease in the corresponding row.

5.2.5. Analysis of the Results of Simulations

In this section, compare the results of the simulations and evaluate the controllers for robot manipulator.

The scenario of the analysis is as follows:

(1.) Comparison the estimation of joint velocity $\dot{q}_i$.

(2.) Comparison the tracking data q_i.

(3.) Comparison the sliding variable σ_i.

(4.) Comparison the Controller τ_i.

- **Comparison of accuracy of the estimation of the joint velocity $\dot{q}_i$.**

The estimations of the joint velocity $\dot{q}_i$ are compared in this section. According to the simulation results, the joint velocity $\dot{q}_i$ is estimated with very high precision in each simulation. The biggest estimation error is observed in the simulation with TSMC1-2: Traditional sliding mode control with overestimated controller gain. The size of the error is ± 0.06. In other simulations, the estimation error is ± 0.002. In conclusion of this comparison, the joint velocity $\dot{q}_i$ is estimated accurately in all simulations, and the overestimation of the high-frequency switching controller gain increases the estimation error. Increased chattering generates increased "measurement noise" of joint variables q_1 and q_2. This yields increased error for observer/differentiator. In Figure 5.169, estimation errors are compared.

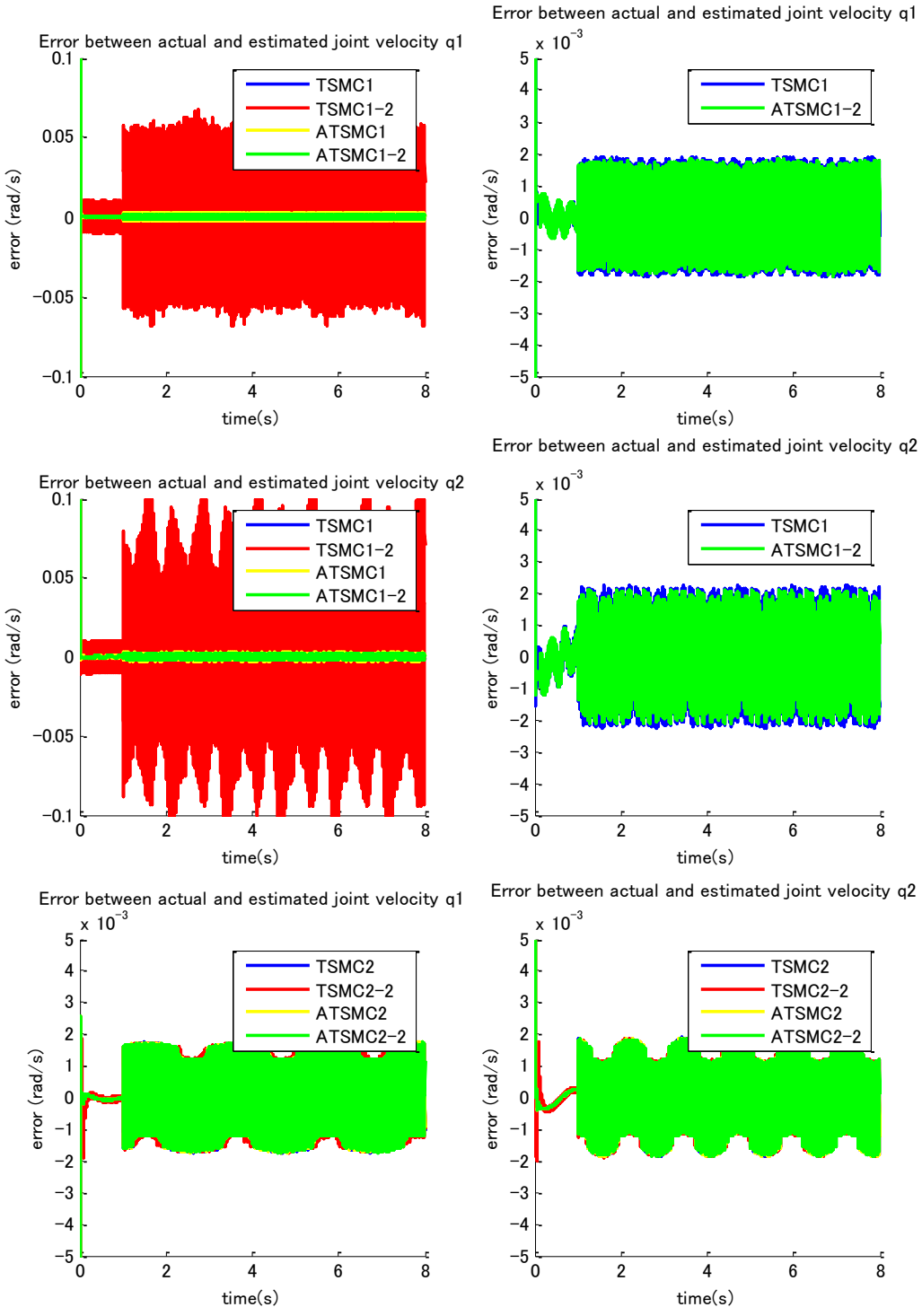

Figure 5.169: Comparison of estimation errors

- **Comparison of the tracking accuracy**

The tracking errors are compared in this section. According to the simulation results, the joint variables q_i track the command q_{ci} with very high precision in each simulation. Comparing the tracking errors in simulations of TSMC1, TSMC1-2, ATSMC1, and ATSMC1-2, the tracking errors of the simulations of TSMC1 and ATSMC1 is very small. The biggest tracking error is observed in the simulation of ATSMC1-2, the maximum error is 0.004 for q_1, and 0.006 for q_2. The second biggest tracking error is in TSMC1-2. The most accurate trajectory is output in the simulation of ATSMC1, which controller is designed without knowledge of the boundary of the disturbances.

Comparing the tracking errors in simulations of TSMC2, TSMC2-2, ATSMC2, and ATSMC2-2, the tracking errors of the simulations of ATSMC2 and ATSMC2-2 are larger than that of the simulations of TSMC2 and TSMC2-2. Especially the adaptive-gain sliding mode controls, ATSMC2 and ATSMC2-2, lose the accuracy for joint variable q_2 in comparison with TSMC2 and TSMC2-2. In Figures 5.170 and 5.171, comparisons of tracking errors are shown. This confirms the efficiency of the adaptive-gain sliding mode controllers.

In conclusion of this comparison, the tracking errors of the simulations of adaptive-gain sliding mode control, ATSMC, are larger than those of the simulations with knowledge of the boundary of the disturbances, TSMC1 and TSMC2, however the tracking errors of the simulations of the adaptive gain sliding mode control, ATSMC1, ATSMC1-2, ATSMC2, and ATSMC2-2, are very small. It is possible to reduce the errors by adjusting the parameters of the gain adaptation.

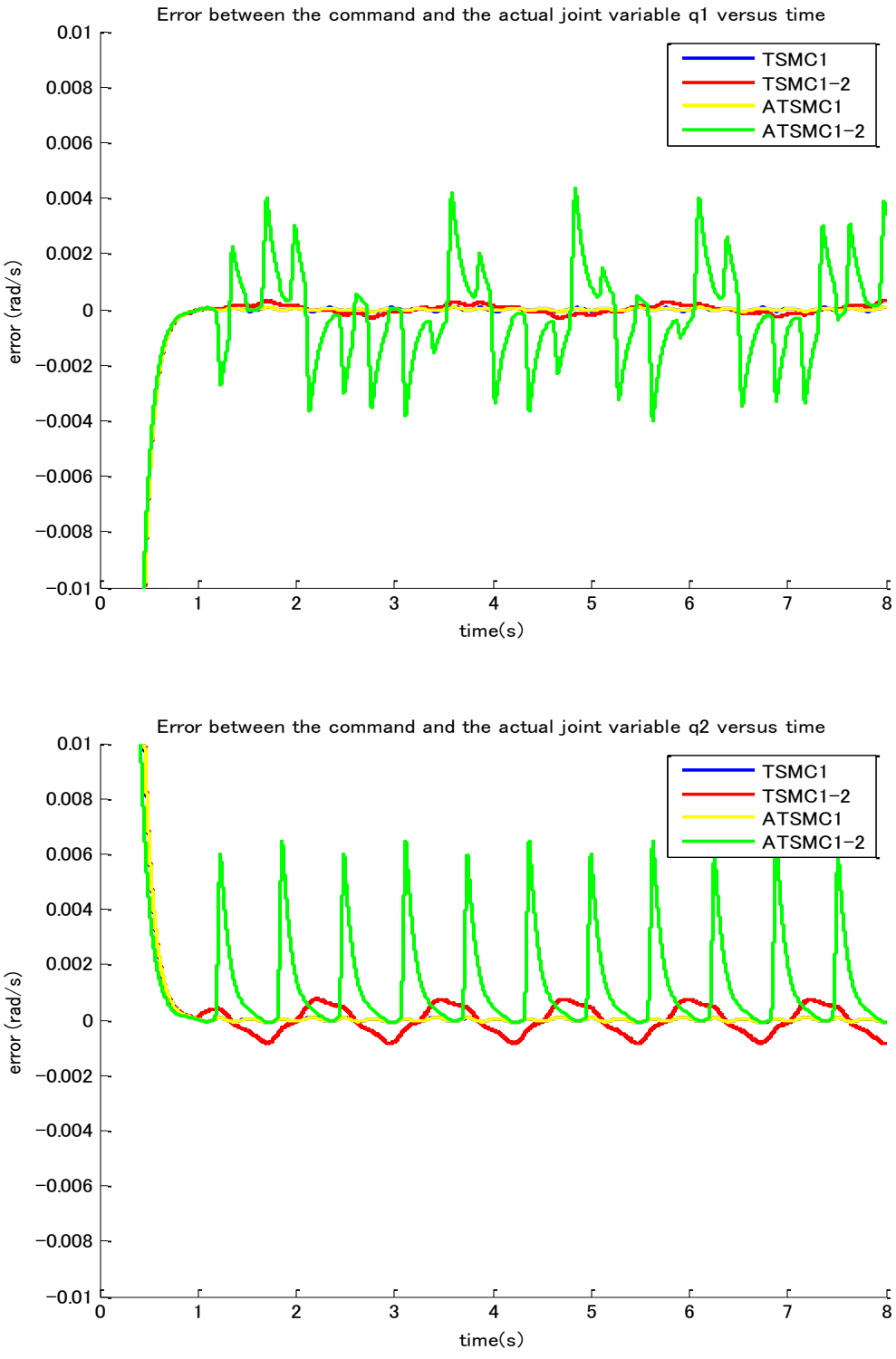

Figure 5.170: Comparison of tracking error 1

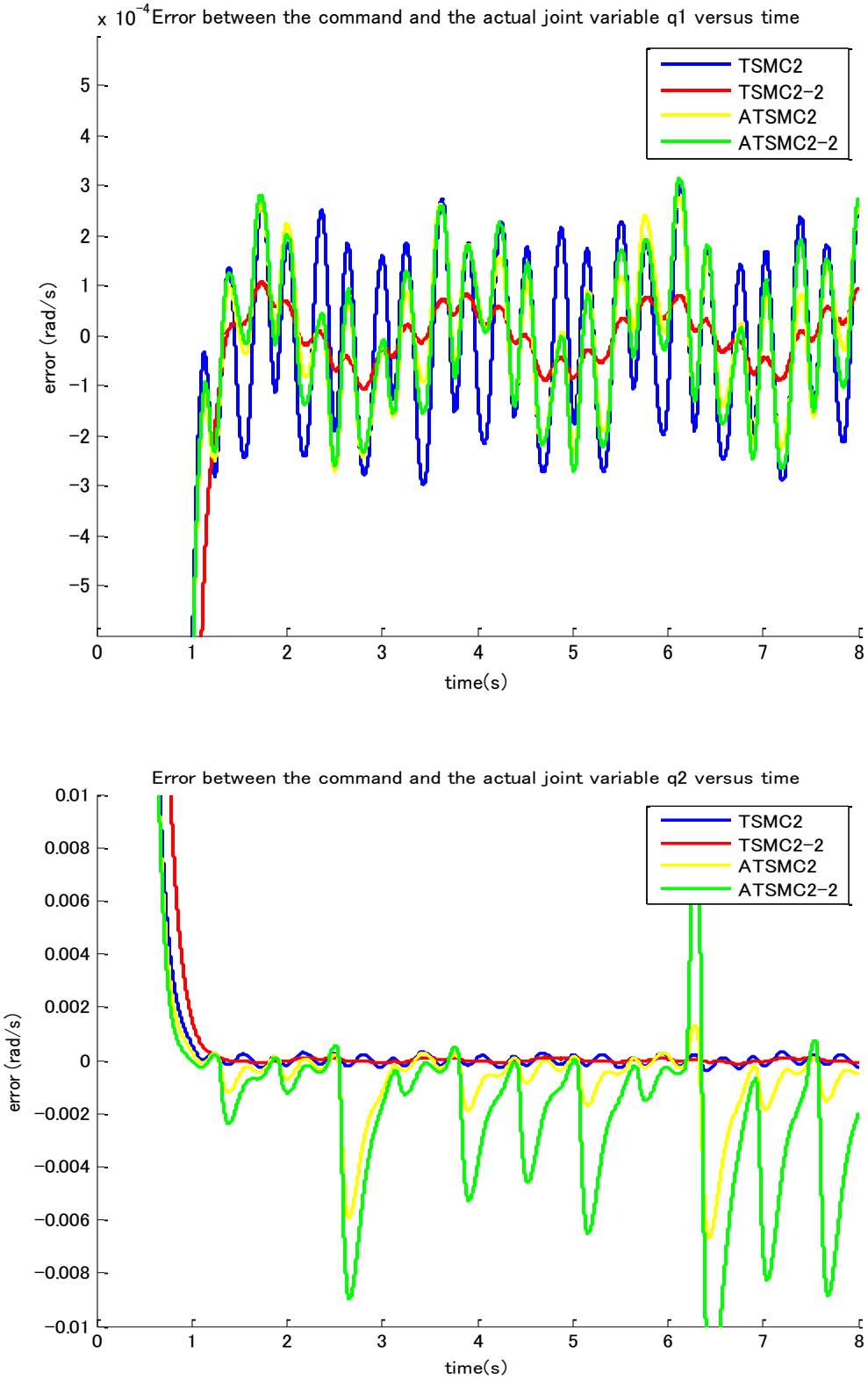

Figure 5.171: Comparison of tracking error 2

- **Comparison of sliding variables σ_i**

Sliding variables of each simulation are compared to examine the stability and the size of chattering for each simulation in this section. There are some spikes in the results of the simulations of ATSMC1-2, ATSMC1-2, and ATSMC2, that means that gain adaptation violates the stability in the simulations of ATSMC1-2, ATSMC2, and ATSMC2-2. Large chattering is observed in the simulation of TSMC1-2. The sliding variables in the simulation of TSMC2-2 keep the best stability and the smallest chattering. The sliding variables in the simulation of ATSMC1 keep better stability and smaller chattering compared with others. Spikes are observed in the simulation of ATSMC1-2, ATSMC2, and ATSMC2-2.

In conclusion of this comparison, sliding variables of the simulations of adaptive-gain sliding mode control, ATSMC1-2, ATSMC2, and ATSMC2-2, have spikes, however the chattering in the sliding variables are very small. The issue of the spikes can be solved by adjusting the parameters of gain adaptation. Chattering of all simulations except for the simulations of overestimated controller gains is very small. In Figures 5.172 and 5.173, all sliding variables of all simulations are shown.

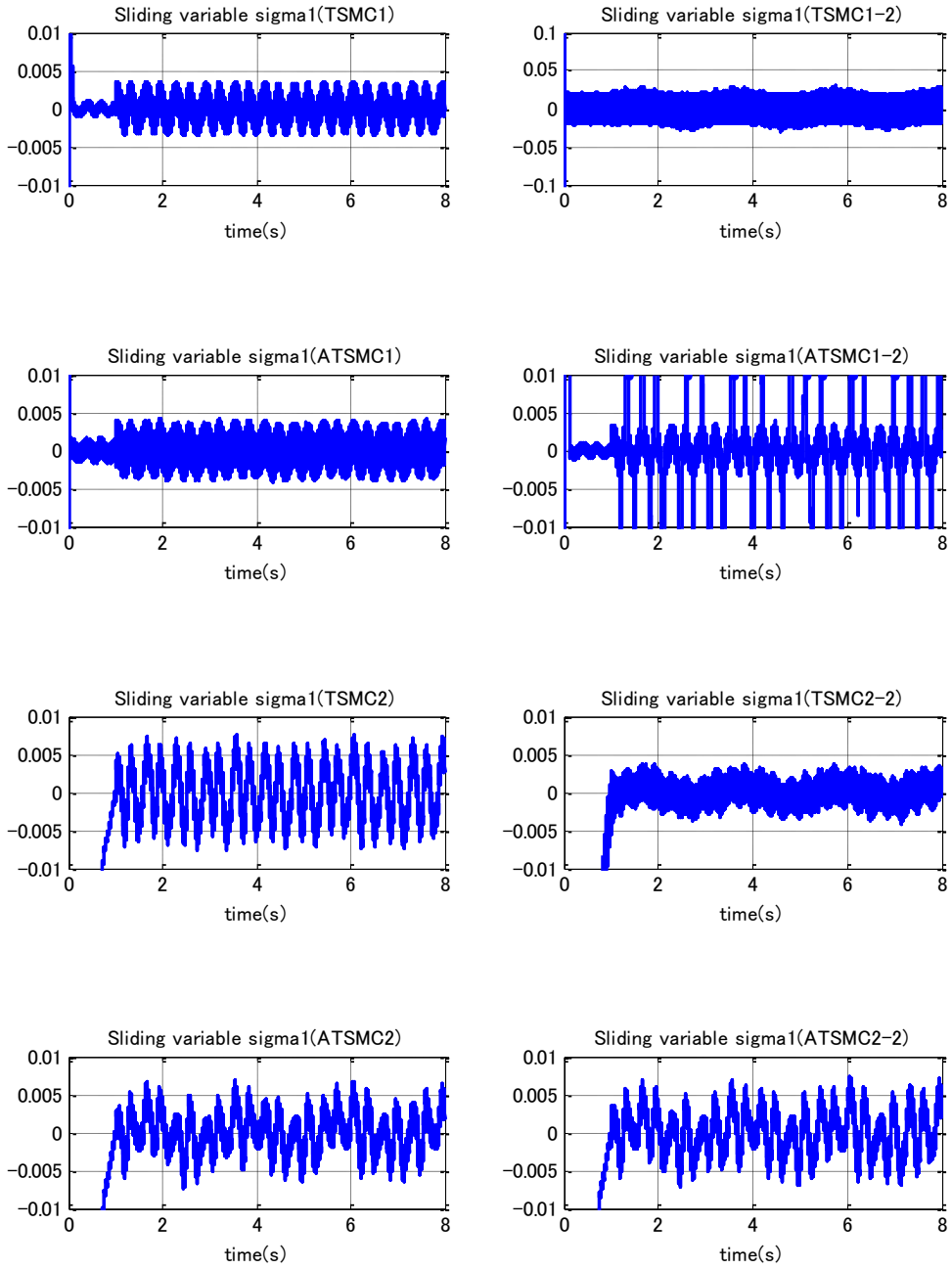

Figure 5.172: Comparison of sliding variable 1

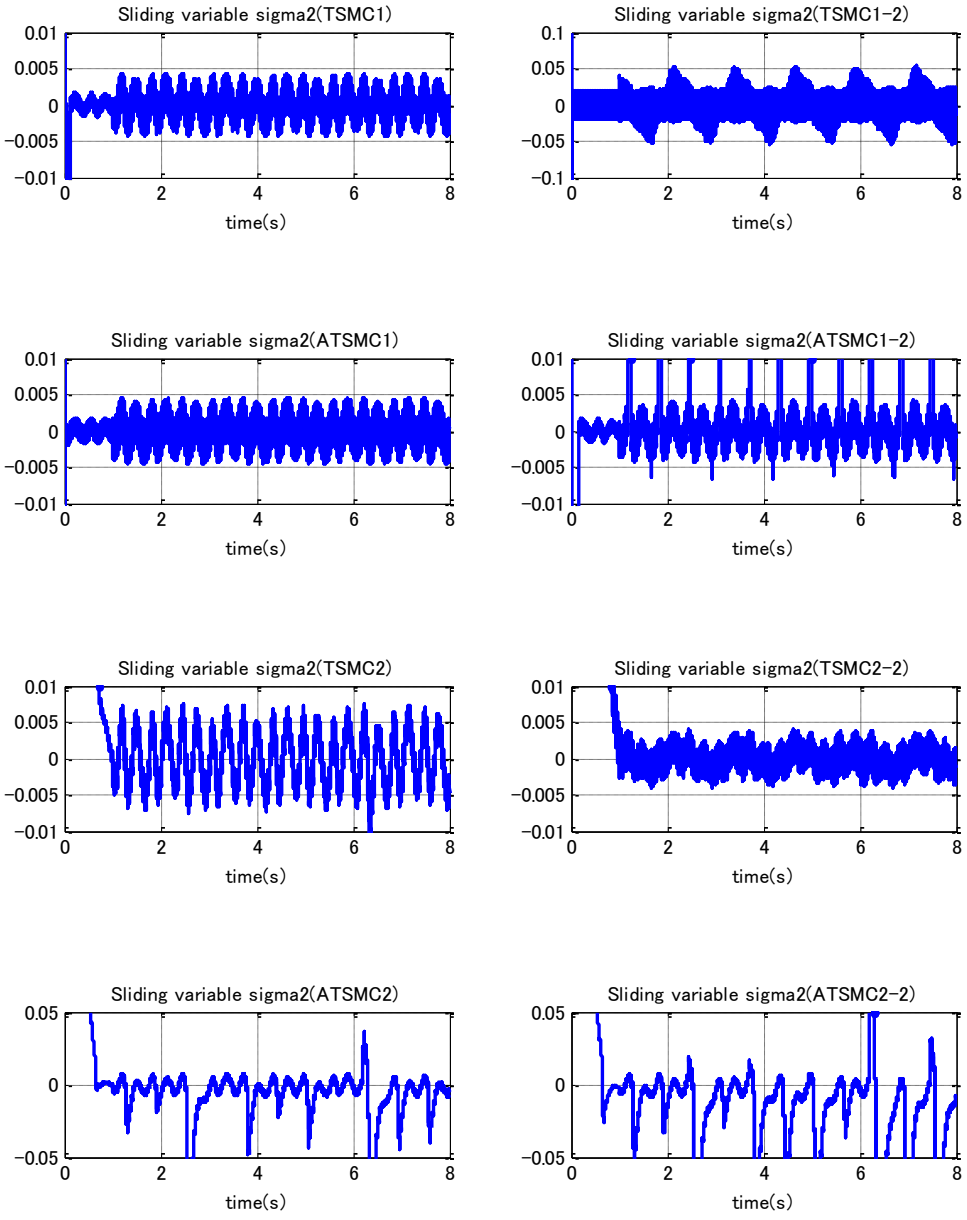

Figure 5.173: Comparison of sliding variable 2

- **Comparison of control force τ_i**

Control forces τ_i of each simulation are compared in this section. At first, the control forces in the simulation of TSMC1, TSMC1-2, ATSMC1, and ATSMC1-2 are discontinuous, while the control forces in the simulations of TSMC2, TSMC2-2, ATSMC2, and ATSMC2-2 are continuous. It is obvious that the overestimation of the controller gain produces large amplitude discontinuous function in comparison TSMC1-2 with TSMC1, and comparison TSMC2 with TSMC2-2. The amplitude of the control forces of the simulations of TSMC1, TSMC1-2, ATSMC1, and ATSMC1-2 are much larger than that of the simulations of TSMC2, TSMC2-2, ATSMC2, and ATSMC2-2. In the control forces, smaller amplitude means less energy. Therefore, the controllers, TSMC2, TSMC2-1, and TSMC2-2 require less energy than the others. In conclusion of this comparison, the adaptive-gain sliding mode controls ATSMC, are similar to the sliding mode control with knowledge of the boundary of the disturbances, TSMC1 and TSMC2. The continuous control functions, TSMC2, ATSMC2, and ATSMC2-2, require small amplitude compared to the discontinuous control functions, TSMC1, ATSMC1, and ATSMC1-2. In Figure 5.174, all control forces are shown.

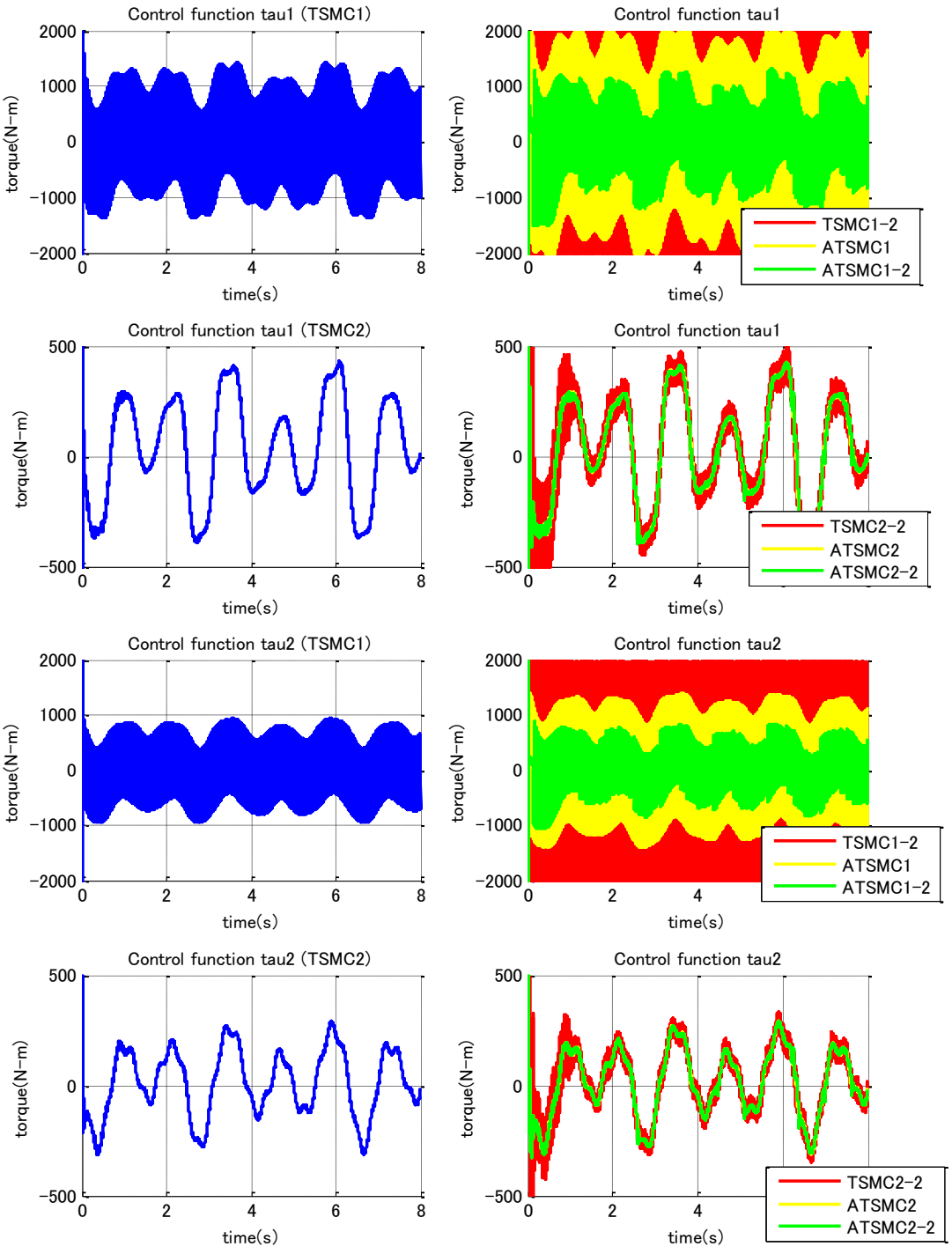

Figure 5.174: Comparison of control forces

- **Summary of Comparison Study**

	Estimation $\dot{q}_1$	Estimation $\dot{q}_2$	Trajectory q_1	Trajectory q_2	Sliding Variable σ_1	Sliding Variable σ_2	Control τ_1	Control τ_2
TSMC 1	Accurate	Accurate	Accurate	Accurate	LC, NS	LC,NS	1500 DC	1000 DC
TSMC 1-2	Less accurate	Less accurate	Accurate	Less accurate	C, NS	C, NS	Over 2000 DC	Over 2000 DC
ATSM C1	Accurate	Accurate	Accurate	Accurate	LC, NS	LC,NS	2000 DC	1300 DC
ATSM C1-2	Accurate	Accurate	Less accurate	Less accurate	LC, LS	LC, LS	1200 DC	1000 DC
TSMC 2	Accurate	Accurate	Accurate	Accurate	LC, NS	LC, NS	400 Con	300 Con
TSMC 2-2	Accurate	Accurate	Accurate	Accurate	LC, NS	LC, NS	500 DC	300 DC
ATSM C2	Accurate	Accurate	Accurate	Less accurate	LC, NS	LC, LS	400 Con	300 Con
ATSM C2-2	Accurate	Accurate	Accurate	Less accurate	LC, NS	LC, LS	400 Con	300 Con

LC- Less Chattering, NS- No Spikes, LS- Large Spikes, C- Chattering.

DC- Discontinuous, Con- Continuous.

As a conclusion of this comparison, the adaptive-gain sliding mode control can provide the accuracy and good stability without the knowledge of the boundary of the disturbances. In the point of trajectory accuracy, the adaptive-gain sliding mode controllers are less accurate compared with TSMC1 and TSMC2 which controllers are designed with knowledge of the boundary of the disturbances, while the errors are very small, less than 0.01 in radian. In the point of sliding variable, the stability is violated by

gain adaptation but also recovered quickly by gain adaptation. In the simulations of ATSMC2 and ATSMC2-2, the controllers provide accurate trajectory with the smallest controller gain.

CHAPTER 6

CONCLUSION

This thesis has studied adaptive sliding mode control design for the dynamics of robot manipulators without knowledge of the boundary of the disturbances/uncertainties, using adaptive sliding mode controls as robust controls for the robot manipulators and as a solution to the problem of chattering. To elucidate this, an adaptive sliding mode control for the n-link robot manipulator which includes the unknown bounded disturbances and uncertainties is studied. A sliding mode control is introduced as a robust control, which provides ultimate accuracy in the presence of the matched bounded disturbances/uncertainties. Chattering is introduced as a problem that accompanies the introduction of a sliding mode control; the chattering may actually damage components and cause loss of accuracy of output. As a solution, gain adaptation is introduced. Gain adaptation mitigates chattering by decreasing the controller gain dynamically when the controller gain is overestimated.

The robot manipulator is chosen as a nonlinear system with unmodeled dynamics, and each adaptive sliding mode control is designed for the robot manipulator system without knowledge of the boundary of the disturbances/uncertainties. As a case study, a

2-link robot manipulator is simulated using the designed observers and the designed adaptive controls.

In the case study, traditional sliding mode controllers, adaptive sliding mode controllers and a second order sliding mode observer are designed for the robot manipulator. The control algorithm of the robot manipulator is to control the joint position/velocity to drive the robot manipulator's end effector to a certain position/motion. The boundary of the disturbances/uncertainties and the joint velocity are assumed as unknown. A traditional sliding mode control is applied to design the control of the robot manipulator. Each joint velocity is estimated with the super-twisting observer. To mitigate chattering and avoid overestimation of the controller gain, two types of gain adaptations are designed for each control. The simulation results for each control design are shown. First, the sliding mode control design for the 2-link robot manipulator, with knowledge of the boundary of the disturbances/uncertainties, is analyzed in terms of the simulation results. Second, the same analysis is performed for the sliding mode control design for the robot manipulator with overestimated gain. Last, the adaptive sliding mode control design for robot manipulator without knowledge of the bounded disturbances/uncertainties is simulated and analyzed.

The efficacy of the adaptive sliding mode control for the robot manipulators has been confirmed in comparison of the simulation results. The adaptive sliding mode control establishes the sliding mode via the sliding mode control laws with gain adaptation, without knowledge of the boundary of the bounded disturbances/uncertainties. The controller gain values are automatically set up and, because these controller gain values are not overestimated, the chattering is mitigated. The tracking errors, chattering in

outputs, and controller gains of the simulations of adaptive-gain sliding mode controls are much close to those of the simulations of traditional sliding mode control with knowledge of the boundary of the disturbances. The greatest achievement of this study is that the adaptive-gain sliding mode control which is designed without knowledge of the boundary of the disturbances, has potential to achieve the accuracy, less chattering, and lower controller gain which are established by the sliding mode control with knowledge of the boundary of the disturbances. To conclude, the adaptive sliding mode control is demonstrated to be the robust control for the unmodeled system, and an effective algorithm to avoid overestimation of controller gains and to mitigate chattering by means of gain adaptation.

REFERENCES

[1] Spong, Mark W., Hutchinson, Seth., and M. Vidyasagar. "Robot Modeling and Control", John Wiley & Sons, Inc. 2006.

[2] Mohammad Mehdi Fateh. "Dynamic Modeling of Robot Manipulators in D-H Frames", World Applied Sciences Journal 6(1):39-44, 2009

[3] Purwar, Shubhi. "Higher Order Sliding Mode Controller for Robotic Manipulator", 22nd IEEE International Symposium on Intelligent Control Part of IEEE Multi-conference on Systems and Control Singapore, 1-3 October 2007

[4] Edwards, Chris, and S.Spurgeon. "Sliding Mode Control", 1st ed. Bristol, PA:CRC Press, 1998.

[5] Huang, Y.-J., Kuo, T.-C., and Chang, S.-H. (2008), "Adaptive Sliding Mode Control for Nonlinear Systems with Uncertain Parameters", IEEE Transactions on System, Man, and Cybernetics

[6] Lee, H., and Utkin, V. I. (2007), "Chattering Suppression Methods in Sliding Mode Control Systems", Annual Reviews in Control.

[7] Plestan, Franck. Shtessel, Yuri. Bregeault, Vincent. Poznyak, Alexander. (2010). "Adaptive sliding mode control for a class of MIMO nonlinear systems application to an electropneumatic actuator"

[8] Plestan, F. Shtessel, Yuri. Bregeault, Vincent. Poznyak, A. (2010). "New methodologies for adaptive sliding mode control"

[9] K. David Young, Vadim I. Utkin, and Umit Ozguner. (1999), "A Control Engineer's Guide to Sliding Mode Control", IEEE TRANSACTIONS OF CONTROL SYSTEMS TECHNOLOGY, VOL. 7, NO. 3

[10] H. Asada and J.-J. E. Slotine, "Robot Analysis and Control", New York: Wiley, 1986, pp. 148-155.

[11] Chandrasekharan, P., C., "Robust Control of Linear Dynamical Systems", Academic Press, 1996.

[12] J. E. Mason, E. W. Bai, L.-C. Fu, M. Bodson, and S. S. Sastry, "Analysis of Adaptive Identifiers in the presence of Unmodeled Dynamics: Averaging and Tuned Parameters", IEEE Transactions on Automatic Control, Vol. 33, No. 10, October 1988